DEVELOPMENT OF AMINE DEHYDROGENASES TOWARD PRODUCTION OF CHIRAL AMINES

A Dissertation
Presented to
The Academic Faculty

by

Samantha K. Au

In Partial Fulfillment
of the Requirements for the Degree
Doctor of Philosophy in the
School of Chemical & Biomolecular Engineering

Georgia Institute of Technology
May 2016

DEVELOPMENT OF AMINE DEHYDROGENASES TOWARD PRODUCTION OF CHIRAL AMINES

Approved by:

Dr. Andreas S. Bommarius, Advisor
School of Chemical & Biomolecular Engineering
Georgia Institute of Technology

Dr. Pamela Peralta Yahya
School of Chemistry and Biochemistry
Georgia Institute of Technology

Dr. Mark Styczynski
School of Chemical & Biomolecular Engineering
Georgia Institute of Technology

Dr. Michael Abrahamson
Principal Process Support Engineer
Abbvie

Dr. Julie Champion
School of Chemical & Biomolecular Engineering
Georgia Institute of Technology

Date Approved: March 15th, 2016

To my parents, David & Michelle Au

ACKNOWLEDGEMENTS

I want to first thank Dr. Andreas Bommarius for being an excellent advisor and giving me direction and guidance throughout my thesis. Thank you for being patient with me as I continually developed as a researcher and I appreciated your constant optimism and support. I want to also thank my committee members: Dr. Mark Styczynski, Dr. Julie Champion, Dr. Pamela Peralta-Yahya and Dr. Michael Abrahamson for their knowledgeable feedback on my thesis.

I want to thank the members of the Bommarius lab for their help over the past couple of years. I want to especially thank Dr. Bettina Bommarius, Dr. Michael Abrahamson and Dr. John (Mick) Robbins. Bettina- I want to thank you for being patient with me when I first joined the lab and taking the time to continually teach and guide me throughout my thesis. I really have enjoyed working with you on the amine dehydrogenase project and look up to you as researcher and mentor. Mike- I want to thank you for training me and doing a good job on your thesis so that I was able to build on such a solid foundation. Mick- I want to thank you for guiding and helping me on the mechanism project and I have enjoyed working with you the past couple of months. I want to also specifically thank the following former and current group members: Dr. Jonathan T. Park (general lab questions and overall guidance), Dr. Mike Rood, Dr. Yuzhi Kang, Dr. Minjeong Sohn, Ryan Clairmont (NMR and mass spectrometry), Matt Mistilis, Marietou Paye, Aditi Sharma, Harrison Rose, Thomas Kwok (Hawaiian rolls), Robert Franklin (amine dehydrogenase mechanism work) and Adam Caparco for their constant support and entertainment. I cherish our friendships and I will miss you all very much. I

also want to thank my undergraduate researchers for their hard work and dedication on the aqueous two-phase extraction project: Rupert (Junxian) Wu and Leandre Kibeho.

I want to thank my parents, David and Michelle Au, for their love and support not only during my thesis, but throughout my life. I appreciate your guidance and patience and I couldn't ask for two better role models. I want to thank my wonderful sister for constantly reminding not to take life too seriously. And most of all, I want to thank my amazing fiancé Jason Gee for his love and support during my thesis. You are the kindest, smartest and most selfless person I know and I'm so blessed to have you in my life. Thank you for always being there for me and listen to me 'tell you stuff'.

I would like to thank funding organizations for their generous support. I would like to thank the Center for Pharmaceutical Development and the U.S. Department of Education's Graduate Assistance in Areas of National Need (GAANN). Lastly, I would like to thank the Georgia Institute of Technology and the School of Chemical and Biomolecular Engineering for allowing me to be part of such an incredible program.

TABLE OF CONTENTS

Page

LIST OF TABLES

LIST OF FIGURES

Page

LIST OF SYMBOLS AND ABBREVIATIONS

ADH	alcohol dehydrogenase
AmDH	amine dehydrogenase
$(NH_4)_2SO_4$	ammonium sulfate
API	active pharmaceutical ingredient
ATPE	aqueous two-phase extraction
$CDCl_3$	deuterated chloroform
cFL1-AmDH	chimeric amine dehydrogenase
DEA	diethylamine
DMBA	dimethyl butyl amine
DMSO	dimethyl sulfoxide
DTT	dithiothreitol
E. coli	*Escherichia coli*
e.e.	enantiomeric excess
F-AmDH	phenylalanine amine dehydrogenase
FDH	formate dehydrogenase
GC	gas chromatography
GC pair	guanine-cytosine content
GDH	glucose dehydrogenase
HPLC	high performance liquid chromatography
IMAC	immobilized metal affinity chromatography
IPA	isopropanol

IPTG	isopropyl β-D-1-thiogalactopyranoside
k_{cat}	catalytic rate constant
kDa	kilodaltons
Keq	equilibrium constant
K_M	Michaelis-Menten constant
L-AmDH	leucine amine dehydrogenase
LB	Luria Bertani
LeuDH	leucine dehydrogenase
MIBK	methyl isobutyl ketone
MTBE	methyl tert-butyl ether
NADH	reduced nicotinamide adenine dinucleotide
NaCl	sodium chloride
NaOH	sodium hydroxide
NH_4OH	ammonium hydroxide
Ni-NTA	nickel nitrilotriacetic acid
NMR	nuclear magnetic resonance
Nox	NADH oxidase
OD_{600}	optical density at 600 nm
PCR	polymerase chain reaction
PDB	protein data bank
PEA	phenylethylamine
PEG	polyethylene glycol
PheDH	phenylalanine dehydrogenase

*p*FPA	*para*-fluoro phenyl acetone or 4-fluorophenyl acetone
*p*FPAm	1-(4-fluorophenyl)-propyl-2-amine
SDS-PAGE	sodium dodecyl sulfate polyacrylamide gel electrophoresis
STL	slope of tie-line
TA	transaminase
T_M	melting temperature
TCA	trichloroacetic acid
TFA	trifluoroacetic acid
TFAA	trifluoroacetic anhydride
TLL	tie-lie length
UV-VIS	ultraviolet–visible spectroscopy
VDH	valine dehydrogenase
V-AmDH	valine amine dehydrogenase
WT	wild-type

SUMMARY

One in four of the top 200 selling pharmaceutical drugs contain a chiral amine. Chiral amines often require difficult synthesis through traditional heterogeneous catalysts. As a result, the use of biocatalysts in industrial applications to create amines has been increasingly desired and developed. Amine dehydrogenases (AmDHs) are a novel class of enzymes that catalyze the reaction of prochiral ketones to chiral amines. Through protein engineering on existing amino acid dehydrogenase scaffolds, ketones instead of carboxylic acids are now substrates of the AmDH. This work will describe the use of biocatalysts, specifically the AmDHs, as a green alternative to catalyze ketones to enantiomerically pure amines.

Three different amine dehydrogenases have been developed so far: leucine amine dehydrogenase (L-AmDH), phenylalanine amine dehydrogenase (F-AmDH) and chimeric amine dehydrogenase (cFL1-AmDH). The AmDHs exhibits excellent (*R*)-enantioselectivity (>99% *e.e.*) and can also catalyze the reverse oxidative deamination reaction of amine to ketone. This work will focus on the further development and application of the amine dehydrogenases. Many of the desired pharmaceutical intermediate targets are bulkier substrates and exhibit low solubility. The first goal of this work will focus on the development of a biphasic organic solvent reaction system in order to allow for conversion of hydrophobic substrates. In a biphasic system, the enzyme and hydrophilic cofactors are envisioned to stay in the aqueous phase, while the hydrophobic substrate will partition from the organic top phase, thereby, reducing any chance of enzyme deactivation from the solvent.

The second goal of this work will involve protein and reaction engineering to obtain mechanistic insight on the binding of the ammonia substrate of the amine dehydrogenase. Amino acid mutations were performed within the active site expecting to improve the electrostatic interactions and binding toward the ammonia substrate. The activity of the AmDH was tested in various buffer conditions and substrate concentrations in order to determine its mechanism. The third goal of this work will focus on kinetic resolution of racemic chiral amine mixtures to allow for isolation of the opposite enantiomer. An AmDH naturally catalyzes formation of only the (*R*)-enantiomer, but many pharmaceutical drug intermediates are comprised of the (*S*)-enantiomer. Through optimization of reaction conditions, the enantiomerically pure (*S*)-amine was successfully obtained through complete oxidative deamination of the racemic amine mixture. The substrate profile of the AmDH was additionally investigated and mutations were introduced to improve the activity in the oxidative deamination direction.

The potential of AmDHs as a biocatalytic alternative for production toward chiral amines has led us to develop a scalable, efficient purification strategy for these enzymes. An aqueous two-phase extraction (ATPE) system consists of a polymer top phase and an aqueous salt buffer for the bottom phase. The ATPE can selectively partition the desired enzyme into the top layer, while the remaining cell debris and lysate remain in the bottom layer, resulting in a simple and efficient enzymatic purification. This was successfully achieved for the phenylalanine amine dehydrogenase, F-AmDH, and further work has applied the ATPE to other dehydrogenases. Furthermore, the phase diagram of the ATPE consisting of a binodal curve and tie-lines was established.

Lastly, the future application and conclusion of this work will be discussed with a focus on expanding the substrate specificity, improving the binding toward the ammonia substrate and switching the enantioselectivity of the AmDH.

CHAPTER 1

INTRODUCTION

1.1 Biocatalysis

Biocatalysis is the use of natural catalysts, such as enzymes, to perform chemical transformations. Enzymes are widely known for their rate enhancement that can range from 10^7 to 10^{19}-fold increase in reaction rates [1]. Enzymes also feature high selectivity, including regio-, chemo-, and enantioselectivity. They operate under environmentally friendly process conditions involving moderate temperature, pressure and aqueous reaction mediums [2, 3]. In addition, enzymes are both renewable and biodegradable. The use of biocatalysts as a green alternative to traditional heterogeneous catalysts has been increasingly investigated in the synthesis of chemical compounds and active pharmaceutical ingredients (APIs) [4, 5].

1.2 Chiral Amines

Chiral amine compounds with high enantioselectivity can be difficult to prepare by many types of traditional catalysts. In 2006, 80% of small-molecule pharmaceutical drugs approved by the FDA contained chiral centers and 75% were single enantiomers [6]. Enantiomers have the same physical properties but can exhibit different chemical properties in a chiral environment, such as the human body and with protein receptors; therefore, they should be treated as separate compounds during drug development. Some enantiomers have shown to be inactive or toxic in the human body. For the case of the anti-inflammatory drug ibuprofen, the (*S*)-enantiomer is a hundred times more potent

than the (*R)*-enantiomer [7]. Each enantiomer requires a separate toxicity study and clinical trial so it is important to produce enantiomerically pure pharmaceutical drugs.

Chiral products, including chiral amines, can be synthesized through three catalytic routes: 1) resolution of a racemic mixture, 2) chiral synthon pool and 3) asymmetric synthesis [8]. In kinetic resolution, the catalyst has different reaction rates toward each enantiomer and the undesired enantiomer can be reacted away. This procedure leaves a mixture containing 50% of the product from the undesired enantiomer and 50% of the desired pure enantiomer. The second method involves a chiral starting material that is incorporated into a chiral product. The third method focuses on asymmetric synthesis from a prochiral starting material to develop a final chiral molecule product.

In 2010, 80% of the 200 most prescribed brand name drugs in the U.S. contain nitrogen, with a chiral amine in 40% of these compounds [9]. Examples of current APIs with amine groups containing chiral centers include Januvia® and Tamiflu® (Figure 1.1). Heterogeneous catalysts to enantiomerically pure amines often feature low selectivity, less environmentally friendly solvents and difficult separation of the amine product [10-13]. As previously mentioned, biocatalysts are desired to create enantiomerically pure amines because of their selectivity and mild processing conditions. The development of biocatalysts suitable towards the production of chiral amines is still relatively limited and unestablished. The American Chemical Society's Green Chemistry Institute Pharmaceutical Roundtable (ACS GCIPR) has focused on increasing green chemistry such as the use of biocatalysts into the pharmaceutical industry. In 2007, the

Pharmaceutical Roundtable determined amination of ketones as a top aspirational reaction (Table 1.1) [14].

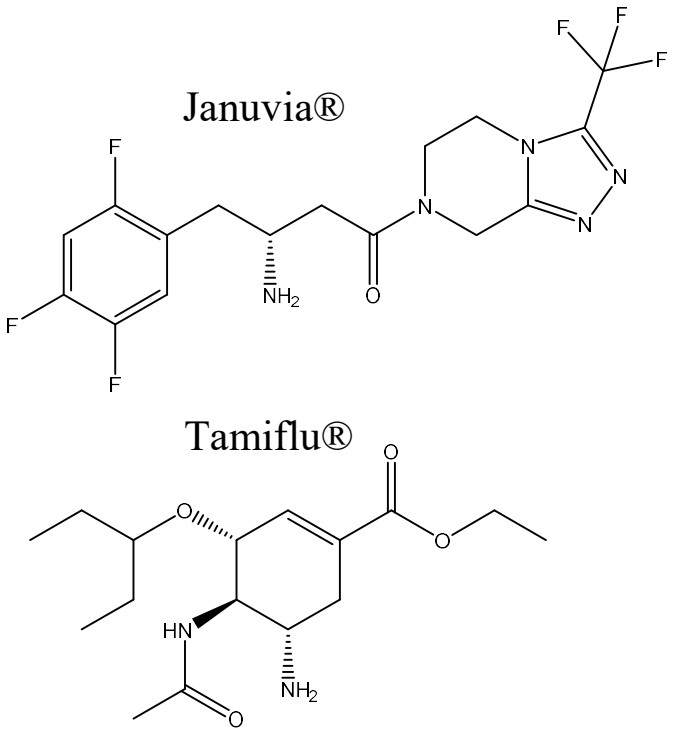

Figure 1.1 Examples of pharmaceutical drugs with chiral amines

Table 1.1 Aspirational reactions challenging the pharmaceutical industry determined by the ACS GCI Pharmaceutical Roundtable [14]

Research Area	**Number of Roundtable companies voting for research area as a priority**
C-H activation of aromatics (cross coupling reactions avoiding the preparation of haloaromatics)	6 votes
Aldehyde or ketone + NH_3 + "X" to give chiral amine	4 votes
Asymmetric hydrogenation of unfunctionalized olefins/enamines/imines	4 votes
New greener fluorination methods	4 votes
N-Centered chemistry avoiding azides, hydrazine etc	3 votes
Asymmetric hydramination	2 votes
Green sources of electrophilic nitrogen (not TsN_3, nitroso, or diimide)	2 votes
Asymmetric hydrocyanation	2 votes

1.3 Transaminases (TAs)

The most established and well-known enzymatic route to chiral amines involves transaminases. ω-transaminase transfers an amine group from an amino donor onto the carbonyl moiety of the amino acceptor (Figure 1.2). The main disadvantages of transaminases include the use of a sacrificial amine source and the need to overcome an unfavorable equilibrium. The ketone co-product must be constantly removed during the reaction to shift the equilibrium and prevent product inhibition in order to achieve conversion much beyond about 50% [15-18].

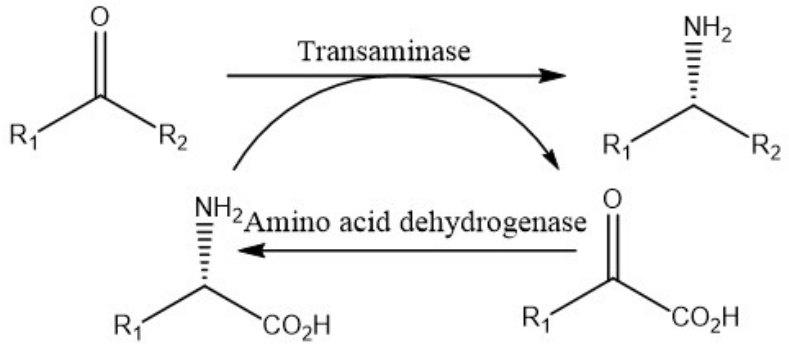

Figure 1.2 Transaminase reaction scheme

Transaminases transfer an amino group from an amine donor to a carbonyl acceptor with PLP as a cofactor. Transaminases possess a dual binding pocket, with a large binding pocket accommodating bulkier substituents and a smaller pocket for smaller substituents. [19, 20]. This smaller pocket causes the ω-transaminase to naturally possess steric constraints that limit the enzyme to convert substituents smaller than a propyl group. Recent work has been successfully developed to expand its limited substrate range to pharmaceutical intermediates [21-24]. Transaminases naturally possess (*S*)-selectivity but recently (*R*)-selective enzymes have been developed [25, 26]. In addition, recent work

has focused on increased stability [27] and by-product removal activity assays to allow for favorable equilibrium and higher conversion [28, 29].

The most successful application of biocatalysts for chiral amine production was achieved by Merck and Codexis involving an (*R)*-selective transaminase for sitagliptin (Januvia®) (Figure 1.3) [30].

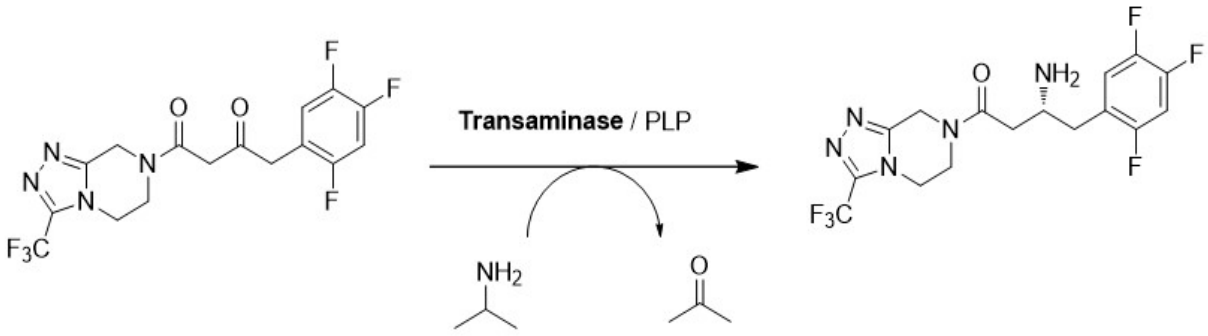

Figure 1.3 Enzymatic transamination for the synthesis of Sitagliptin [30]

1.4 Amine Dehydrogenases (AmDHs)

Amine dehydrogenases were recently developed through protein engineering using existing amino acid dehydrogenase as scaffolds (Figure 1.4). The amine dehydrogenase converts the analogous ketone (as opposed to the alpha-keto acid, the substrate of the amino acid dehydrogenase) to its respective amine with the addition of cofactor NADH and ammonia (Figure 1.5) [31]. Reductive amination of a ketone by amine dehydrogenases offer a distinct advantage over transamination by avoiding equilibrium limitations and requiring a sacrificial amine donor- it is the most direct biocatalytic route to produce chiral amines. Prior to this work, there was no developed enzymatic route toward amines by amination of prochiral ketones. Three different amine dehydrogenases have been developed: leucine amine dehydrogenase (L-AmDH) [32], phenylalanine amine dehydrogenase (F-AmDH) [33] and a chimeric amine dehydrogenase (cFL1-

AmDH) [34] (Figure 1.5). Each amine dehydrogenase has a different ketone substrate profile.

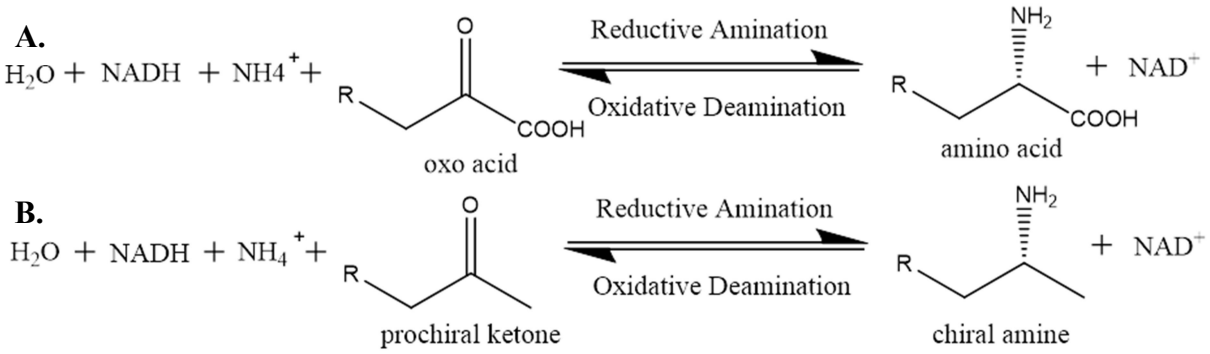

Figure 1.4 Reaction scheme of wild-type amino acid dehydrogenase (A) and amine dehydrogenase (B) [31]

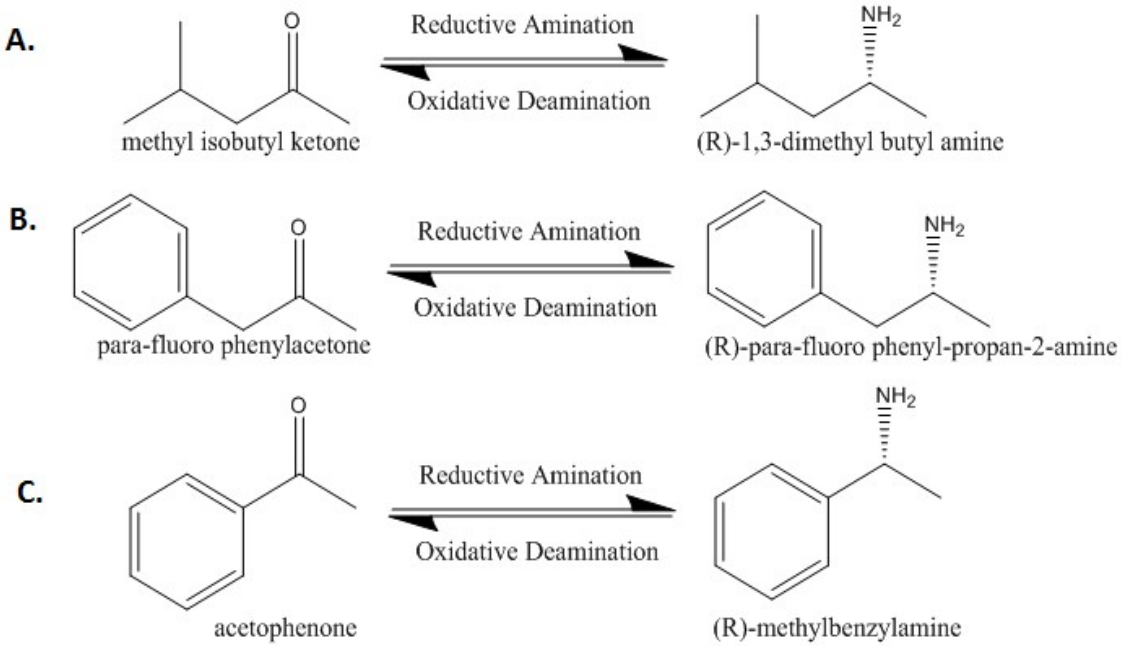

Figure 1.5 Reaction scheme for a model substrate of leucine amine dehydrogenase (L-AmDH) (A), phenylalanine amine dehydrogenase (F-AmDH) (B), and chimeric amine dehydrogenase (cFL1-AmDH) (C) [31]

1.4.1 Leucine Amine Dehydrogenase (L-AmDH)

The first amine dehydrogenase developed was the leucine amine dehydrogenase (L-AmDH). L-AmDH was developed from mutations to the active site of the *Bacillus stearothermophilus* leucine dehydrogenase. L-AmDH converts methyl isobutyl ketone (MIBK) to (*R*)-1,3-dimethylbutylamine (1,3-DMBA). A high-throughput absorbance-based assay based on NADH/NAD^+ at 340 nm and cell density measurement at 600 nm was employed to screen variants of the two-site library 67DDK/260DDK. Eleven rounds of protein engineering resulted in a successful variant K67S/N260L with a k_{cat} value of 0.46 s^{-1}. Lab-scale reaction on a 30 mg scale with L-AmDH and cofactor regeneration with formate dehydrogenase (FDH) resulted in 92.5% conversion and 99.8% *e.e.* [32].

1.4.2 Phenylalanine Amine Dehydrogenase (F-AmDH)

The second amine dehydrogenase developed was the phenylalanine amine dehydrogenase (F-AmDH) and was created by introducing mutations to *Bacillus badius* phenylalanine dehydrogenase scaffold. F-AmDH converts 4-fluoro phenylacetone (*p*FPA) to (*R*)-1-(4-fluorophenyl)-propyl-2-amine (*p*FPAm). Phenylacetone was not used because it is regulated as a Schedule 2 controlled substance. Another high-throughput library was screened for F-AmDH activity but, unexpectedly, the best F-AmDH variant consisted of the same two mutations present in the L-AmDH. Use of a restricted codon DDK at each of the two mutation sites was implemented for more efficient screening. Twenty-one unique F-AmDH variants were identified with k_{cat} values greater than 1 s^{-1}. The top variant (K77S/N275L) achieved a k_{cat} of 6.85 s^{-1} in the presence of all saturated substrates. Successful lab-scale reaction with a cofactor regeneration system was

achieved with 93% conversion and 99.8% *e.e.* (Figure 1.6) [33]. In addition, the F-AmDH from *Rhodococcus sp.* M4 has been recently developed [35].

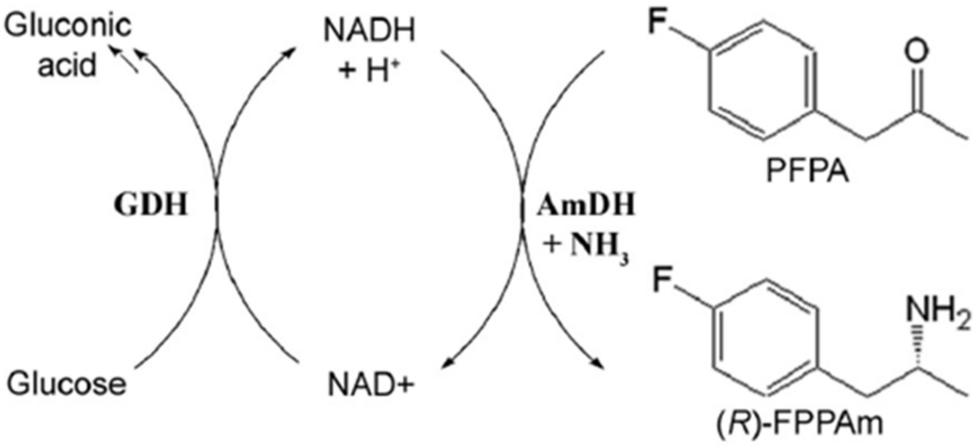

Figure 1.6 F-AmDH reaction scheme with cofactor regeneration [33]

1.4.3 Chimeric Amine Dehydrogenase (cFL1-AmDH)

The chimeric amine dehydrogenase (cFL1-AmDH) was created by combining the ketone-binding domain from the F-AmDH (residues 1-151 of *B. badius* PheDH) and the cofactor binding domain from the L-AmDH (residues 141-368 of *B. stearothermophilus* LeuDH). The cFL1-AmDH possesses unique properties as it can now take benzylic ketones as substrates, in addition to the substrates of F-AmDH. The model reaction for cFL1-AmDH is the conversion of acetophenone to (*R*)-1-phenylethylamine (1-PEA). In addition, cFL1-AmDH has a higher temperature optimum of 60°C compared to the F-AmDH temperature optimum of 50°C. Thus, the development of cFL1-AmDH has further expanded the amine dehydrogenase family [34].

1.4.4 Chiral cascades with alcohol dehydrogenases (ADH)/ amine dehydrogenases (AmDHs)

Multi-enzyme cascade reactions to synthesize chiral amines are highly desired because they avoid isolation and purification of intermediates, use less raw materials and can be used to overcome thermodynamically unfavorable equilibriums [36, 37]. The alcohol dehydrogenase (ADH) oxidizes the alcohol to form the ketone and the amine dehydrogenase (AmDH) subsequently reductively aminates the ketone to a chiral amine (Figure 1.7). This reaction is redox-neutral and allows the cofactor NADH/NAD^+ to be constantly recycled between both reactions. Through this cascade reaction, high conversion was achieved (up to 96%) and excellent enantioselectivity (>99% *e.e.*) was obtained for the (*R*)-amine [38-40].

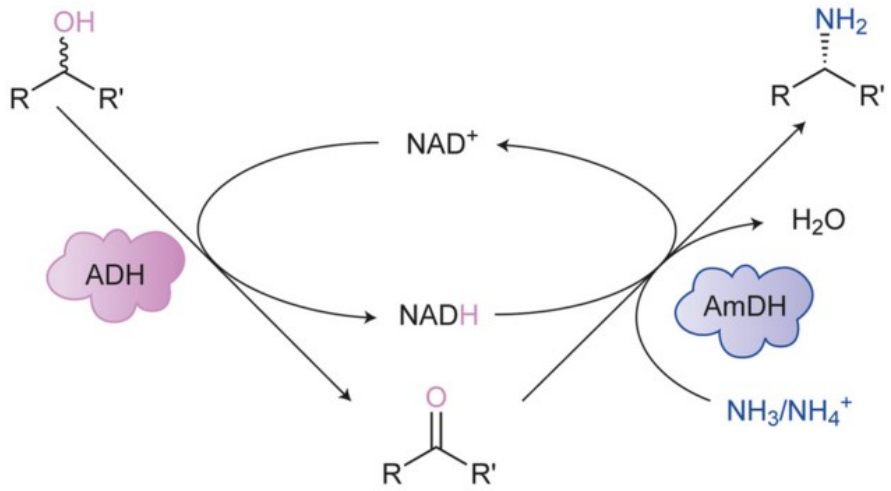

Figure 1.7 ADH/AmDH reaction scheme to create chiral amines from alcohols [39]

1.5 Cofactor Regeneration

Dehydrogenases, including the amine dehydrogenase, use nicotinamide cofactors NADH/NAD^+ as substrates. However, due to their high costs, it is not economic to use

the cofactor in stoichiometric quantities (Table 1.2). Therefore, this section will focus on implementation of an *in situ* cofactor regeneration system paired with the amine dehydrogenase.

Table 1.2 Cost of nicotinamide cofactors [41] and regeneration systems [42]

Compound	Price ($/mol)
NADH	3,580
NADPH	96,530
$HCOONH_3$ (formate)	0.2
Glucose	0.2

1.5.1 Formate Dehydrogenase

Reduction of the oxidized form of the NADH cofactor can be performed with several enzymes (Figure 1.8). In this thesis work, the cofactor regeneration enzyme glucose dehydrogenase (GDH) [43] was replaced with *Candida boidinii* formate dehydrogenase (*Cb*-FDH) [44-47]. The main advantage is the reaction can be performed in an ammonium formate solution, which i) buffers at a pH value of around 6.8, ii) supplies NH_4^+ and formate as the substrate for AmDH and *Cb*-FDH, respectively, thus, leading to improved atom economy. Another advantage of employing *Cb*-FDH is the co-product carbon dioxide, which is more easily removed than gluconic acid, the co-product of the GDH regeneration system. As gluconic acid is formed in the glucose dehydrogenase reaction, the pH value will eventually drop and the reaction system will no longer be at its optimum. A base will have to constantly be added to keep the optimum pH value. In addition, the *Cb*-FDH had a favorably wide range for pH optimum from 6.0-9.0, which is important because the amine dehydrogenase has a basic pH optimum of 9.6.The C23S

mutation was added to the FDH to improve it thermostability but there was no improvement observed in its thermostability or kinetic constants.

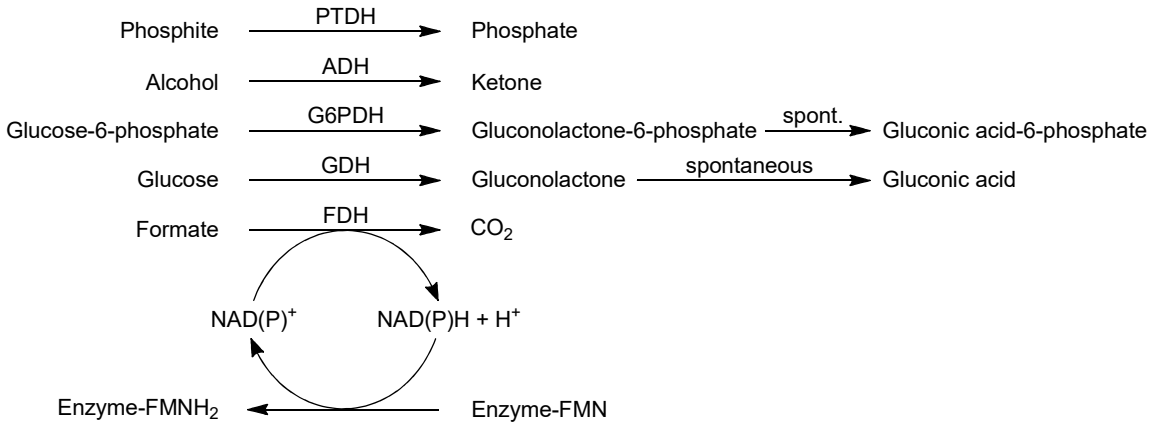

Figure 1.8 NADH regeneration scheme with various enzymes

1.5.2 NADH Oxidase

NADH oxidases (Noxs) catalyze the reaction from NADH to NAD^+ and will be utilized in kinetic resolution reaction schemes described in Chapter 4. There are two types of Noxs: 1) nox1 catalyzes a two-electron transfer to produce hydrogen peroxide as a by-product and 2) nox2 catalyzes a four-electron transfer to produce water as a by-product. This work will only involve nox 2 enzymes and there are several well-known and studied nox2 enzymes: *L. rhamnosus* [48], *L. plantarum* [49], *L. sanfrancensis* [50, 51], *L. brevis* [52-54] and *S. pyogenes* [55]. Noxs are flavin-dependent enzymes and protein engineering has been successfully performed to improve its thermostability [55] and its oxidative stability [49]. This thesis work will focus on the nox2 from *Lactobacillus plantarum* because it has already been previously studied and purified in our lab.

1.6 Protein Engineering

Due to wild-type enzymes being limited to a narrow range of substrates, mutations can be introduced with the expectation of expanding the substrate specificity. Protein engineering methods have rapidly improved over the years because of increased mechanistic, structural and sequence-based knowledge built on previous successful mutations. Increasing availability of crystal structures provides important structural information and allows for better prediction of the enzyme's interaction with its substrates and catalytic mechanism. Novel protein engineering tools include iterative saturation mutagenesis (ISM), combinatorial active-site saturation testing (CASTing) and restricted libraries. ISM involves mutating individual residues within an active site to encompass all possible residues that may be beneficial and aims for synergistic effects through iteration. CASTing is a more systematic approach and chooses to saturate small portions of the active site based on structural knowledge. Codon restriction allows for focus on a small amount of target libraries with selective codon choices that allow for more efficient screening [56]. Accumulation of beneficial mutations mirrors the evolutionary path of nature but protein engineering has steadily evolved to allow for more efficient high-throughput screening and identification of beneficial mutations [57, 58]. Both directed evolution and rational design have improved enzyme properties such as catalytic activity, substrate affinity and selectivity, and enzyme stability and both methods will be utilized in this thesis work.

1.7 Map of Dissertation

This thesis focuses on the development and application of the amine dehydrogenase for synthesis of chiral amines. Chapter 2 discusses the use of a biphasic organic solvent reaction system to allow for enzymatic conversion of hydrophobic substrates. Chapter 3 investigates the mechanism of the amine dehydrogenase and looks to understand and improve its binding toward the ammonia substrate. Chapter 4 implements a kinetic resolution reaction of a racemic amine mixture to obtain the enantiomerically pure (*S*)-enantiomer. Chapter 5 develops an aqueous two-phase extraction system for efficient purification of dehydrogenases. Chapter 6 summarizes the main findings in each chapter and discusses recommendations for future work.

CHAPTER 2

DEVELOPMENT OF A BIPHASIC ORGANIC SOLVENT SYSTEM TO ALLOW FOR ENZYMATIC CONVERSION OF HYDROPHOBIC SUBSTRATES

2.1 Introduction & Motivation

Enantiomerically pure amines are commonly used as precursors for active pharmaceutical ingredients (APIs). The amine dehydrogenases (AmDHs) have been developed to catalyze the reductive amination of prochiral ketones into chiral amines with the addition of the cofactor NADH and ammonia. The main challenge of the newly developed amine dehydrogenases is their limited substrate acceptance. It is our goal to expand the range of substrates for AmDH towards intermediates important for pharmaceuticals or crop protection. The limited substrate acceptance is largely due to the hydrophobicity and thus low solubility of potential substrates in aqueous medium. Reactions in organic solvents have many advantages beyond increased solubility of substrates, including suppression of hydrolysis side reactions, easy product removal, and overcoming an unfavorable equilibrium [59, 60].

Biocatalytic reactions involving organic solvents often accelerate deactivation of enzymes. Despite this notion, many reactions have been successfully achieved, including amination of prochiral ketones by transaminases performed in water/DMSO [61, 62]. Dehydrogenases, however, have been scarcely employed in these water-miscible systems because of their limited stability in organic solvents, and low solubility and stability of the cofactor has prevented successful applications [63-65]. To incorporate biocatalysts

into organic solvents, work can be either performed on the biocatalyst to improve its stability or on the medium to optimize reaction conditions [66, 67]. Optimization of reaction conditions in the presence of organic solvents is the focus of the current work.

In biphasic aqueous-organic solvent systems, enzymes and hydrophilic cofactors, such as NADH, are envisioned to stay in the aqueous phase while the hydrophobic substrate preferentially partitions into the organic phase (Figure 2.1). Enzyme interaction with the organic solvent should be minimal [68]. Alcohol dehydrogenases have been used successfully in a biphasic reaction system coupled with cofactor regeneration using *Candida boidinii* FDH (*Cb*-FDH) [69, 70]. Previous work specifically involving phenylalanine dehydrogenases in organic solvents has included immobilization of the enzyme [71] or additional mutations [72] to improve stability, none of which will be included in this work.

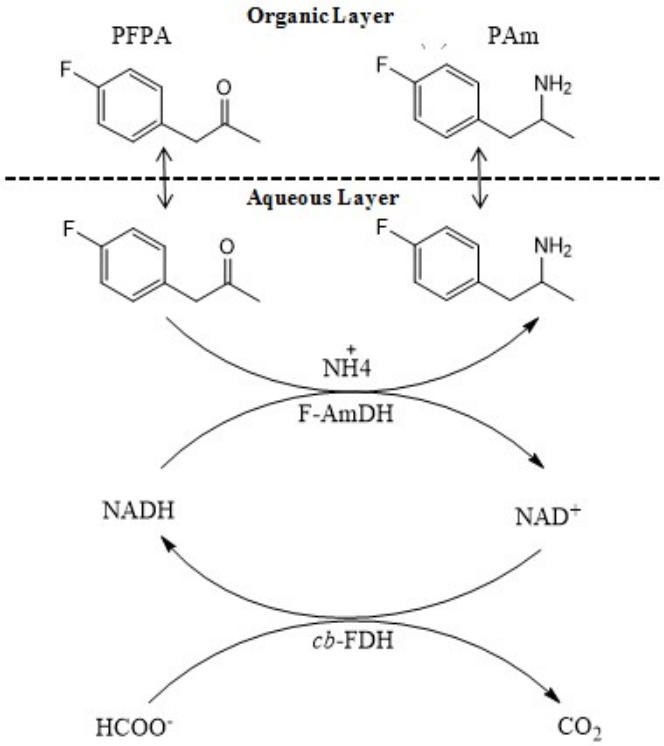

Figure 2.1 Biphasic system reaction scheme involving F-AmDH and *p*FPA

This current work focuses on the incorporation of water-immiscible organic solvents to establish an efficient biocatalytic route using AmDH to produce chiral amines, often scaffolds for active pharmaceutical intermediates (APIs), from hydrophobic ketones. The substrate range for AmDH is expanded because the biphasic reaction system allows for conversion of desired substrates that previously could not be converted to chiral amines as a result of their insolubility (Figure 2.2, substrates **3** and **4**). The amine products of *p*FPA (**1a**) and 1-adamantyl methyl ketone (**3a**), which is the 1-(4-fluorophenyl)-propyl-2-amine and 1-adamantyl-ethyl-1-amine respectively, mimic APIs of sitagliptin (Januvia®) [73] and saxagliptin (Onglyza®) [74], respectively, two anti-Type II diabetes drugs.

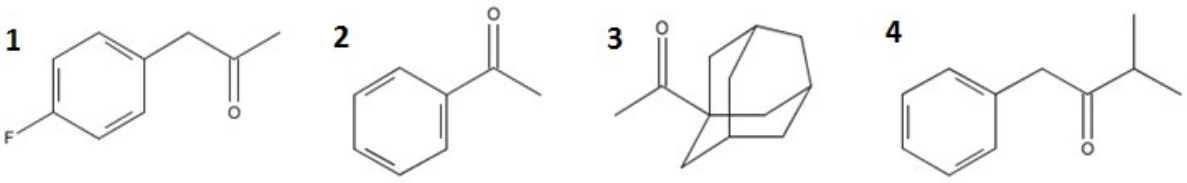

Figure 2.2 Hydrophobic substrates of the amine dehydrogenase. **1**: *para*-fluoro phenyl acetone (*p*FPA), **2**: acetophenone, **3**: 1-adamantyl methyl ketone, **4**: 3-methyl-1-phenyl-2-butanone

2.2 Materials & Methods

2.2.1 General

Substrates were obtained from suppliers and used without further purification. NADH was obtained from Amresco (Solon, OH). 4-fluorophenyl acetone, 1-phenylethylamine and butyl acetate were obtained from Acros Organic (Morris Plains, NJ). *(R/S)*-1-(4-fluorophenyl)-propyl-2-amine, 3-methyl-1-phenyl-2-butanone and imidazole were obtained from Alfa Aesar (West Hill, MA). Acetophenone, 1-adamantyl methyl ketone,

(R/S)-1-(1-adamantyl) ethylamine hydrochloride, 4-(dimethylamino)pyridine, NAD^+, chloroform, trifluoroacetic acid (TFA) and trifluoroacetic acid anhydride (TFAA) were obtained from Sigma Aldrich (St. Louis, MO). Heptane and methyl-*tert*-butyl ether (MTBE) was obtained from J.T. Baker (Phillipsburg, NJ). HPLC grade methanol, toluene and acetonitrile were obtained from Fisher Scientific (Fairlawn, NJ). IPTG was obtained from Gold Biotechnology (St. Louis, MO).

2.2.2 Protein expression and purification

Both amine dehydrogenases were expressed in a pET-28a, BL21 (DE3) (Invitrogen) system at 18°C in Luria Bertani medium (United States Biological). Expression was induced with 0.5 mM IPTG at an OD_{600} value of 0.5 and continued for 12 hours. Overexpression was determined by observing a prominent band at 44 kDa on an SDS-PAGE gel. His-tagged proteins were purified by employing immobilized metal affinity chromatography (IMAC) through a Ni-NTA resin (Thermo Scientific). Protein concentration is measured through Bradford assay [75].

2.2.3 Spectrophotometric and activity analysis

Specific activity is determined using an NADH-dependent (340 nm, λ_{340}= 6220 M^{-1} cm^{-1}) spectrophotometric assay. Activity is calculated from the stoichiometric oxidation of NADH to NAD^+ as measured by the change in absorbance over time. One unit of activity is defined as the amount of enzyme that catalyses the formation of 1 μmol of product amine in 1 minute. Reductive amination activity is measured in 5 M $NH_4/CHOO^-$ pH 9.6

buffer and measured at 25°C. Protein concentration is measured through Bradford assay [75].

2.2.4 High-performance liquid chromatography (HPLC) analysis

Liquid chromatography was performed on a Shimadzu UFLC-2010 with a Beckman Coulter Ultrasphere column (4.6 mm x 25 cm). The samples are run at 1 mL min^{-1} with a column temperature at 40°C. Detection occurs at 255 nm. Methods for detecting conversion to amine are summarized in Table 2.1.

Table 2.1 HPLC method and retention times for ketones and their respective amines

	pFPA/ pFPAm	**Acetophenone/ 1-PEA**	**3-methyl-1-phenyl-2-butanone**
Method	MeOH-H_2O-(0.5 M sodium acetate-glacial acetic acid, pH 3.40) (60:35:5) with 0.1% TFA [76]	MeOH-H_2O-(0.5 M sodium acetate-glacial acetic acid, pH 3.40) (40:55:5) with 0.1% TFA [76]	Acetonitrile (0.1% TFA)-water (30:70)
r.t. ketone (min)	4.3	10.2	9.1
r.t. amine (min)	3	3.8	3.9

2.2.5 Gas chromatography (GC) analysis

Gas chromatography was performed on a Shimadzu GC-2010 gas chromatography apparatus with a Restek Rt-BDEXcst column (length: 30 m; inner diameter: 0.32 mm; film thickness: 0.25 μm). 1-adamantyl methyl ketone does not absorb in the UV range so detection of amine was determined by gas chromatography (GC) with Flame Ionization Detector (FID). The reaction mixture is derivatized by trifluoroacetic acid anhydride (TFAA). To derivatize the compounds, 150 mM (approximately one crystal) of 4-(dimethylamino) pyridine, which acts as a catalyst, and 2 μL of TFAA were added to 200 μL of the sample. The derivatized sample was allowed to react for 10 minutes before GC

analysis. The linear velocity is 60 cm/s and the carrier gas was helium air mixture. When the aqueous layer was analyzed, chloroform is added to extract any leftover ketone and amine into the organic layer.

2.2.6 Partition coefficient

The ratio of the amount of the compound present in the organic phase compared to the aqueous phase was calculated to determine the partition coefficient. The aqueous medium is ammonium formate (5M NH_4HCO_2/OH pH 9.6). 25 mM of the hydrophobic substrate was added to the biphasic mixture. The partitioning was conducted in a glass vial (diameter= 0.5 cm, height= 4 cm) and allowed to equilibrate at 30°C for five hours. Different phase ratios were observed in a total reaction volume of 1 mL. When stirring was required, the sample was stirred at 150 rpm. Both the organic and aqueous layers were analyzed *via* HPLC. As for the 1-adamantyl methyl ketone, both layers were analyzed *via* GC.

2.2.7 Conversion in purely aqueous systems (without presence of organic solvents)

To determine conversion to the amine, reactions were performed in the presence of the respective amine dehydrogenase and the regeneration enzyme in a 5 mL glass vial. Time points were taken up to 24 hours. Only 10 mM of *p*FPA was added due to solubility issues while 30 mM of acetophenone was added into the reaction. In the case of *p*FPA, 0.1 mg of F-AmDH and 0.25 mg of *Cb*-FDH were added to the aqueous reaction medium of 5 M NH_4HCO_2/OH pH 9.6. The reaction was performed at 35°C. In the case of acetophenone, 0.25 mg of cFL1-AmDH and 0.5 mg of the thermostable *Bs*-GDH was

added to the reaction medium of 5 M NH_4Cl/OH pH 9.6. The reaction was conducted at 50°C and 100 mM of glucose was added to the reaction. 1 mM NADH/NAD^+ was added to all reactions. All reactions were stopped by diluting with methanol and analyzed using HPLC for amine peaks. After 24 hours, the product amine was extracted with MTBE and analyzed using ^{1}H NMR (20 Hz) in $CDCl_3$. No stirring was implemented.

2.2.8 Biphasic conversion

To determine conversion to the amine, reactions were performed in the presence of the respective amine dehydrogenase and the regeneration enzyme in a 1 mL volume and time points were taken. 150 mM of the substrate was added to the organic solvent. 0.1 mg and 0.25 mg of F-AmDH was added for the *p*FPA and 3-methyl-1-phenyl-2-butanone reactions, respectively. The aqueous reaction medium was 5 M NH_4HCO_2/OH pH 9.6 and the reaction was performed at 35°C. 0.25 mg of cFL1-AmDH was added to the reactions involving acetophenone and 1-adamantyl methyl ketone. The aqueous reaction medium was 5 M NH_4Cl/OH pH 9.6 and the reaction was performed at 50°C. Twice as much regeneration enzyme activity (*Cb*-FDH, *Bs*-GDH) was added to ensure that the reversible reaction would not occur and that enough co-substrate NADH was always present during the reaction. 1 mM NADH/NAD^+ was added to the reactions. All reactions were stopped by adding methanol and analyzed by HPLC to detect of amine peaks. After 24 hours, the products *p*FPAm and PEA were extracted with MTBE and analyzed *via* $_1$H NMR in $CDCl_3$. Mass spectrometry was used to determine product amine with reactions involving 1-adamantyl methyl ketone and 3-methyl-1-phenyl-2-butanone. No stirring was implemented.

2.3 Results & Discussion

2.3.1 AmDH deactivation in presence of organic solvents

The model substrate of F-AmDH is *para*-fluoro phenyl acetone (*p*FPA). *p*FPA has limited solubility (10 mM at pH 9.6 and 25°C) in aqueous ammonium formate buffer compared to phenylalanine due to the replacement of the carboxyl group with a methyl group (solubility decreases over 10-fold). The necessity to increase solubility of hydrophobic substrates initially led us first to monophasic aqueous-organic solvent reaction systems. In the presence of organic co-solvents that previously achieved success, including acetone, methanol, dimethyl sulfoxide (DMSO) and ethylene glycol (10-30%, v v^{-1}) [77, 78], F-AmDH quickly lost most of its catalytic activity (within one minute) toward *p*FPA as compared to *Candida boidinii* FDH (*cb*-FDH) (Figure 2.3). This led to a transition into biphasic aqueous-organic solvent reaction systems.

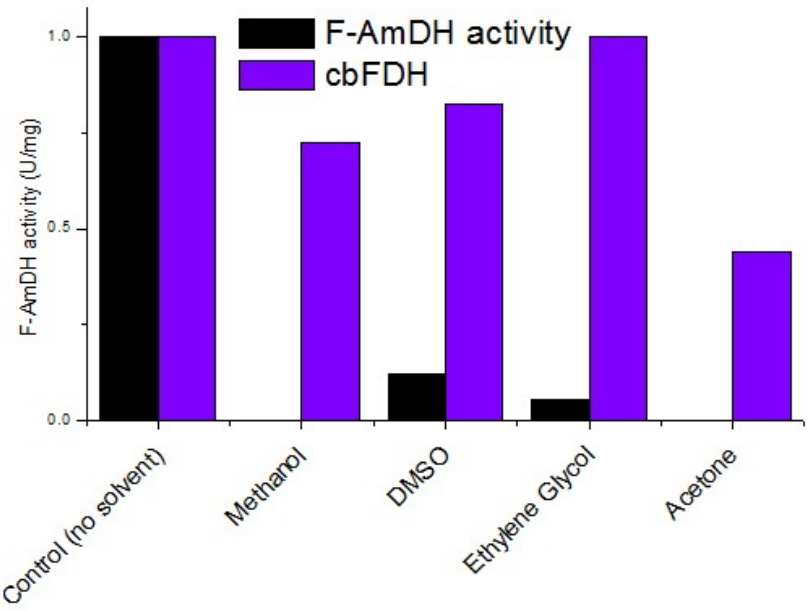

Figure 2.3 F-AmDH and *cb*-FDH residual activity in 20% (v/v) organic solvents (normalized to 1, highest specific activity observed without an organic solvent present).

2.3.2 Partition coefficients of organic solvents and identification of heptane as the optimal organic solvent

The first step towards developing a biphasic organic solvent reaction system is to identify potential solvents that are immiscible with water, achieved previous success [64, 69, 70], and exhibit minimal environmental impact to maintain benefits of biocatalysts according to the ACS GCI PR solvent selection guide [79]. Heptane was chosen as a representative example of aliphatic hydrocarbons, toluene for aromatic compounds, methyl *tert*-butyl ether (MTBE) for ethers and butyl acetate for esters [80]. Chloroform was also additionally chosen because of its ease of extraction of the amine product, especially involving analytical-scale work. Ketones were excluded because of probable cross-reactivity as a substrate.

According to the solvents' log P values (Table 2.2), heptane is the least polar solvent (highest organic-aqueous partition coefficient) [81]. Hydrophilic solvents are known to remove water molecules from the surface of the enzyme essential for catalysis and subsequently often lead to enzyme deactivation [59]. Therefore, heptane did not deactivate the enzymes compared to other solvents, likely because less of it enters the aqueous phase [82]. In addition, we measured the log P value of *p*FPA in all four organic solvents between the aqueous reaction buffer and organic solvent (Table 2.2, Figure A.1). The partition coefficient of *p*FPA in heptane is relatively small compared to other solvents, so that a good portion of the substrate distributes into the aqueous phase. In addition, the cofactor regeneration enzyme *Cb*-FDH is known to have low stability in the presence of common water-immiscible organic solvents, such as toluene and MTBE, but was previously found to show stability around aliphatic hydrocarbons such as hexane and heptane [69, 70]. Since the enzyme may come into contact with the interface between the

organic and aqueous phases during the reaction, it is beneficial for the enzymes to have high stability in the presence of organic solvents. Heptane was ultimately chosen as the organic solvent for the biphasic reaction system based on these partition coefficient results.

Table 2.2 Partition coefficient of *p*FPA in various organic solvents

	Heptane	**MTBE**	**Butyl Acetate**	**Toluene**	**Chloroform**
*p*FPA	1.11	2.12	2.25	2.27	2.56
Log P values of solvents (reported in literature) [a]	4.27	1.29	1.80	2.72	1.94

[a]Estimated with Advanced Chemistry Development (ACD/Labs) Software V11.02 [81]

2.3.3 Partition coefficient of the hydrophobic substrates and phase ratios

Next, the partition coefficients were experimentally determined for desired hydrophobic substrates and their corresponding amines in heptane (Table 2.3). Larger partition coefficients indicate that less of the substrate moves into the aqueous phase and conversion becomes harder to achieve. The partition of amines is important to determine the ease of product extraction, and the transition of amine into the organic layer can help avoid product inhibition. While the partition coefficient is the most common criterion to predict enzyme success in organic solvents [83, 84], prediction of enzyme behavior within a biphasic system likely cannot be captured by just a single variable [80]. Enzymes can easily deactivate or perform poorly in various non-optimal reaction conditions, such as temperature, pH, enzyme concentrations, and substrate concentrations.

Partition coefficients are also reported here for varying phase ratios for the case of stirred solution (Table 2.3). Previous work in biphasic media had found the optimal phase ratio to be 1:4 for heptane to water [64, 69, 70]. Substrate concentration decreases with a smaller ratio of organic to aqueous phase because more of the substrate is partitioned into the aqueous phase (Figure 2.4, Figure A.2). A phase ratio of 1 to 4 is employed for the remaining biphasic reactions. 1-Adamantyl methyl ketone (**2a**) is the exception because the log P values are extremely skewed, as very little of the adamantyl substrate partitioned into the aqueous phase. Therefore, a more concentrated organic phase is observed. This result explains also the issue of low conversion of the 1-adamantyl methyl ketone to 1-(1-adamantyl) ethylamine as very little of the substrate diffuses into the aqueous phase regardless of the solvent.

Table 2.3 Partition coefficient of substrates in heptane (a: ketone, b: amine)

Phase ratio	1a	1b	2a	2b	3a	3b[a]	4a
1:1	1.11	-0.02	1.35	-0.14	3.28	2.65	2.21
1:2	1.12	-0.03	1.37	-0.15	3.72	2.56	2.1
1:4	1.22	-0.1	1.35	-0.17	4.95	2.28	1.75
1:4 stirring	1.21	-0.04	1.39	-0.18	4.94	2.36	1.79

[a]Average of two log P values: racemic 1-(1-adamantyl ethylamine) is split into two peaks with two retention times on the chiral GC column. For 3-methyl-1-phenyl-2-butanone (**4a**), the respective amine (α-(1-methylethyl)-benzene ethanamine)), compound **4b**, is not available for partition coefficient data.

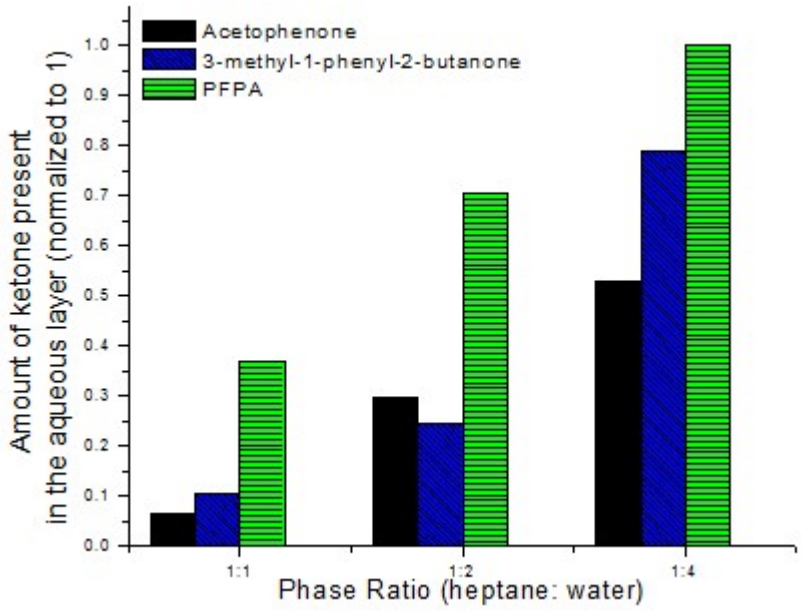

Figure 2.4 The amount of hydrophobic substrates in the aqueous layer as a function of phase ratio (normalized to **1a**, the amount of *p*FPA in the aqueous phase).

2.3.4 Effect of stirring and mass transfer limitations

The effect of stirring on the system was also investigated. Previous biphasic reaction systems were gently stirred to improve distribution of the hydrophobic substrate at the interface [85]. However, stirring can lead to enzyme precipitation caused by shear stress. In addition, stirring did not show a significant difference in specific activity and is not critical to the overall reaction because mass transfer, as expected, is fast compared to kinetics. The rate limiting step of mass transfer is the movement of the substrate across the interface. This interfacial mass transfer occurs fast enough to ensure the reaction is always saturated with the adequate amount of substrate to proceed in the absence of mass transfer limitations (Figure A.3). The time scale for a reaction is given by Equation 2.1. The k_{cat} value at 25°C and pH 9.6 for F-AmDH towards *p*FPA is 6.8 s^{-1}. This reaction is chosen because it is the fastest reaction from ketone to amine investigated in this work and would be most likely to be slowed by mass transfer limitations.

$$\tau_{reaction} = {}^{1}/_{k_{cat}} = {}^{1}/_{6.8} = 0.158 \text{ seconds} \qquad \text{[Equation 2.1]}$$

The mass transfer across the interface after the system has reached steady-state is described by Equation 2.2. The flux of the substrate is based on the concentration gradient across the interface and the mass transfer coefficient in the aqueous phase. The mass transfer coefficient can be roughly estimated (Equation 2.3) using film theory and the value for the diffusion coefficient of the hydrophobic substrates in aqueous medium [86, 87]. The concentrations of the substrates in each phase can be estimated by the partition coefficients found in Table 2.3. The flux of *p*FPA is found to be 0.1 $M \cdot s^{-1}$, which shows 10 mM of the substrate can be transferred every 0.1 seconds. The K_M value of *p*FPA is approximately 6 mM so at the given mass transfer rate, the enzyme will always be saturated with enough substrate to proceed at near maximum specific activity.

$$J = k_L a\left(C_{org} - C_{aq}\right) = 0.1\ {}^{M}/_{S} \qquad \text{[Equation 2.2]}$$

$$k_L = \frac{D_{aq}}{\Delta x} = \frac{D_{aq}}{\delta} \qquad \text{[Equation 2.3]}$$

2.3.5 Impact of biphasic organic solvent system on specific activity and volumetric productivity

An increased volumetric productivity is observed for *p*FPA and acetophenone in a biphasic reaction system as compared to a reaction without organic solvents (Figure 2.5). *p*FPA exhibits limited solubility (up to 10 mM) without the presence of organic solvent; consequently, the limit on the amine that can be produced likewise is around 10 mM in purely aqueous systems. However, this problem is resolved through the incorporation of organic solvents and the volumetric productivity doubles for *p*FPA and is very apparent

after 6 hours. Substrate conversion and thus specific activity are measured *via* HPLC (Figure A.4 and Figure A.5).

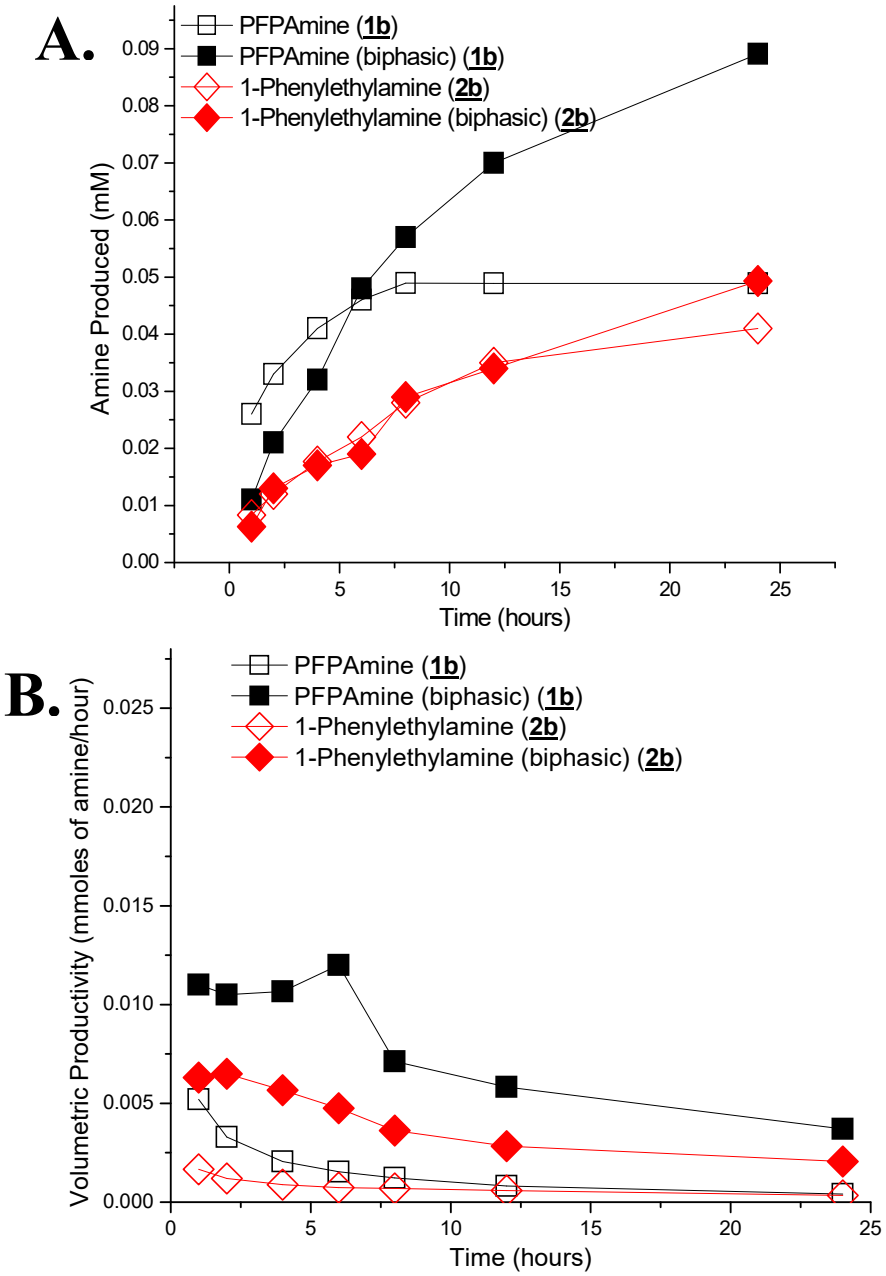

Figure 2.5 Amount of amine product over time for *p*FPA and acetophenone in a biphasic organic solvent reaction system (A). Increased volumetric productivity over time for *p*FPA and acetophenone in a biphasic organic solvent reaction system (B)

Specific activity of the amine dehydrogenase towards its respective substrates was measured over one hour. Comparable specific activity involving the model substrates is achieved between reaction systems with and without the presence of organic solvents (Table 2.4, biphasic versus monophasic). In addition, similar specific activity is observed between time point measurements by the HPLC and the UV-spectrometer. For highly hydrophobic substrates (substrates **3** to **4**), specific activity can only be measured in a biphasic reaction system. The specific activity of cFL1-AmDH with respect to 1-adamantyl methyl ketone is lower because very little of the substrate diffuses into the aqueous phase due to its high hydrophobicity.

Table 2.4 Specific activity ($U \cdot mg^{-1}$), calculated over one hour (N.D.= not determined because of solubility issues)

	1	**2**	**3**	**4**
Biphasic (HPLC)	3.7	0.45	0.035	0.17
Monophasic (HPLC)	4.3	0.55	N.D.	N.D.
Monophasic (UV-spec)	5.5	0.3	N.D.	N.D.

2.3.6 Organic solvents are necessary to achieve conversion

The amount of amine present in the system is shown to increase over time and successful conversion to amine is achieved for all hydrophobic substrates (Figure 2.6). A reaction system that does not include organic solvents cannot be used for highly hydrophobic substrates **3** and **4** because of little to no solubility in aqueous medium. This again emphasizes the importance and necessity of a biphasic organic solvent system for these substrates.

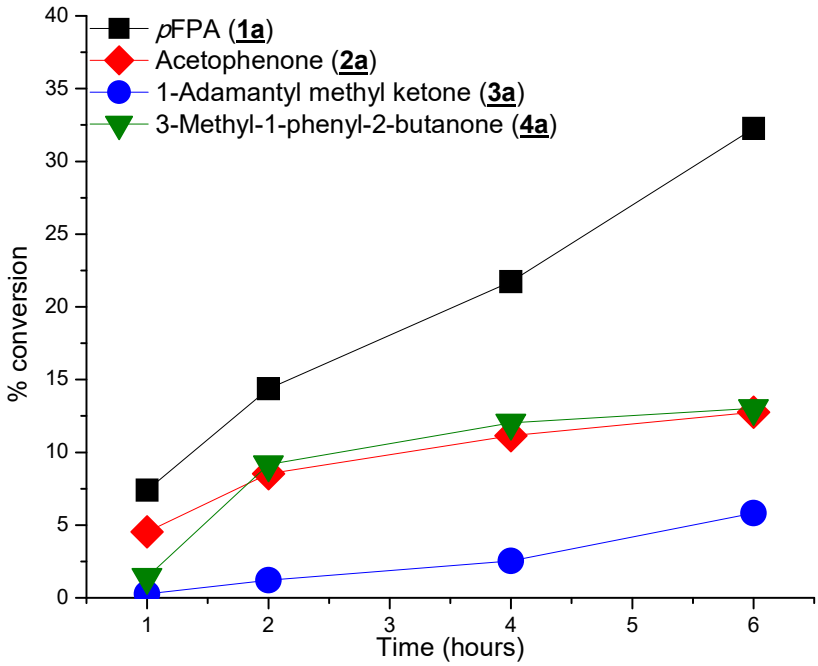

Figure 2.6 Percent conversion over time in a biphasic organic solvent reaction system

2.3.7 Impact on enantioselectivity

Enzymes, such as lipases can have their enantioselectivity controlled by the presence of organic solvents [88, 89]. Biphasic systems had no negative impact on enantioselectivity of the amine dehydrogenases, as compared to monophasic systems without any organic solvents as shown in Figure 2.7. The monophasic system produces the *(R)-p*FPAm with 99.88% *e.e.* The biphasic system produces the *(R)*-amine with 99.67% *e.e.* in the organic layer and with >99.99% *e.e.* in the aqueous layer. With regards to the adamantyl ketone, the biphasic system produces the (*R*)-amine with 98.69% *e.e.* in the aqueous layer.

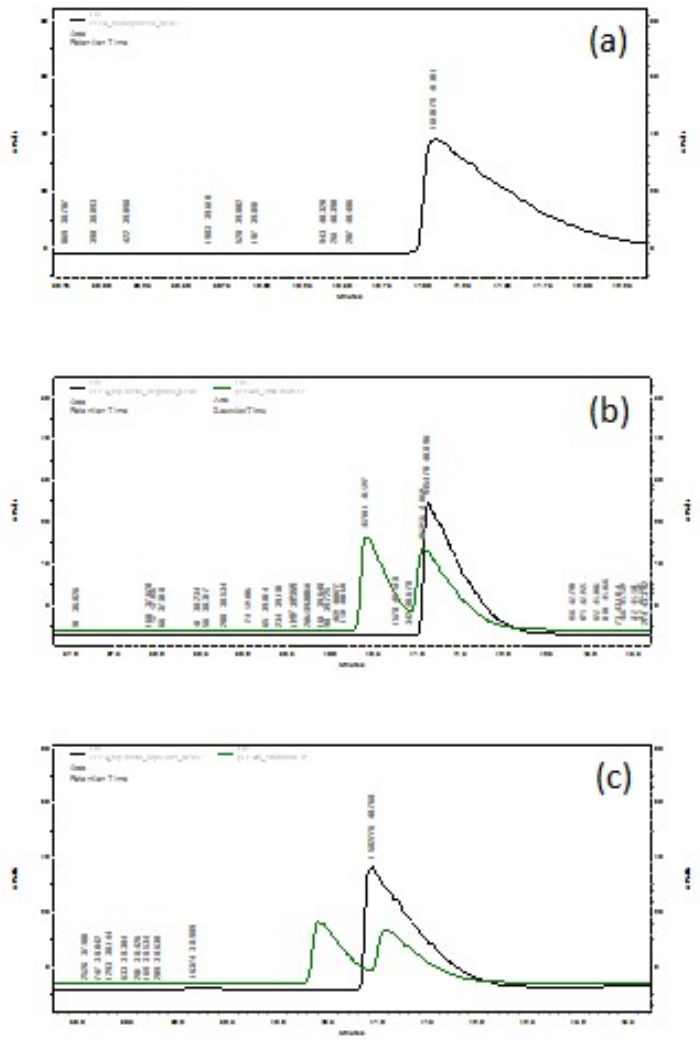

Figure 2.7 Impact of biphasic organic solvent systems on enantioselectivity: monophasic (a), biphasic organic layer (b) and biphasic aqueous layer (c). Chromatograms were obtained by GC.

2.4 Conclusion

The present work demonstrates the development of a biphasic aqueous-organic solvent reaction system for ketone reduction to enantiomerically pure amines catalyzed by the novel amine dehydrogenases and FDH/GDH for regeneration. Owing to deactivation of most dehydrogenases by organic solvents and low solubility of the nicotinamide cofactor, dehydrogenases rarely have been incorporated into water-miscible organic systems. By

developing a biphasic aqueous/water-immiscible organic solvents reaction media for AmDH/ (FDH/GDH), we achieved two goals: i) for moderately water-soluble ketones substrates, we increase overall solubility and volumetric productivity, as enzymatic activity is comparable between aqueous and biphasic media, and ii) for highly hydrophobic ketones with very low water solubility, several of them reagents for APIs, we are able to demonstrate that they are substrates of AmDH. The results of this work can be applied towards further development of a biphasic organic solvent system for additional substrates of amine dehydrogenases.

CHAPTER 3

INVESTIGATION OF THE K_M VALUE OF AMMONIA AND MECHANISTIC INSIGHT OF THE AMINE DEHYDROGENASE THROUGH RATIONAL AND PROTEIN ENGINEERING

3.1 Introduction & Motivation

All amine dehydrogenases were created by the introduction of two mutations within the active site of an amino acid dehydrogenase scaffold (lysine mutated to serine and asparagine mutated to leucine, respectively). The K_M value towards ammonia of F-AmDH significantly increased from the wild-type PheDH. The F-AmDH features a K_M value of 557 mM towards ammonia at its optimum pH of 9.6, while the wild-type PheDH has a K_M value of 37.6 mM. A possible reason for a decreased affinity toward ammonia is due to the methyl group attached to the alpha carbon instead of the carboxyl group [33]. This leads to a loss of the negatively charged group that attracts the partially positively charged ammonia at the basic pH value of 9.6.

A low affinity towards the ammonia substrate requires the AmDH-catalyzed reactions to run at ammonia concentrations greater than 2 M. At these ammonia concentrations, solubility of the ketone substrate decreases and there is an increased chance of chemical side reactions. There is also sign of substrate inhibition caused by the ammonia substrate. In multi-enzyme cascade reactions involving amine dehydrogenases paired with NADH/NAD^+ cofactor regeneration enzymes (formate and glucose dehydrogenase, NADH oxidase), the high concentration of ammonia negatively affects other enzymes. In addition, the high concentration of ammonia leads to higher overall

cost of substrate. From a purely scientific perspective, it is important to understand the cause for this lower affinity for the ammonia substrate. In addition, the work in this chapter will also focus on developing insight into the overall mechanism of the amine dehydrogenases.

3.2 Materials & Methods

3.2.1 Chemicals

Substrates were obtained from suppliers and used without further purification. NADH was obtained from Amresco (Solon, OH) and NAD^+ was obtained from Gold Biotechnology (St. Louis, MO). Ammonium formate, 1-(4-fluorophenyl)-propyl-2-amine and L-phenylalanine were obtained from Alfa Aesar (West Hill, MA). Ammonium chloride was obtained from BDH Chemicals (West Chester, PA). Ammonium hydroxide was obtained from Ricca Chemical Company (Arlington, TX). *p*FPA (4-(fluorophenyl) acetone) was obtained from Matrix Scientific (Columbia, SC) and phenylpyruvic acid was obtained from Sigma Aldrich (St. Louis, MO). Cyclohexanone was obtained from Mallinckrodt Raker (Paris, KY).

3.2.1 Cloning

Mutations are introduced by overlap extension PCR [90, 91] of the *Bacillus badius* F-AmDH gene. The mutated gene is amplified with T7 forward and reverse primers and then restricted overnight with *Nde*I and *Xho*I. The gene is inserted into the pET-28a vector and the vector was transformed into BL21-(DE3) competent cells. Clones were screened for overexpression of protein. The enzyme was grown in LB medium at 30°C

and induced with 0.5 mM IPTG at an OD_{600} value of 0.5 absorbance or grown and expressed in Overnight Express™ EMD Millipore media at 30°C (Billerica, MA). Overexpression was determined by observing a prominent band at 44 kDa on an SDS-PAGE gel. Primers and sequencing results are obtained from MWG operon (Huntsville, AL).

3.2.2 Protein expression and purification

AmDH were purified using the same procedure described in Section 2.2.2.

3.2.3 Enzyme activity assays

All UV-VIS analysis was performed as described in Section 2.2.3. Ammonia buffers were obtained by mixing solutions of ammonium hydroxide and ammonium formate at known concentrations to the desired pH. Unless otherwise stated, all measurements were performed at 25°C at pH 9.6. The ammonium hydroxide concentration was determined by titration with phenolphthalein.

3.2.4 High throughput screening of restricted libraries

Restricted libraries are grown in 96-well plates at 37°C and expressed at 30°C. The clones from the libraries are resuspended in B-PER® to lyse the cells and screened for activity at 340 nm ($NADH/NAD^+$ absorbance change) and 600 nm to account for any changes in the cell mass. The T123/D124/M125 library was screened at 500 mM, 100 mM and 50 mM ammonia concentrations to identify any changes in binding of ammonia substrate (Figure

3.1). The clones exhibiting the best activities were grown in 50 mL express media and purified and tested for activity.

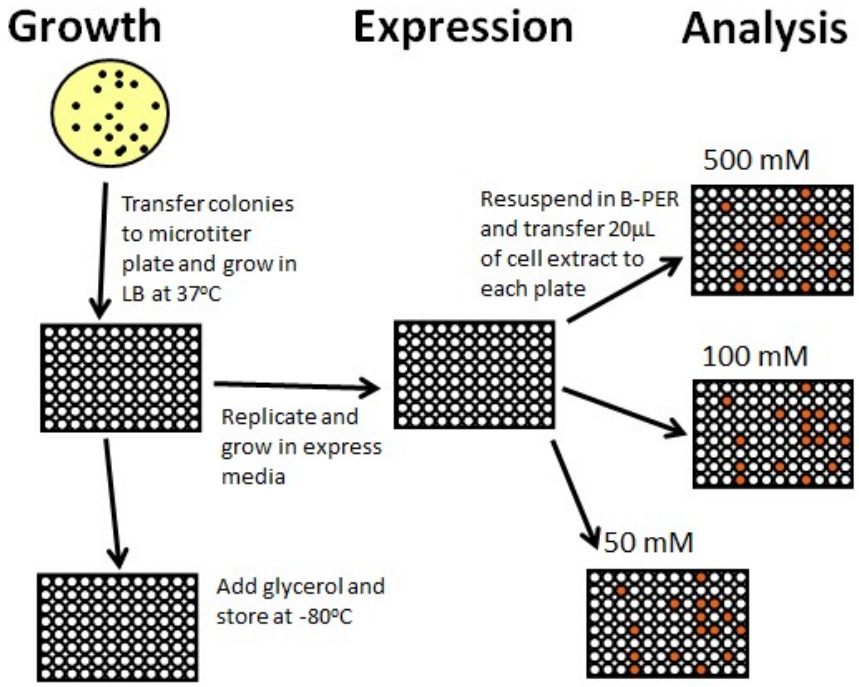

Figure 3.1 High throughput screening of restricted libraries

3.3 Results & Discussion

3.3.1 Investigation of active site residues within the amine dehydrogenase

The kinetic mechanism of the *Rhodococcus* sp. PheDH has been extensively studied through structural analysis of the active site. The *Rhodococcus sp.* and *Bacillus badius* PheDH show a 32% sequence identity and 50% sequence similarity and the crystal structure alignment is shown in Figure 3.2. There are numerous amino acid residues around the active site that exhibit a charged side chain, specifically lysine and aspartate, which possibly affect the ammonia binding through electrostatic interactions. Studies

have revealed a pH dependence of the mechanism because at varying pH values there are changes in the k_{cat} and K_M values with respect to the substrate phenylpyruvate [92]. In addition, protonation of ammonia occurs at a pH values lower than its pKa value of 9.24.

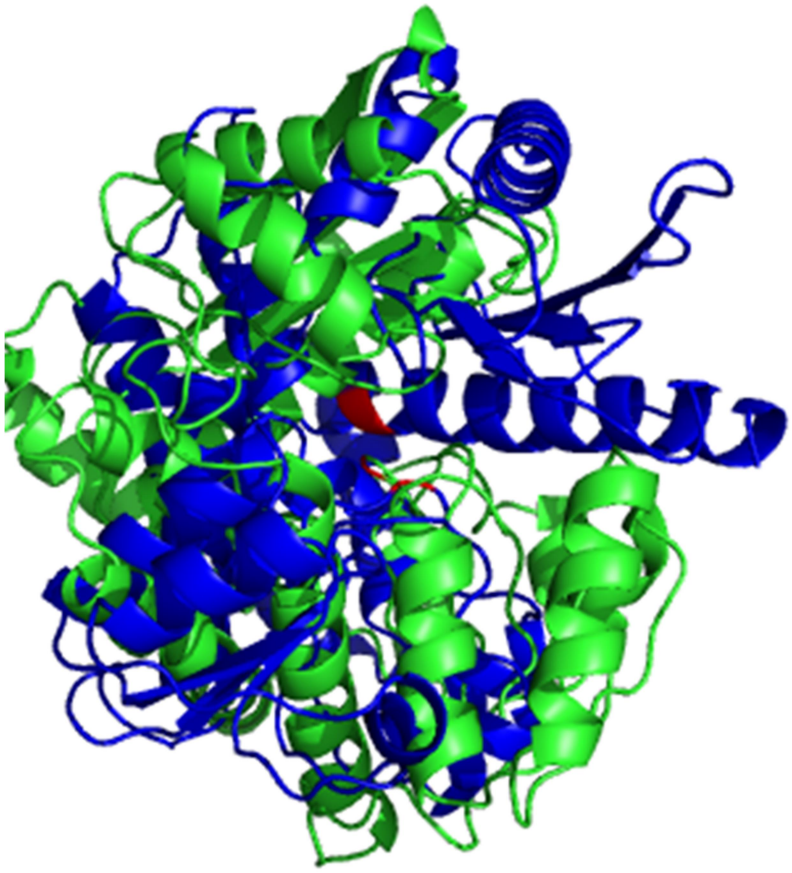

Figure 3.2 Crystal alignment of the *Rhodococcus sp.* PheDH (blue) and homology model of *Bacillus badius* PheDH (green). Catalytic residues K77 and N275L are highlighted in red.

The residue proposed to bind to ammonia in the *Rhodococcus* sp. PheDH is the negatively charged aspartate at position 118. The corresponding amino acid in the *Bacillus badius* PheDH is aspartate 124 and is suspected to have favorable electrostatic and hydrogen bonding interactions with the free ammonium [92, 93] (Figure 3.3). A single mutation was introduced at that position to introduce another negatively charged residue glutamate to check if activity could be retained. However, this mutation

decreased the activity of enzyme by 100-fold and did not change the K_M value of ammonia. Glutamate is a larger residue and could have posed steric constraints on the binding pocket [data not shown]. Therefore, it is hypothesized that aspartate 124 is not directly responsible for the binding of ammonia.

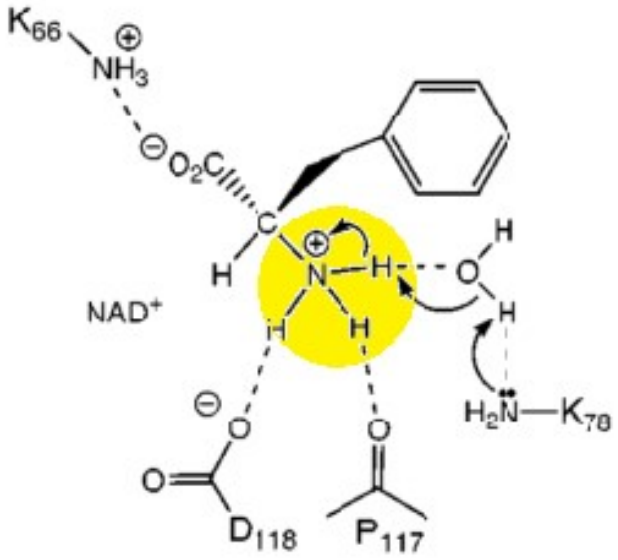

Figure 3.3 Proposed binding mechanism of ammonia in *Rhodococcus sp.* PheDH [92]

A restricted library was performed simultaneously at T123/D124/M125 on the F-AmDH. The following codons were implemented to allow for efficient screening: T123MVT, D124VAW and M125ADK. 768 colonies were expressed and screened for activity at 500 mM, 100 mM and 50 mM concentrations of ammonia to see if any mutations would have an impact on the binding of ammonia. 20 clones exhibiting the best activities were purified but no improvement in activity or binding of ammonia was observed. None of the clones contained any mutations at the D124 and M125 residue and only glycine and asparagine mutations were found in the T123 residue. All additional site-specific mutations performed on the active site of the F-AmDH are located in Appendix B.

3.3.2 Incorporation of lysine into active site to improve electrostatic interactions

As previously mentioned, the amine dehydrogenase (AmDH) exhibits roughly a 20 times fold decrease in binding for the ammonia substrate as compared to the amino acid dehydrogenase (aaDH). The two main differences between the AmDH and aaDH are 1) loss of the positive charge with the lysine to serine mutation (on residue 77) and 2) loss of the carboxylic group (negatively charged group) in the substrate. It was hypothesized that another positively charged lysine residue plays a role in the binding of ammonia and further investigation is performed on lysine residue 89. The lysine 66 and 78 residues of the *Rhodococcus sp.* PheDH (as shown in Figure 3.4) align with lysine 77 and 89 of the *Bacillus badius* PheDH.

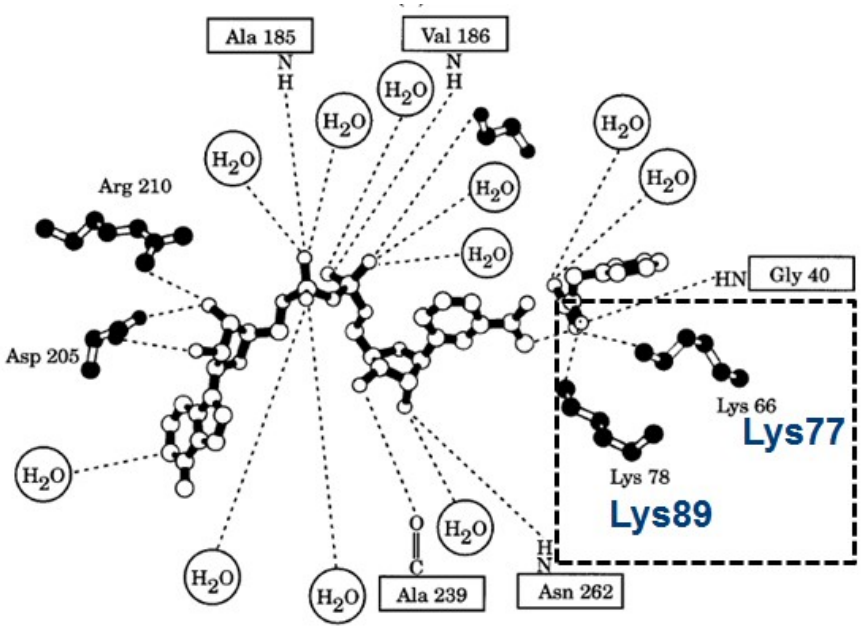

Figure 3.4 Amino acids within active site of the *Rhodococcus sp.* PheDH [93]

The K89S mutation was introduced into the *Bacillus badius* phenylalanine dehydrogenase. As shown in Table 3.1, the activity was dramatically decreased over a 1000 times fold (25 compared to 0.017 U/mg). However, when that same mutation is

introduced into the F-AmDH, the activity decreased just over 1.5 times (5.5 compared to 3 U/mg). This indicates a possible difference in the mechanism between the two enzymes, since the introduction of the K89S mutation shows very different results with regards to catalytic activity for both enzymes. Furthermore, the K89S mutations drastically decreased the binding of ammonia of the F-AmDH (K_M > 1.5 M). It was hypothesized that this lysine residue was not necessarily important for catalytic activity but instead critical for the binding of ammonia. It was further hypothesized that additional lysine residues within the active site would improve electrostatic interactions and increase the F-AmDH binding toward its ammonia substrate.

Table 3.1 K89S variants on the *B. badius* F-AmDH and the PheDH

	***p*FPA (U/mg)**	**L-Phe (U/mg)**
PheDH	Not active	25
K89S	Not active	0.017
N275L	0.13	0.023
K89S/N275L	0.024	0.0006
K89S/K77S	0.065	Not active
K89S/K77S/N275L	3	Not active
F-AmDH (K77S/N275L)	5.5	Not active

As shown in Table 3.2, lysine residues were individually incorporated into the active site to replace twelve amino acid residues and the affinity for ammonia and catalytic activity was measured. Not only did the lysine residues not improve the binding toward the ammonia substrate, the introduction often made it worse. In addition, lysine at residue 77 was introduced back into the F-AmDH (K77K/N275L) and the binding toward ammonia did not improve. Furthermore, when lysine was introduced at residue 275 (K77S/N275K), the binding toward ammonia dramatically decreases (K_M > 1.5 M) (Figure 3.5). This data, along with the variants listed in Table 3.2, leads to the conclusion

that the introduction of additional lysine into the active site of the F-AmDH does not help the binding to the ammonia substrate.

Table 3.2 Lysine mutations within the active site of the *B. badius* F-AmDH. All activity was measured in 5 M $NH_4OH/CHOO^-$ buffer at 25°C.

Mutation	Effect on K_M value of ammonia	Effect on specific activity
G50K	Did not express	N/A
G51K	Not active	N/A
R53K	Worsen (>1.5 M)	No change
Y76K	No change	No change
D82K	No change	1/4 less active
G88K	Did not express	N/A
G122K	Not active	N/A
T123K	Worsen (>1.5 M)	1/4 less active
D124K	Not active	N/A
D131K	Worsen (>1.5 M)	2/3 less active
S155K	Not active	N/A
N276K	Worsen (>1.5 M)	2/3 less active

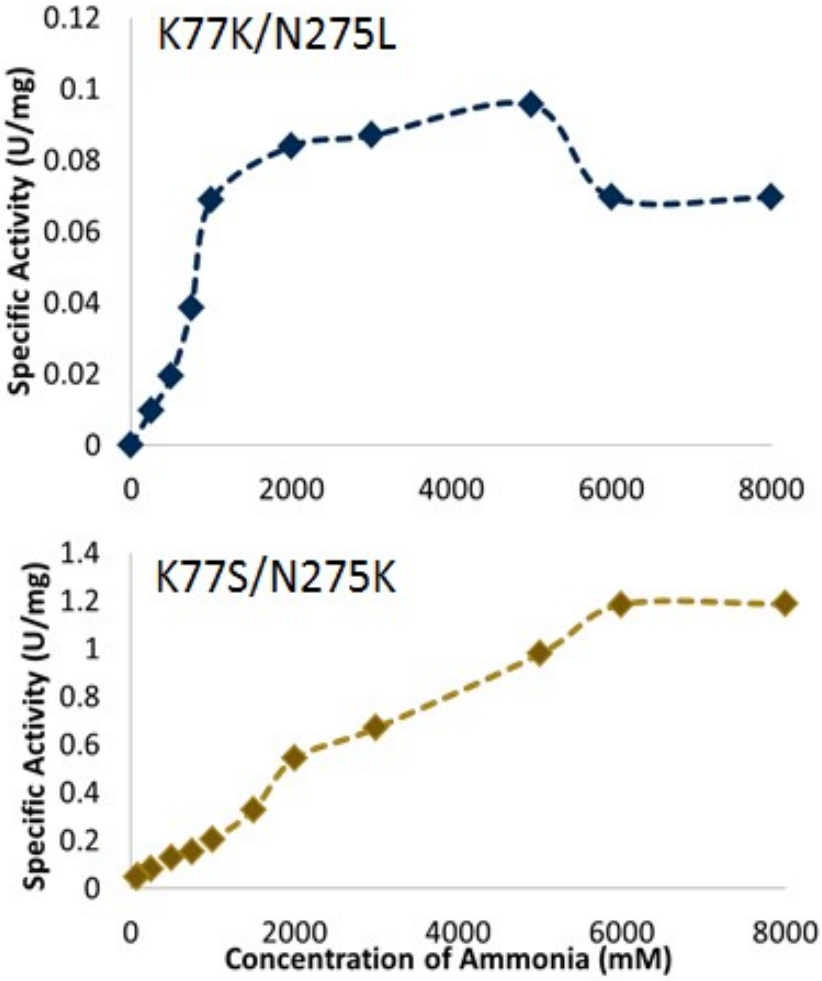

Figure 3.5 Mutation of lysine back into the active site of the F-AmDH

3.3.3 Equilibrium constant of the F-AmDH

An estimate of the equilibrium constant of the F-AmDH was determined to gain further insight on the reaction mechanism. The reaction of the F-AmDH is reversible, as shown in Figure 1.4 and Figure 1.5. The equilibrium constant represents the ratio of the concentration of the reactants to products at equilibrium and is described by Equation 3.1. The true equilibrium constant must also take into account the proton released during the reaction (to be determined by the final pH).

$$K_{eq}' = \frac{[NADH][4-\text{flurophenylacetone}][NH_4^+]}{[NAD^+][1-(4-\text{fluorophenyl})\text{propyl}-2-\text{amine}]} \qquad \text{[Equation 3.1]}$$

Brunhuber et al. determined the K_{eq} of the *Rhodococcus sp.* phenylalanine dehydrogenase by monitoring the amount of NADH that is present once equilibrium is reached and then determining the concentration of each substrate [92]. Once the NADH concentration does not change, the forward and reverse reactions are moving at the same rate. It is important that in the reaction conditions, all substrates are in equimolar quantities as to not drive the reaction past equilibrium (La Chatelier's principle). Due to the high K_M value of ammonia, at least 50 mM of ammonia must be added to the reaction to observe catalytic activity. In addition, ammonia had to be added in the oxidative deamination direction because the amount of ammonia released from *p*FPAm is not enough to drive the reaction. 200 µM NADH, 200 µM *p*FPA and 50 mM ammonia were added for the reaction in the forward direction; 200 µM NAD^+, 400 µM *p*FPAm (because of racemic mixture) and 50 mM ammonia were added in the reverse direction. The change in absorbance on the UV-VIS is shown in Figure 3.6 (red/green lines represents reductive amination direction and blue/purple lines represents oxidative deamination direction).

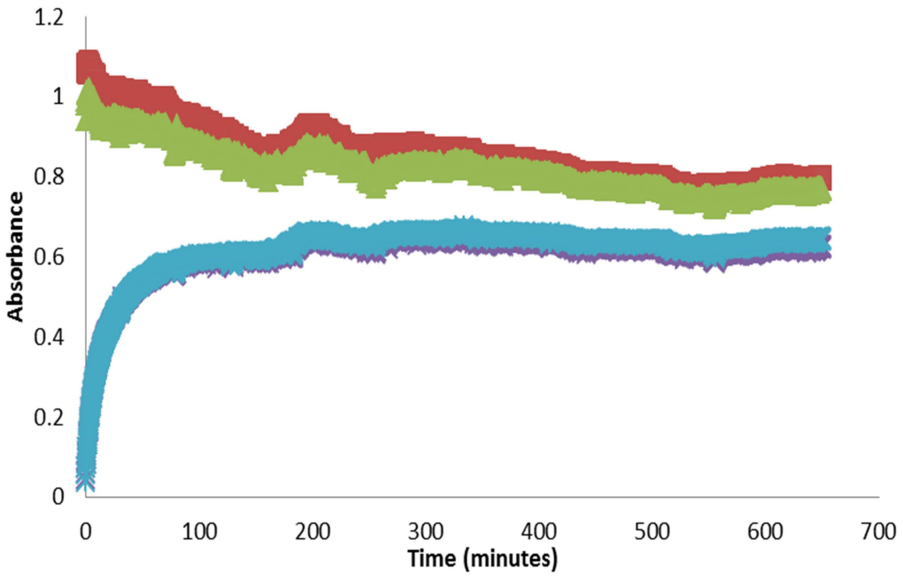

Figure 3.6 Equilibrium constant determination of the F-AmDH. Reductive amination activity was performed in 5 M $NH_4OH/CHOO^-$ buffer pH 9.6 and oxidative deamination activity performed in 0.1 M glycine pH 10.4 at 25°C.

The K_{eq} in the reductive amination direction was calculated to be 3.89 x 10^{-9} M^2. The K_{eq} in the oxidative deamination direction was calculated to be 1.52 x 10^{-9} M^2. The differences in the equilibrium constants are probably due to the fact that ammonia had to be added in the oxidative deamination direction to obtain any catalytic activity. For the *Rhodococcus sp.* phenylalanine dehydrogenase, the K_{eq} was 4.5 x 10^{-14} M^2, which is typical of other amino acid dehydrogenases [92, 94]. The difference in the equilibrium constants between the AmDH and aaDH is due to the high amount of ammonia that must be present in order for reaction to occur. In both cases, the equilibrium constant value is determined to be less than one and the amine/ amino acid synthesis is favored thermodynamically.

3.3.4 Hammett correlation

The substrate profile of an enzyme can help to determine the mechanism of any enzyme. The transaminase has a dual substrate recognition active site that impacts its substrate range and mechanism [19, 20, 95]. The Hammett correlation on various substituents on the phenyl ring of acetophenone was investigated for the chimeric amine dehydrogenase (Table 3.3). The data was fit to each substrate's sigma, hydrophobic and steric parameters. There was no correlation for these substrates, as shown in Figure 3.7.

Table 3.3 Impact on activity with various substituents on phenyl ring of acetophenone

Substrate	**Vmax (U/mg)**	**$K_{M\text{-}ketone}$ (mM)**
Acetophenone	0.4	1.93
4-methoxy	0.016	14.2
4-chloro	0.31	6.88
4-nitro	Not active	N/A
4-acetobenzylnitrile	0.036	12.16
4-methyl	0.21	7.62
4-amino	0.079	N/A
4-dimethyl amino	Not soluble	N/A
4-methyl sulphonyl	Not active	N/A

Activity was performed in 5 M $NH_4OH/CHOO^-$ buffer pH 9.6 at 30°C

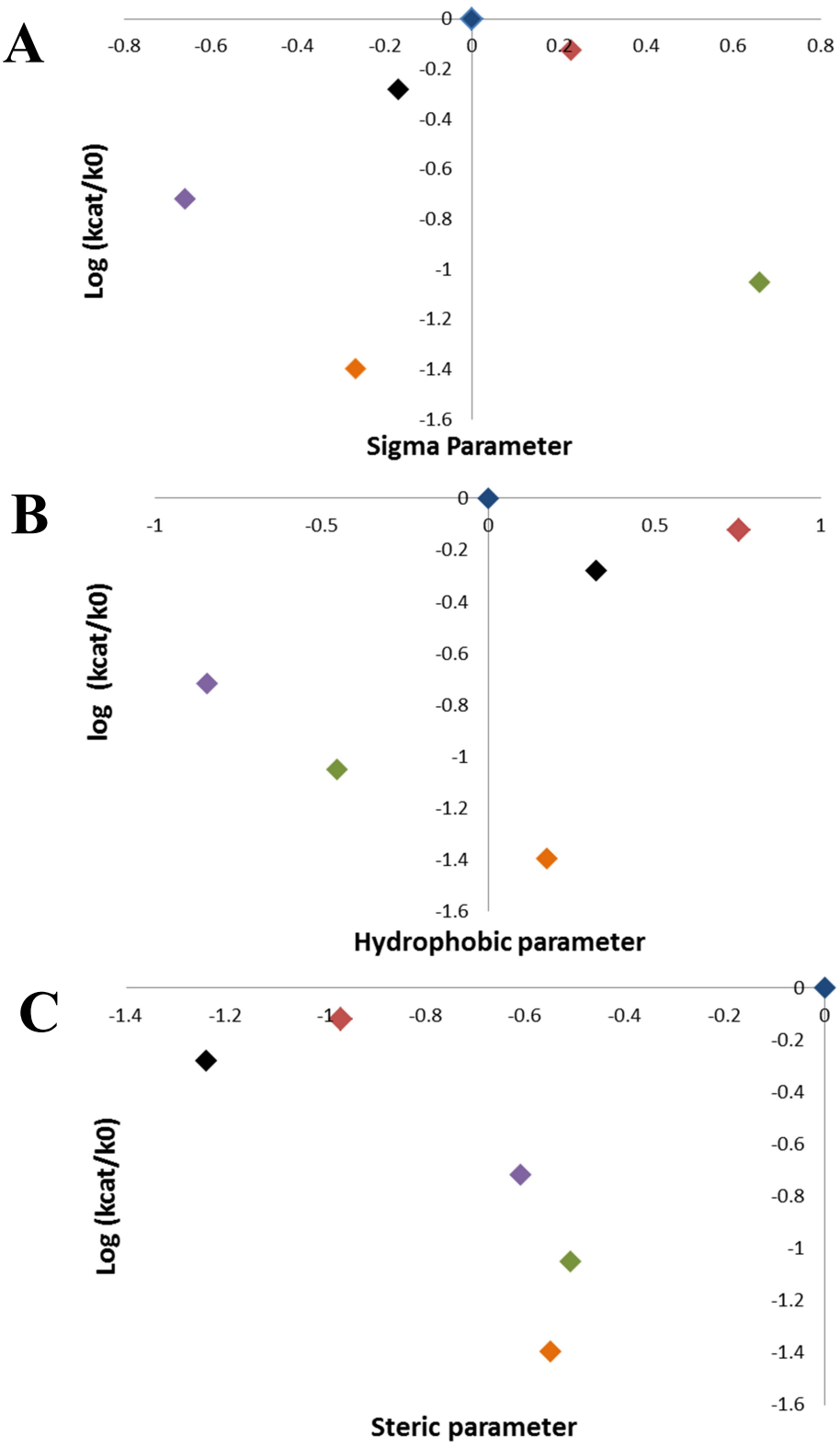

Figure 3.7 Hammett correlation of the cFL1-AmDH with respect to (A) sigma, (B) hydrophobic and (C) steric parameters. Acetophenone (dark blue), 4-methoxy (orange), 4-chloro (red), 4-acetylbenzylnitrile (green), 4-methyl (black) and 4-amino (purple).

3.3.5 Mechanistic insight of the amine dehydrogenases

In the reductive amination direction, the amine dehydrogenase reaction represents a terreactant mechanism with three substrates- NADH, *p*FPA and ammonia. The initial velocity is collected at various concentrations of the three substrates (A and B but at a fixed concentration of C; at various concentration of A and C but a fixed concentration of B; and at various concentrations of B and C but at a fixed concentration of A) as shown in Figure 3.8 through 3.10. Measurements are performed around the K_M value and as close to saturation as possible with respect to each substrate. The data was fit to the Michaelis-Menten equation using non-linear regression analysis through KaleidaGraph (done with help by Dr. John M. Robbins).

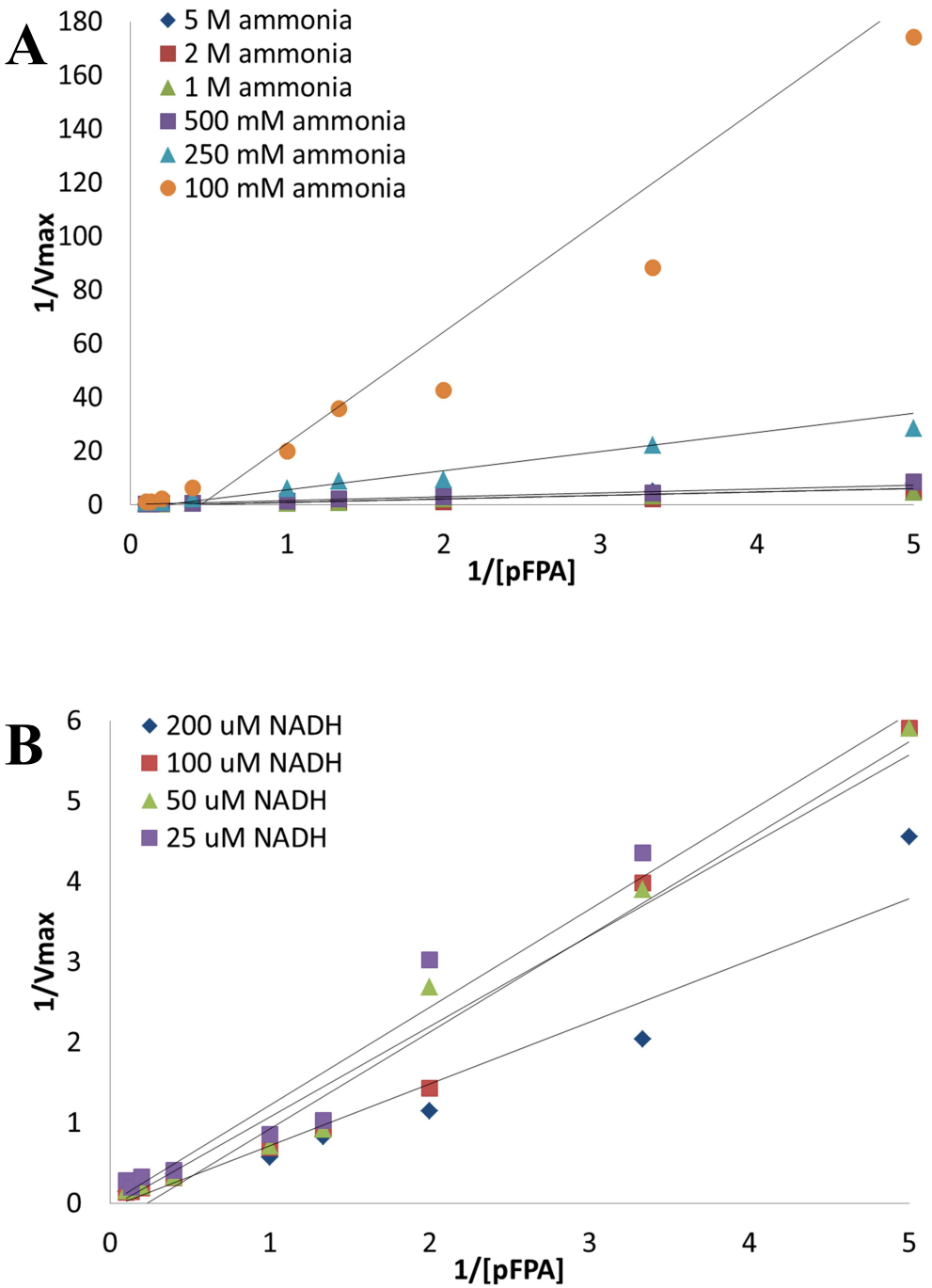

Figure 3.8 Lineweaver-Burk plots of concentration of *p*FPA versus velocity at (A) various fixed concentrations of ammonia: 5 M (dark blue), 2 M (red), 1M (green), 500 mM (purple), 250 mM (light blue), 100 mM (orange) at 200 µM NADH concentration and (B) various fixed concentrations of NADH: 200 µM (dark blue), 100 µM (red), 50 µM (green) and 25 µM (purple) at 2 M ammonia concentration. Converging lines indicate sequential mechanism. Data was fit to Equation 3.3 and best fit parameters are listed in Table 3.4.

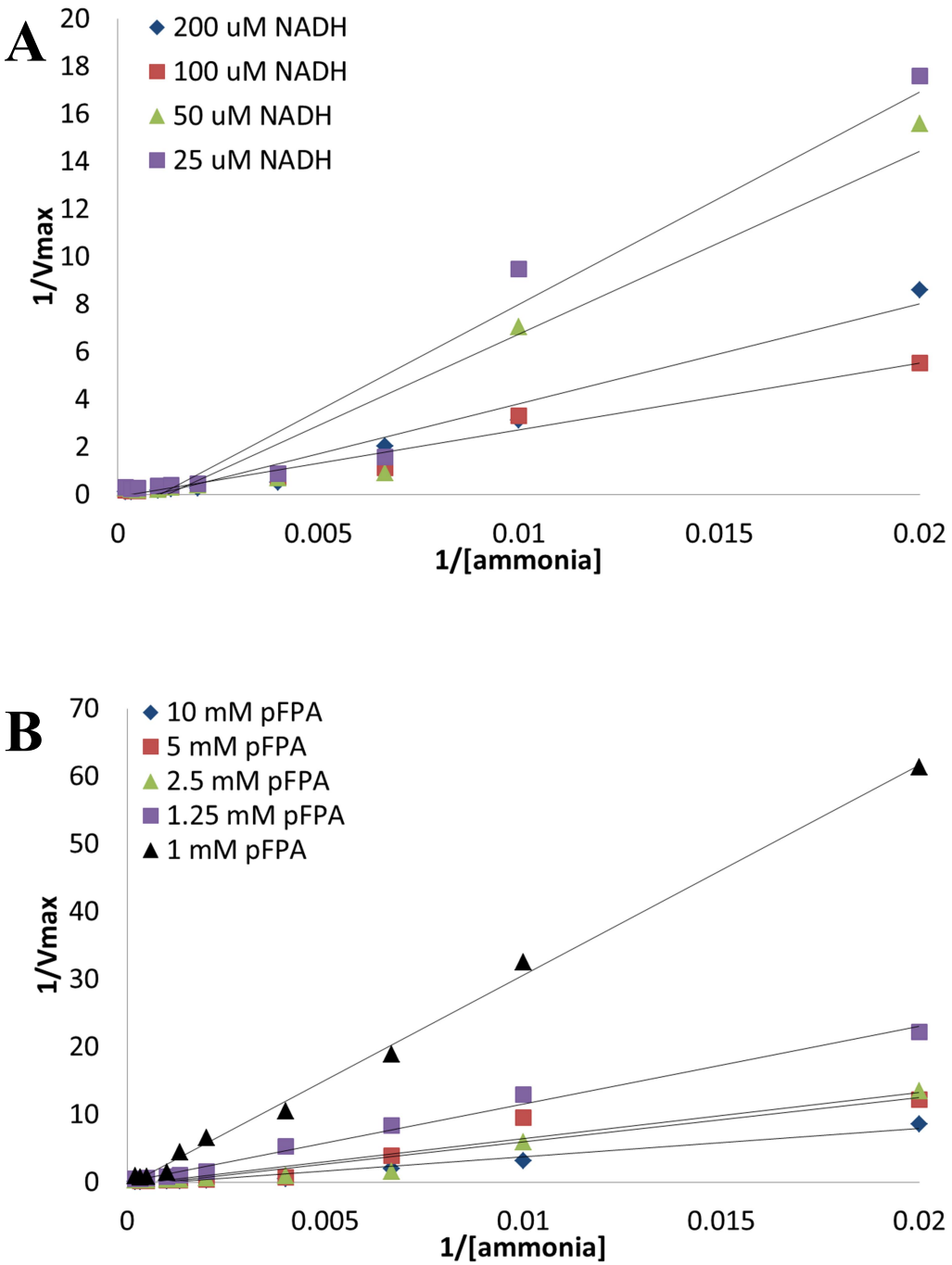

Figure 3.9 Lineweaver-Burk plots of concentration of ammonia versus velocity at (A) various fixed concentrations of NADH: 200 µM (dark blue), 100 µM (red), 50 µM (green), 25 µM (purple) at 10 mM *p*FPA concentration and (B) various fixed concentrations of *p*FPA: 10 mM (dark blue), 5 mM (red), 2.5 mM (green), 1.25 mM (purple) and 1 mM (black) at 200 µM NADH concentration. Converging lines indicate sequential mechanism. Data was fit to Equation 3.3 and best fit parameters are listed in Table 3.4.

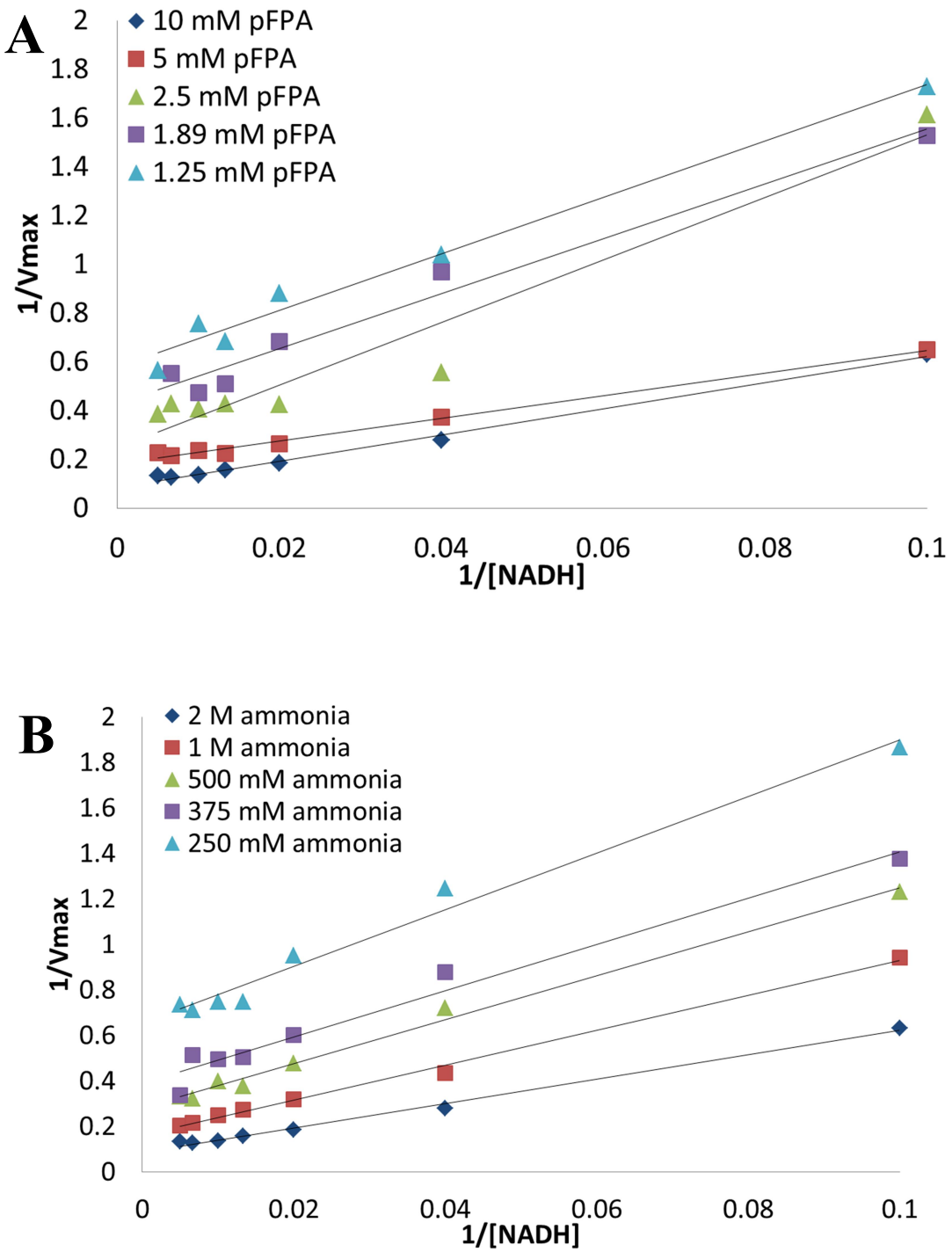

Figure 3.10 Lineweaver-Burk plots of concentration of NADH versus velocity at (A) various fixed concentrations of *p*FPA: 10 mM (dark blue), 5 mM (red), 2.5 mM (green) and 1.89 mM (purple) and 1.25 mM (light blue) at 200 µM NADH concentration and (B) various fixed concentrations of ammonia: 2 M (dark blue), 1 M (red), 500 mM (green), 375 mM (purple) and 250 mM (light blue) at 10 mM *p*FPA concentration. Parallel lines indicate ping pong mechanism. Data was fit to Equation 3.3 and best fit parameters are listed in Table 3.4.

With the exception of the Lineweaver-Burk plots employing varying concentrations of NADH at different fixed concentrations of ammonia and *p*FPA (Figure 3.10), all double reciprocal plots of velocity versus substrate concentration demonstrate a converging pattern indicative of a sequential mechanism. This is similar to results obtained in literature for the wild-type *B. badius* PheDH [96]. Parallel lines are indicative of a ping pong component to the mechanism. A terreactant reaction mechanism is described by Equation 3.2 [97-99] (substrate A= NADH, B=*p*FPA, C=ammonia). 'V' represents the maximum velocity and K_A, K_B and K_C are Michaelis-Menten constants observed when all other substrates are at saturation. The equation is fitted to the data in the reductive amination direction with F-AmDH and *p*FPA (fitting performed by Robert D. Franklin in Mathematica).

$$v = \frac{\mathrm{V}\mathbf{ABC}}{\mathrm{const} + (\mathrm{coefA})\mathbf{A} + (\mathrm{coefB})\mathbf{B} + (\mathrm{coefC})\mathbf{C} + \mathrm{K_A}\mathbf{BC} + \mathrm{K_B}\mathbf{AC} + \mathrm{K_C}\mathbf{AB} + \mathbf{ABC}} \qquad \text{[Equation 3.2]}$$

The best fit of the data presented in Figure 3.8 through Figure 3.10 to Equation 3.2 show the coefficients terms of the *p*FPA (B) and ammonia (C) are not statistically different from zero and are therefore determined to be missing, leading to the data to be fit to Equation 3.3 instead. The values of the respective parameters from this best fit are listed in Table 3.4. This suggests a sequential mechanism with steady-state addition of NADH first to the enzyme followed by a random addition of *p*FPA and ammonia. This mechanism is similar to a citrate cleavage enzyme [100]. The theoretical Vmax value of 37.86 U/mg is never reached because the enzyme becomes inhibited before it can reach saturation (especially with respect to the ammonia substrate) and the ketone becomes insoluble before it can reach full saturation. Saturation of ammonia and *p*FPA cannot be

achieved under experimental conditions. As a result, the K_M value listed is higher than the apparent K_M value measured because this equation is fitted with respect to all three substrates and therefore is more accurate by taking into account any substrate or product inhibition.

$$v = \frac{\mathrm{V}\mathbf{ABC}}{\mathrm{const} + (\mathrm{coefA})\mathbf{A} + \mathrm{K_A}\mathbf{BC} + \mathrm{K_B}\mathbf{AC} + \mathrm{K_C}\mathbf{AB} + \mathbf{ABC}} \qquad \text{[Equation 3.3]}$$

Table 3.4 Coefficients of the F-AmDH/*p*FPA reductive amination reaction (R^2= 0.9597). A=NADH, B=*p*FPA, C=ammonia

Coefficients	Value
V (U/mg)	37.86 ± 8.89
const	470.6 ± 124.18
coefA	14913 ±3372.98
K_A(mM)	0.114 ± 0.032
K_B (mM)	22.35 ± 6.56
K_C (mM)	1798 ±675.18

The same experiments were performed in the oxidative deamination direction as shown in Figure 3.11. In the oxidative deamination direction, the amine dehydrogenase reaction represents a bireactant mechanism with two substrates- NAD^+ (A) and *p*FPAm (B). The data was fit to Equation 3.4, indicating a sequential reaction (fitting performed by Robert D. Franklin in Mathematica). It cannot be concluded if the binding is ordered or random until inhibition studies have been completed. The values are listed in Table 3.5.

$$\mathrm{v} = \frac{\mathrm{V}\mathbf{AB}}{\mathrm{K_{IA}K_B} + \mathrm{K_B}\mathbf{A} + \mathrm{K_A}\mathbf{B} + \mathbf{AB}} \qquad \text{[Equation 3.4]}$$

Table 3.5 Coefficients of the F-AmDH/*p*FPAm oxidative deamination reaction (R^2=0.9899)

Coefficients	Value
V (U/mg)	0.827 ± 0.029
K_{IA} (mM)	0.036 ± 0.015
K_A (mM)	0.395 ± 0.0037
K_B (mM)	0.279 ± 0.045

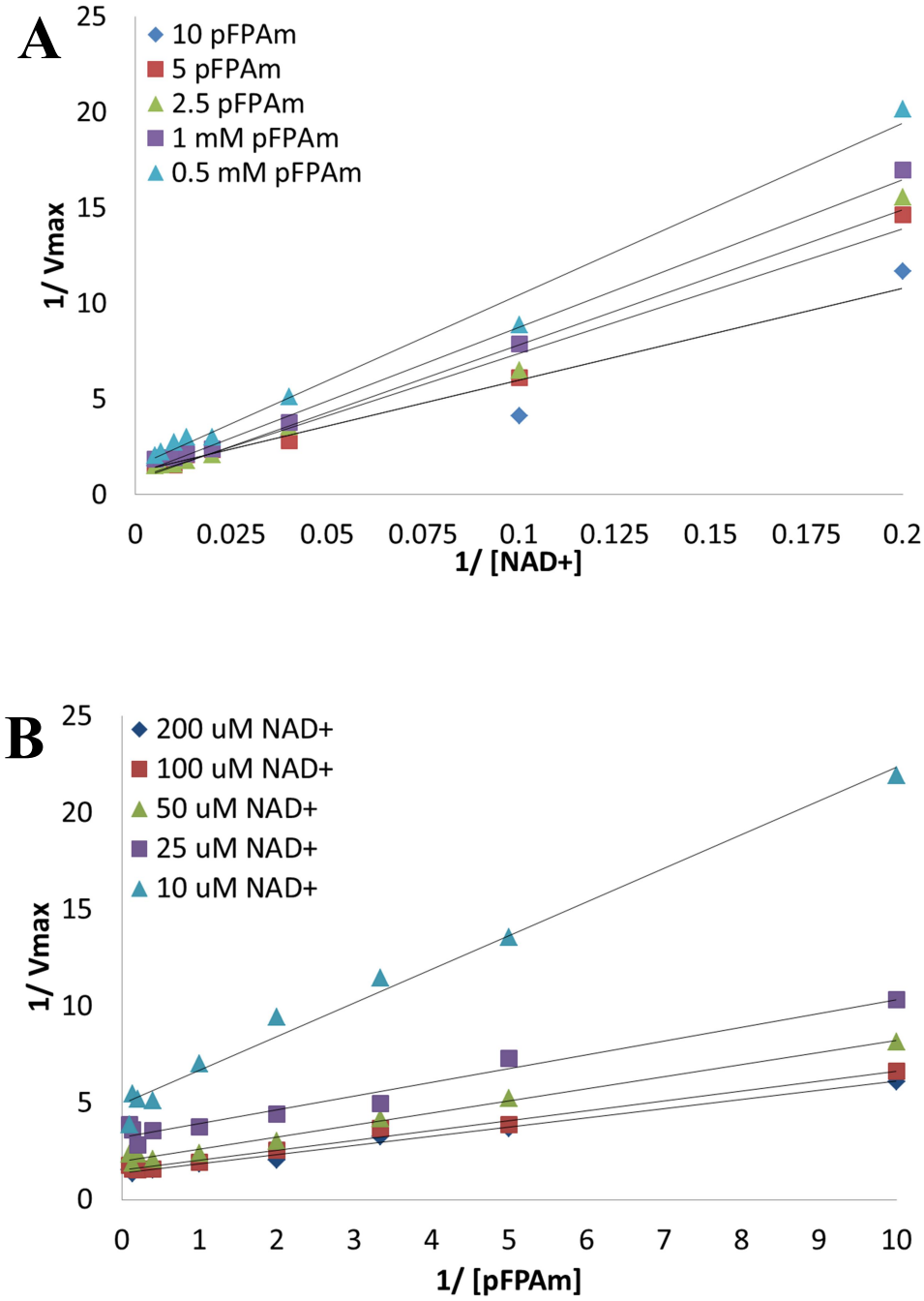

Figure 3.11 Lineweaver-Burk plots of (A) various concentrations of NAD^+ versus velocity at various fixed concentrations of *p*FPAm: 10 mM (dark blue), 5 mM (red), 2.5 mM (green), 1 mM (purple) 0.5 mM (light blue) and (B) various concentrations of *p*FPAm versus velocity at various fixed concentrations of NAD^+: 200 µM (dark blue), 100 µM (red), 50 µM (green), 25 µM (purple), 10 µM (light blue). Data was fit to Equation 3.4 and best fit parameters are listed in Table 3.5.

3.3.6 Chemical reaction of substrates in the presence of ammonia

There is a drastic difference in the binding of ammonia in the amine dehydrogenase reaction compared to the amino acid dehydrogenase reaction. It is hypothesized that the difference may be attributed not to any changes to the enzyme but rather to the substrate itself (ketone versus keto acid). When acetophenone (substrate of the chimeric amine dehydrogenase reaction) is placed in the presence of high concentration of ammonia (up to 5 M), no chemical interaction that leads to a new intermediate is observed through carbon NMR. There is no presence of a tetrahedral intermediate or imine formation and the spectrums are nearly identical (Figure 3.12).

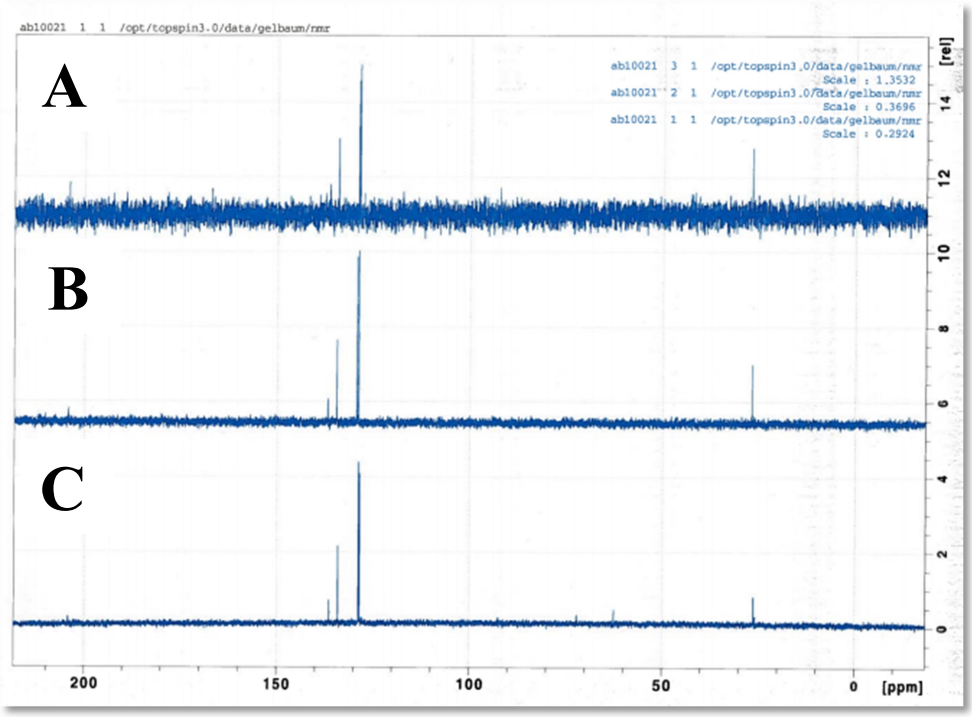

Figure 3.12 Acetophenone in the presence of 5 M ammonia pH 9.0 (A), 5 M ammonia pH 11.0 (B) and water (C).

Next, phenyl pyruvic acid was placed in 100 mM ammonia buffer. Shifts in the carbon NMR spectrum are detected and the presence of a tetrahedral intermediate and imine are hypothesized to form (Figure 3.13). Additional peaks are observed at 45, 100, 170 and

205 ppm in the ammonia buffer (assignments of the peaks are difficult because no experimental spectrum of the isolated imine or tetrahedral intermediate have been reported). It is hypothesized that the presence of more electron withdrawing groups attached to the methyl group would allow for the formation of an imine or tetrahedral intermediate (Figure 3.14). The enzyme can then convert the imine intermediate into an amine. 2-chloro-acetophenone was tested for activity as an example of a more electron withdrawing group on the methyl but cFL1-AmDH does not show any activity (although no activity could also be attributed to a chemical reaction of 2-chloro-acetophenone in the presence of high ammonia concentrations).

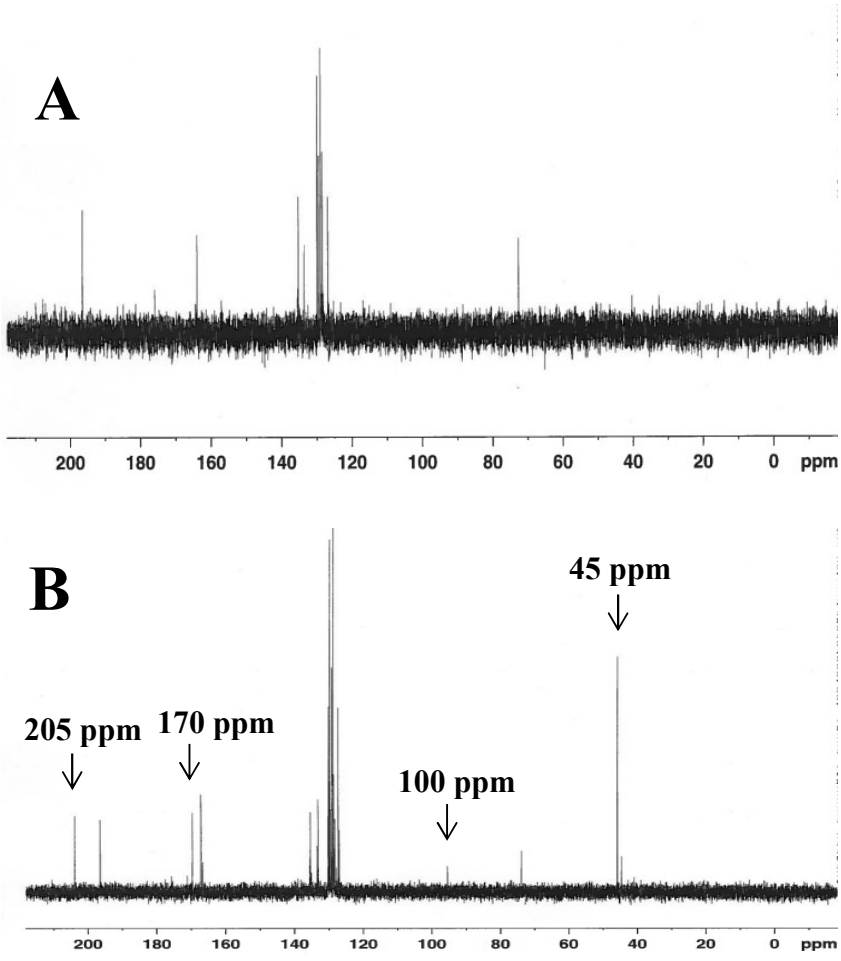

Figure 3.13 Phenyl pyruvic acid in the presence of water (A) and 100 mM ammonia pH 9.6 (B)

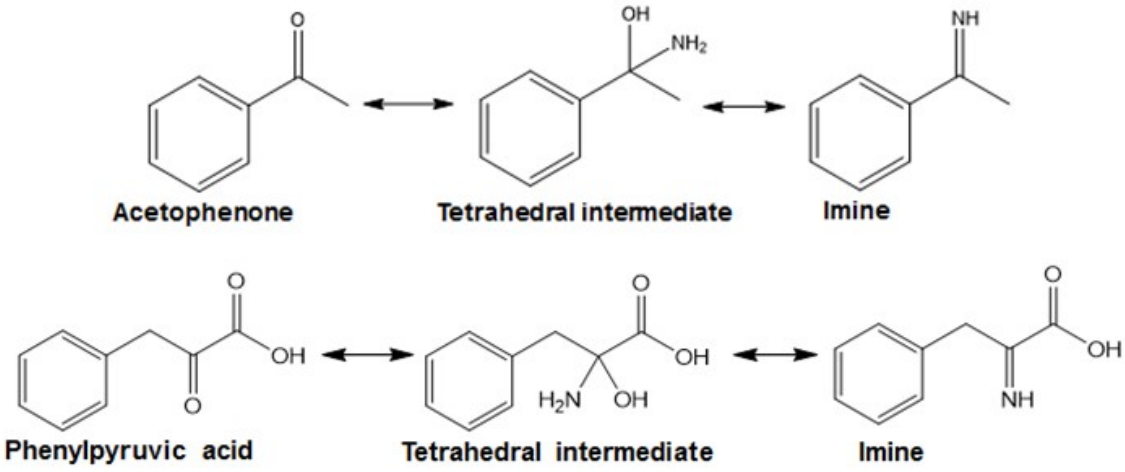

Figure 3.14 Hypothesized formation of tetrahedral intermediate and imine

3.3.7 pH dependence profiles of the amine dehydrogenases

The affinity towards ammonia was measured in various buffer conditions. Different ammonia buffers (formate, chloride, acetate, bicarbonate, data located in Figure C.1) and various substituents on the phenyl ring of the ketone (Figure C.2) influenced the specific activity but did not change the affinity toward the ammonia substrate. However, different K_M values towards ammonia were observed at various pH values (Table C.3) and further investigation was needed.

The enzymatic activity of the F-AmDH towards *p*FPA was measured at various pHs and the data was fitted to the double ionization model [101] (Equation 3.5) using KaleidaGraph (version 3.5.2). The pKa of the reaction is obtained from fitting this equation. 'y' is k_{cat} or k_{cat}/K_M, 'C' is the pH-independent value of y, which in this case is the maximum value of k_{cat} or k_{cat}/K_M, H is $[H^+]$ and K_1 and K_2 represent the dissociation constant and are directly related to the pKa values.

$$\log y = \log\left[C/\left(1 + \frac{H}{K_1} + \frac{K_2}{H}\right)\right] \qquad \text{[Equation 3.5]}$$

The k_{cat} (orange curve) and k_{cat}/K_M (red curve) are shown in Figure 3.15. The same curve trend is observed, which indicates the same ionizable group contributes to both catalysis and the binding of ammonia. This result indicates that to improve the binding of ammonia (to either the active site or the ketone) surrounding residues (not the catalytic residue) need to be mutated to maintain the desired protonation state. An identical trend was observed with another ketone substrate of the F-AmDH with lower specific activity, cyclohexanone (Figure 3.16). Table 3.6 lists the pKa1 value of around 7.5 and the pKa2 value of around 11. A cysteine or histidine residue is suspected to be responsible for pKa1 and a lysine residue is responsible for pKa2. The lysine residue is suspected to be the lysine at position 77 for the F-AmDH. In addition, the same experiment was performed with the wild-type *Bacillus badius* phenylalanine dehydrogenase and fit to a double ionization model (Figure 3.17). Interestingly, a higher pKa1 value of 8.82 is observed compared to the F-AmDH (Table 3.6). This difference could be indicative of an overall difference in the active site environment between the wild-type PheDH and F-AmDH.

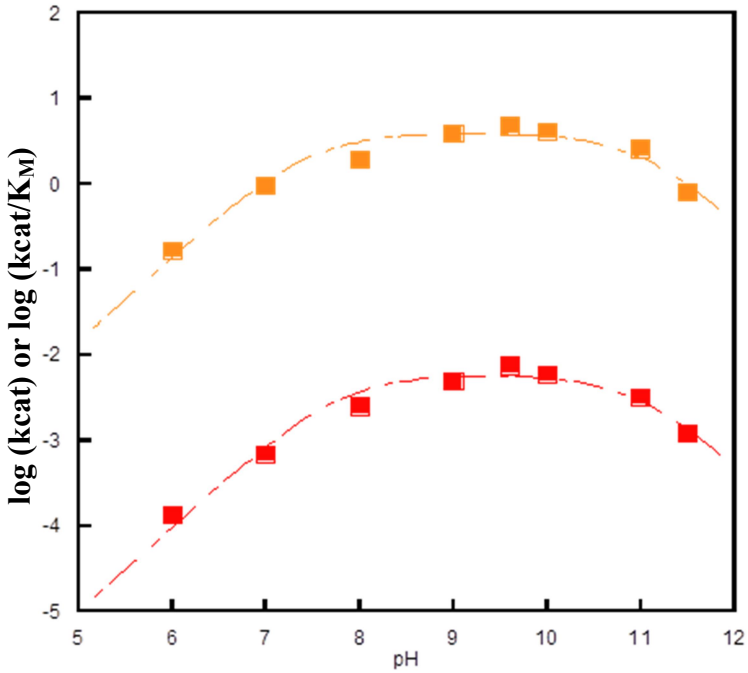

Figure 3.15 Double ionization models to describe pH dependence of F-AmDH/ *p*FPA, k_{cat} (orange curve), k_{cat}/K_M (red curve). Activity was measured in $NH_4OH/CHOO^-$ buffer at 25°C.

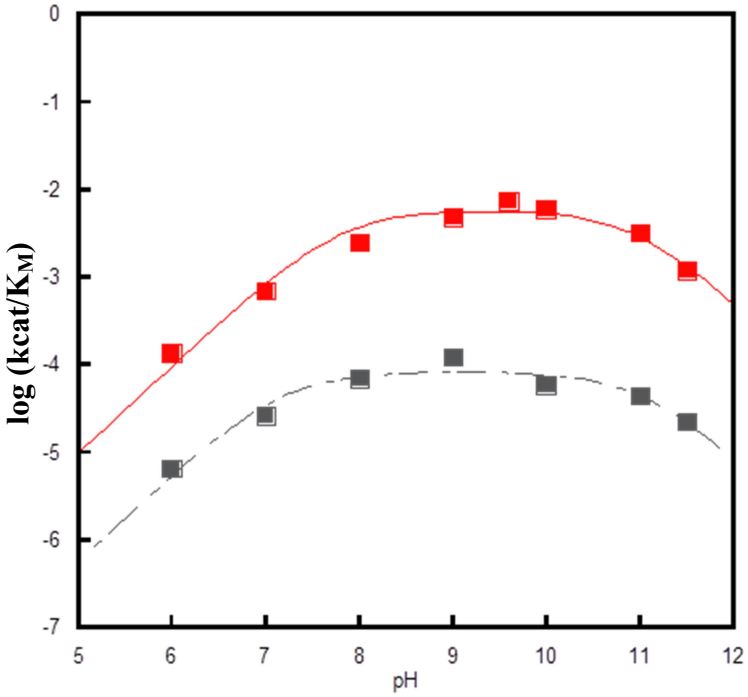

Figure 3.16 Double ionization models to describe pH dependence of F-AmDH/ *p*FPA (red curve) versus F-AmDH/ cyclohexanone (grey curve). Activity was measured in $NH_4OH/CHOO^-$ buffer at 25°C.

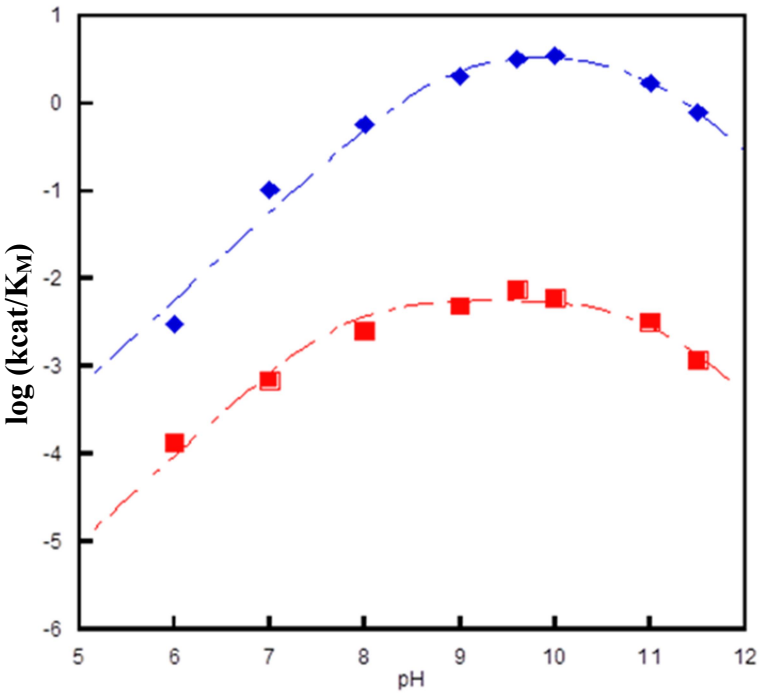

Figure 3.17 Double ionization models to describe pH dependence of F-AmDH/ *p*FPA (red curve) versus WT PheDH/ phenyl pyruvic acid (blue curve). Activity was measured in $NH_4OH/CHOO^-$ buffer at 25°C.

Table 3.6 pKa1 and pKa2 values of the *B.badius* F-AmDH and PheDH reactions

	Substrate	Enzyme	pKa1	pKa2
$\mathbf{k_{cat}}$	*p*FPAcetone	F-AmDH	7.44 ± 0.139	10.99 ± 0.185
$\mathbf{k_{cat}/K_M}$	*p*FPAcetone	F-AmDH	7.78 ± 0.134	10.96 ± 0.185
$\mathbf{k_{cat}/K_M}$	phenylpyruvic acid	PheDH	8.82 ± 0.192	10.89 ± 0.279

3.4 Conclusion

The F-AmDH exhibits a significantly decreased affinity for ammonia than the amino acid dehydrogenase. Mutations within the active site did not improve the binding of the ammonia substrate. The activity of the AmDH was tested in various buffer conditions and substrate concentrations in order to determine its mechanism. Results from initial rate studies indicate the steady-state addition of NADH followed by the random addition of *p*FPA and ammonia. Results from carbon NMR studies suggest that there is a chemical

reaction to form the imine (ammonia and ketone) before proceeding to enter the active site of the enzyme. In addition, pH studies suggest that a cysteine or histidine residue likely contributes to the binding of ammonia and future work should focus on mutating surrounding residues to favor the correct protonation state within the active site.

CHAPTER 4

EXTENDING THE UTILITY OF THE AMINE DEHYDROGENASE: SYNTHESIS OF THE (*S*)-AMINE THROUGH KINETIC RESOLUTION

4.1 Introduction & Motivation

Kinetic resolution of amines has been extensively studied in the literature and offers a viable alternative when asymmetric synthesis is not possible. Transaminase and amine oxidases are widely known for their enzymatic production of chiral amines. Numerous accounts of kinetic resolution of racemic chiral amines have been successfully achieved through ω-transaminases [102-106] and monoamine oxidases [107-110]. For example, ω-transaminase has been used for deracemization of mexiletine, an intermediate for an analgesic oral drug [23]. In addition, dynamic kinetic resolution of ibuprofen to obtain the (*S*)-enantiomer has been described in the literature [7].

The recently developed amine dehydrogenase (AmDH) class of enzymes shows extremely high enantioselectivity for production of (*R*)-amines (>99% *e.e.*) from prochiral ketones [32-34, 111]. So far, no success of switching the enantioselectivity of the AmDH has been achieved through protein engineering within the active site. As a result, we turn to kinetic resolution of the racemic amine mixture to obtain the enantiomerically pure (*S*)-amine (Figure 4.1). The amine dehydrogenase reaction is reversible, making it an ideal candidate for enantiomerization reactions.

Regeneration of NAD^+ from NADH is afforded by coupling the AmDH reaction with the NADH oxidase-catalyzed reduction of molecular oxygen to water [50, 52]. In

the present work, racemic amine substrates of 1-phenylethylamine (**1**), 1-(2-napthyl)ethylamine (**2**), 2-aminohexane (**3**), 1,3-dimethylbutylamine (**4**) and 3,3-dimethyl-2-butylamine (**5**) were successfully deracemized to obtain their respective (*S*)-amine (Figure 4.2).

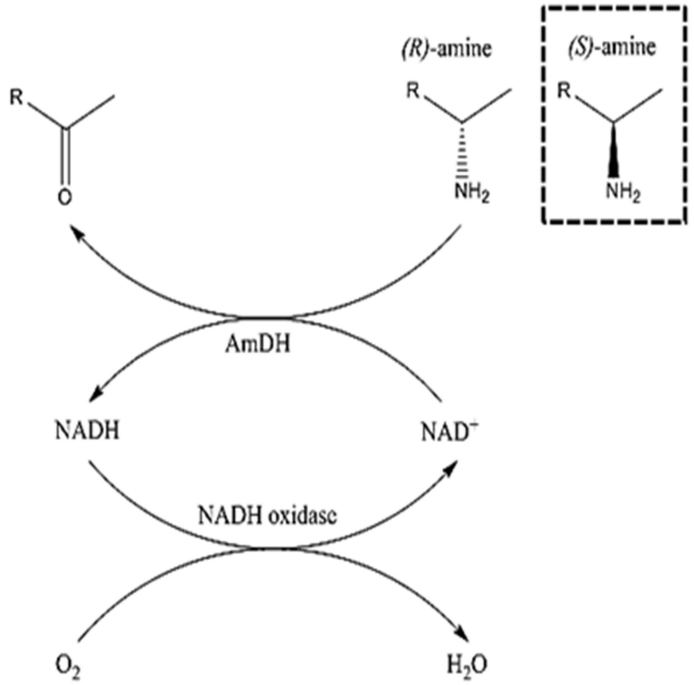

Figure 4.1 Kinetic resolution reaction scheme by the amine dehydrogenases

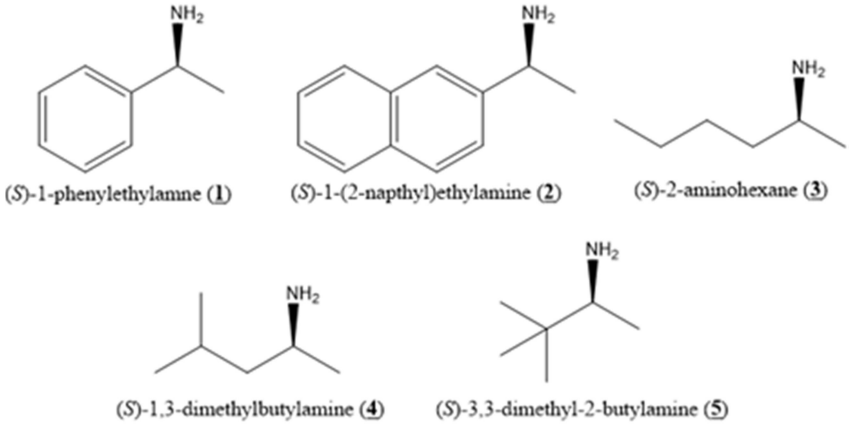

Figure 4.2 Production of (*S*)-enantiomer through oxidative deamination of racemic amines by amine dehydrogenases

4.2 Materials & Methods

4.2.1 Chemicals

Chemicals were obtained from suppliers and used without further purification. Acetophenone, methyl isobutyl ketone, (*R/S*)-1,3-dimethylbutylamine, (*R*)-phenylethylamine, chloroform and 4-(dimethylamino) pyridine were obtained from Sigma Aldrich (St. Louis, MO). (*R/S*)-1-phenylethylamine (1-PEA) and HPLC grade n-hexane were obtained from Acros Organic (Morris Plains, NJ). (*R*)-(+)-1-(2-napthyl)ethylamine, (*S*)-*(-)*-1-(2-napthyl)ethylamine, 2-acetylnapthalene, (*R*)-2-aminohexane, (*R*)-3,3-dimethyl-2-butylamine and (*R/S*)-3,3-dimethyl-2-butylamine were obtained from Alfa Aesar (Ward Hill, MA). (*R/S*)-2-aminohexane was obtained from Pfaltz and Bauer (Waterbury, CT). 2-hexanone and 2-pinacolone were obtained from Aldrich Chemical Company (Milwaukee, WI). NADH was obtained from Amresco (Solon, OH). NAD^+ and dithiothreitol (DTT) were obtained from Gold Biotechnology (St. Louis, MO). Isopropanol was obtained from Fisher Scientific (Fairlawn, New Jersey).

4.2.2 Protein Expression and Purification

AmDHs were purified using the same procedure as described in Section 2.2.2. NoxV and the K147R variant were expressed in a pET-28a, BL21 (DE3) (Invitrogen) system at 30°C in Overnight Express^{TM} Instant TB medium (Novagen). NoxV was expressed and purified based on a protocol previously described [49]. Cell pellets were resuspended in 50 mM Tris-Cl buffer pH 7.5 with 5 mM DTT (Buffer A). The suspension was sonicated at 14 W for 1 minute ten times. Sonicated cells were centrifuged at 10,000 rpm for 30 minutes. The clarified cell lysate was subjected to 50% ammonium sulfate precipitation.

The supernatant was filtered through a 0.8 μm microfiltration membrane (Pall Corporation, Ann Arbor, MI) and loaded onto a HiPrep 16/10 butyl hydrophobic column on an AKTAexplorer™. A gradient separation was performed starting from Buffer A with 50% ammonium sulfate decreasing down to 15%. The fractions with highest activity were collected and dialyzed against 50 mM Tris-Cl buffer pH 7.5 with 5 mM DTT (Buffer A). The sample was loaded onto a HiPrep 16/10 DEAE anionic exchange column on an AKTAexplorer™. A gradient separation was performed starting from buffer A with 150 mM NaCl increasing up to 250 mM NaCl. The fractions with highest activity were collected as pure protein. The purification yield is shown in Table 4.1 and the SDS-PAGE gel is shown in Figure 4.3.

Table 4.1 Purification of *L. plantarum* NADH oxidase (NoxV)

	Volume (mL)	**Protein (mg)**	**S.A. ($U.mg^{-1}$)**	**Yield (%)**
Cell lysate	15	164.4	5.89	100
50% $(NH_4)_2SO_4$	7.5	94.2	5.07	48.7
Butyl HIC	40	14	14.1	20.4
DEAE AEX	30	0.8	126	10.4

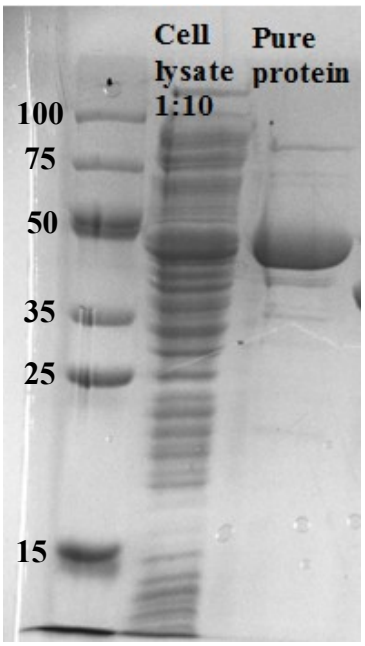

Figure 4.3 Purification of *L. plantarum* NADH oxidase (SDS-PAGE gel)

4.2.3 Spectrophotometric and activity analysis

All analysis was performed as described in Section 2.2.3.

4.2.4 High-performance liquid chromatography (HPLC) analysis

Liquid chromatography was performed on a Shimadzu UFLC-2010 with a Daicel Chiralpak AS column to separate 1-(2-napthyl)ethylamine. Its enantiomers do not separate on the GC. The samples are run at 1 mL min^{-1} with column temperature at 25°C. Detection occurs at 225 nm and 1 μL of sample was injected. The mobile phase was a gradient mixture of n-hexane and isopropanol with 0.1% diethylamine (DEA) (from 5% to 20% of isopropanol). The reaction mixture was diluted with isopropanol and filtered with 0.2 μm microfiltration membrane (Pall Corporation, Ann Arbor, MI) before injection.

4.2.5 Gas chromatography (GC) analysis

Gas chromatography was performed on a Shimadzu GC-2010 gas chromatography apparatus with an Astec CHIRALDEX^{TM} B-DM column (length: 30 m; inner diameter: 0.25 mm; film thickness: 0.12 μm). The compounds are extracted into organic solvent chloroform from the aqueous reaction mixture. The reaction mixture is derivatized by trifluoroacetic acid anhydride (TFAA). To derivatize the compounds, 1.5 μL of 1 M solution of 4-(dimethylamino) pyridine in chloroform, which acts as a catalyst, and 1.5 μL of TFAA were added to 200 μL of the sample. The derivatized sample was allowed to react for 10 minutes before GC analysis. The linear velocity was 60 cm/s and the carrier helium air mixture.

4.2.6 Oxidative deamination reaction conditions

Reactions were performed in 0.1 M glycine buffer pH 8.0 in a total volume of 1.5 mL. All reactions were conducted at 35°C, except for the 1-(2-napthyl)ethylamine/cFL1-AmDH reaction which was performed at 45°C. 20 mM of racemic amine mixture of 1-PEA (substrate **1**) was added to the reaction. 10 mM of racemic amine mixture was added of the amine substrates **2** through **5**. 10 mM DTT is added into all reactions. No stirring is implemented.

6 U of the AmDH is added into the reaction to 1 U of the NADH oxidase. 20 mM NAD^+ is added into the reaction mixture. After 24 hours of reaction, an additional 4 U of AmDH and 20 mM NAD^+ were added to the reaction to drive it to completion and stopped after 36 hours. For the 1,3-DMBA/L-AmDH reaction, an additional 10 mM NAD^+ was added and the reaction was left for an additional 4 hours to obtain full

conversion (40 hours total). For the 1-(2-napthyl)ethylamine/ cFL1-AmDH reaction, 20 mM NAD^+, 1.5 U of cFL1-AmDH and 1 U of NADH oxidase was added to the reaction. 1 U of cFL1-AmDH/ 20 mM NAD^+ was added at 24 hours and 1 U of cFL1-AmDH/ 10 mM NAD^+ was added at 36 hours to drive the reaction to completion (48 hours total).

4.3 Results & Discussion

4.3.1 Protein engineering to improve oxidative deamination activity

The use of protein engineering to improve oxidative deamination activity of the AmDHs was investigated. The same two catalytic residues are responsible and essential to create amine dehydrogenase activity: L-AmDH (K67/N260) [32], F-AmDH (K77/N275) [33], cFL1-AmDH (K77/N270) [34]. Mutation of the lysine to a serine and the asparagine to a leucine was the top variant for reductive amination activity for all amine dehydrogenases. It was hypothesized that different amino acid residues are optimal for the desired reverse reaction, the oxidative deamination reaction. Reducing reductive amination activity is also crucial to prevent the reverse reaction from the ketone back to the amine and assist in the equilibrium of the reaction. Mutation of that catalytic lysine to methionine and asparagine to valine, respectively, created the top variant for oxidative deamination activity for all three AmDHs (mutations to the L-AmDH were previously performed [32]) (Table 4.2). The most dramatic improvement was observed for the cFL1-AmDH: relative oxidative deamination towards 1-phenylethylamine (**1**) was increased 10-fold, while reductive amination was decreased 10-fold towards acetophenone (Figure 4.4).

Table 4.2 Top variants for reductive amination and oxidative deamination activity

	Reductive Amination (U/mg)	Oxidative Deamination (U/mg)
L-AmDH (K67S/N260L) [a]	0.46	1.76
L-AmDH (K67M/N260V) [a]	0.059	1.87
F-AmDH (K77S/N275L) [b]	3.19	1.39
F-AmDH (K77M/N275V) [b]	1.23	1.70
cFL1-AmDH (K77S/N270L) [c]	0.3	0.066
cFL1-AmDH (K77M/N270V) [c]	0.044	0.52

a) Activity toward L-AmDH substrate, methyl isobutyl ketone and 1,3-dimethylbutylamine [32]; b) Activity toward F-AmDH substrates, *para*-fluoro phenyl acetone (*p*FPA) and *para*-fluoro phenyl amine;. c) Activity toward cFL1-AmDH substrates, acetophenone and 1-phenylethylamine; d) Reductive amination activity was performed in 5 M $NH_4OH/CHOO^-$ buffer pH 9.6 and oxidative deamination activity performed in 0.1 M glycine pH 10.4 at 25°C.

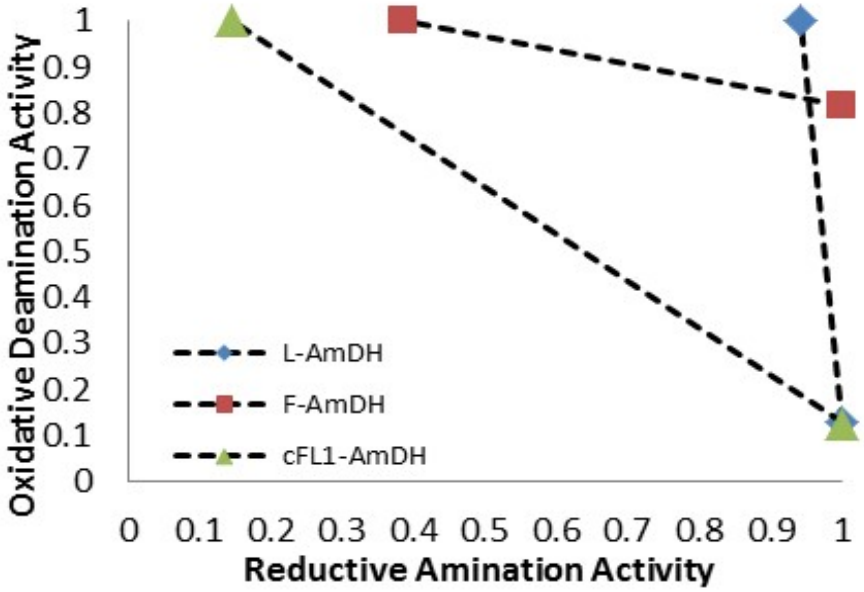

Figure 4.4 Impact of amino acid changes at catalytic residues in L-AmDH (blue), F-AmDH (red) and cFL1-AmDH (green)

4.3.2 Protein engineering to improve thermostability of the NADH oxidase

Cofactor recycling of $NADH/NAD^+$ is performed through *Lactobacillus plantarum* NADH oxidase (NoxV). Previous characterization of the NoxV showed a T_{opt} of 40°C and loss of enzyme activity after just 2 hours at room temperature [49]. Protein

engineering to improve temperature stability was performed in hopes to achieve optimal reaction conditions. Lysine residues mutated to arginine residues often show improved protein stability [112]. Recent work on *S. pyogenes* NADH oxidase showed that a single point mutation K184R improved activity by 50% and improved thermostability by increasing the half-life at 30°C by 46.6% [55]. Sequence alignment showed that this surface lysine is conserved among several NADH oxidases. The K147R mutation was introduced to the *L. plantarum* NoxV and the variant maintained 100% activity after 6 hours, compared to 2 hours for the wild-type. In addition, the enzyme retains 67% of activity after 22 hours. However, the specific activity and optimum temperature of K147 variant of NoxV did not improve (Figure 4.5).

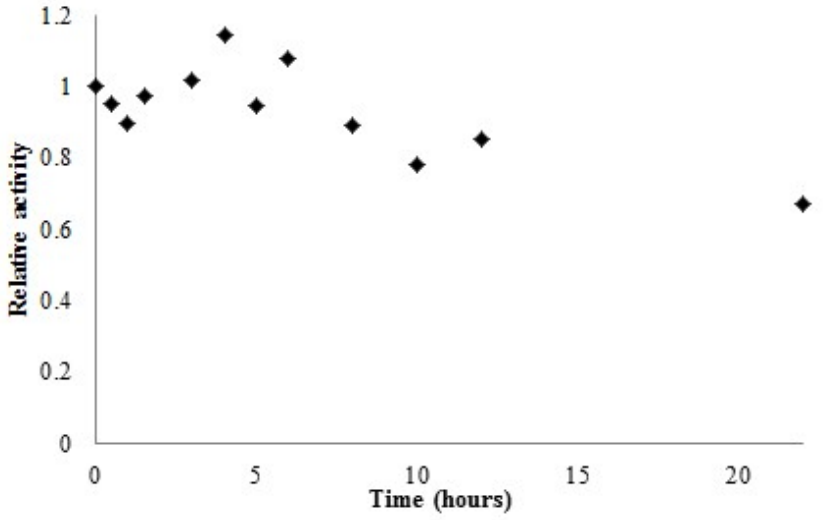

Figure 4.5 Temperature stability of NoxV (K147R) at room temperature

4.3.3 Determination of kinetic parameters in oxidative deamination reactions

The oxidative deamination reaction has been less thoroughly investigated compared to the reductive amination direction. To ensure optimal oxidative deamination reaction

conditions of the racemic amine mixtures, kinetic parameters were obtained *via* UV-VIS spectrometry (Table 4.3). Specific catalytic activity was measured toward the ketone and amine substrates and the K_M value toward the amine substrate was determined. The MIBK/1,3-DMBA (**4**) was the only reaction which utilized the methionine/valine variants described in the previous section.

Despite substantial improvements in increasing the oxidative deamination activity of the cFL1-AmDH (as previously described and shown in Table 4.2 and Figure 4.4), L-AmDH was chosen instead as the enzyme for 1-PEA to acetophenone activity due to its surprisingly higher activity toward 1-PEA and better temperature optimum (Table 4.4). L-AmDH unexpectedly displays 10-fold lower activity in the reductive amination direction towards acetophenone, which is highly beneficial for the desired oxidative deamination reaction. Furthermore, L-AmDH displays little activity toward pinacolone (0.054 U/mg) but displays around 25 times more activity in the oxidative deamination direction (1.43 U/mg, Table 4.4). These interesting but unexpected results of L-AmDH catalytic activity toward the amine but not toward the respective ketone will be further investigated in future work.

(*R*)-1-(1-napthyl)ethylamine is the active pharmaceutical ingredient for Sensipar® (Cinacalcet) [113] and a desired target substrate for the AmDHs. cFL1-AmDH does not show any activity toward the (*R*)-1-(1-napthyl)ethylamine but it does exhibit 0.205 U/mg of enzymatic activity towards the (*R*)-1-(2-napthyl)ethylamine. This is due to the position of the amine group relative to the aromatic ring. No activity was observed for the respective (*S*)-enantiomer making it an ideal candidate for this reaction. The double variant K77M/N270V showed no improvement in the oxidative deamination activity over

cFL1-AmDH (K77S/N270L). In addition, F-AmDH showed no activity toward either substrate, once again displaying the difference in substrate profiles between the two enzymes.

Additionally, despite being an aliphatic substrate, F-AmDH unexpectedly displays higher activity toward 2-aminohexane than L-AmDH (1.59 versus 0.93 U/mg, respectively). The same trend was observed with the ketone substrates 2-hexanone and 2-octanone. F-AmDH may be more accepting of these larger aliphatic substrates because its model substrates traditionally consist of a bulky phenyl ring and therefore, it is more accommodating to larger substrates.

Table 4.3 Kinetic parameters of the AmDHs in their respective reactions

Reaction	**Acetophenone/ 1-PEA (1)**	**2-acetylnapthalene/ 1-(2-napthyl) ethylamine (2)**	**2-hexanone/ 2-aminohexane (3)**
Enzyme	L-AmDH K67S/N260L	cFL1-AmDH K77S/N270L	F-AmDH K77S/N275L
S.A. (Amination)	0.059	0.011	0.38
S.A. (Deamination)	0.97	0.205	1.59
K_M (Deamination)	8.32	3.68	2.65

Reaction	**MIBK/ 1,3-DMBA (4)**	**Pinacolone/ 3,3-DMBA (5)**
Enzyme	L-AmDH K67M/N260V	L-AmDH K67S/N260L
S.A. (Amination)	0.059	0.054
S.A. (Deamination)	1.87	1.43
K_M (Deamination)	5.23	5.62

a) S.A.: specific activity (U/mg). b) K_M value is measurement toward the substrate in the oxidative deamination direction. c) K_M value was measured with racemic amines (both (*R*) and (*S*) amines present in equal amounts). c) Reductive amination activity was performed in 5 M $NH_4OH/CHOO^-$ pH 9.6 buffer and oxidative deamination activity performed in 0.1 M glycine pH 10.4 buffer at 25°C.

Table 4.4 Activity of L-AmDH and various AmDHs towards acetophenone/1-PEA

	Reductive amination of acetophenone (U/mg)	Oxidative deamination of *(R)*-1-PEA (U/mg)	Temperature optimum (°C)
L-AmDH (K67S/N260L)	0.059	0.97	50
F-AmDH (K77S/N275L)	<0.1	0.019	50
cFL1-AmDH (K77S/N270L)	0.3	0.066	>80
cFL1-AmDH (K77M/N270V)	0.044	0.52	>80

a) S.A.: specific activity (U/mg). b) Reductive amination activity was performed in 5 M $NH_4OH/CHOO^-$ buffer pH 9.6 and oxidative deamination activity performed in 0.1 M glycine pH 10.4 at 25°C.

Cofactor inhibition ratios of the L-AmDH/NoxV were investigated. L-AmDH displays a K_M value at 40.56 μM towards NAD^+ and K_I at 259.5 μM towards NADH. Competitive inhibition by NADH was observed experimentally (Figure 4.6). Previous characterization of NoxV by Park et al. showed non-competitive inhibition by NAD^+ [49]. NoxV showed a K_M value at 50.2 μM towards NADH and K_I at 289 μM towards NAD^+. The apparent inhibition ratio must be less than unity in order to allow for theoretical complete conversion. Less than unity inhibition ratios were observed in the L-AmDH/NoxV reaction (Table 4.5).

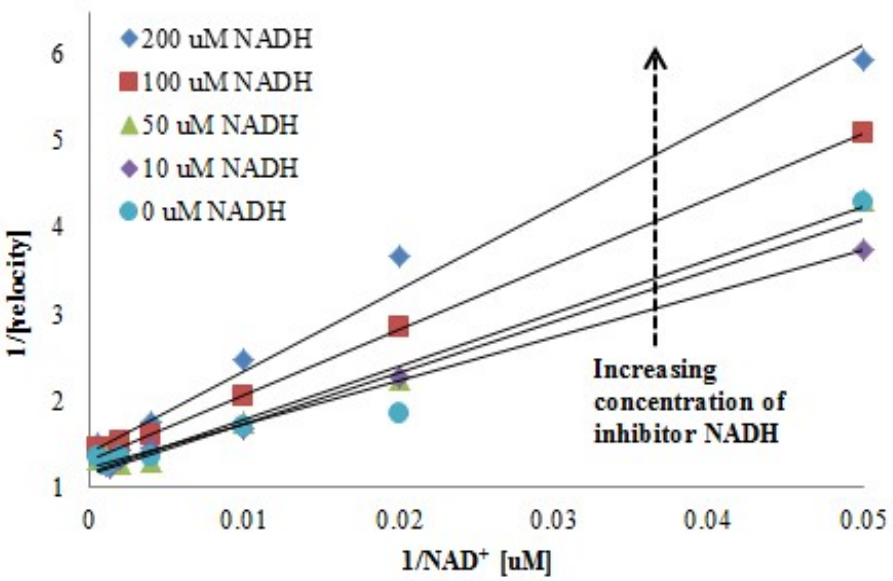

Figure 4.6 Inhibition patterns of L-AmDH towards NADH

Table 4.5 Cofactor inhibition ratios for L-AmDH/NoxV reaction

		Inhibition ratio	Cross inhibition ratio
L-AmDH:	$K_{M\text{-}NAD+}/K_{i\text{-}NADH}$	0.16	
	$K_{M\text{-}NAD+}/K_{i\text{-}NAD+}$		0.14
NADH ox:	$K_{M\text{-}NADH}/K_{i\text{-}NAD+}$	0.17	
	$K_{M\text{-}NADH}/K_{i\text{-}NADH}$		0.19

4.3.4 Optimization of oxidative deamination reaction conditions to achieve pure (*S*)-amine

After obtaining the kinetic parameters of the AmDHs and their respective reactions, reaction conditions were investigated to achieve optimal conversion of the (*R*)-amine. Various conditions were initially investigated in the 1-PEA (**1**) reaction and then further applied to the other oxidative deamination reactions (same reaction conditions unless otherwise noted in Experimental Section). First, various reaction buffers were considered (Table D.1). Ammonium buffer is not needed for the reaction to proceed in the oxidative deamination direction and NoxV deactivates in high ammonium concentrations. 0.1 M

glycine pH 8.0 was ultimately chosen as the buffer for all future oxidative deamination reactions.

The optimum reaction temperature was 35°C (Table D.2) due to the thermal instability of NoxV. Various enzyme ratios of L-AmDH to NoxV were investigated to allow for efficient cofactor regeneration. An optimum ratio of 6:1 of L-AmDH to NoxV was observed and used in further reactions (Table D.3). Different initial NAD^+ concentrations were added into the reaction (Table D.4) and it was found that at least 10 mM NAD^+ must always be present in the reaction solution in order to achieve optimal conversion, indicating poor cofactor recycling. The K_M value towards the cofactor $NADH/NAD^+$ of all AmDHs and NoxV is around 45 μM (as previously described) so the low conversion can solely be attributed to inefficient cofactor regeneration leading to a build-up of NADH. Despite improvement to the thermostability to the NADH oxidase, no improvement was observed with the K147R variant in the reaction and further work must be done to optimize cofactor recycling.

Despite inefficient cofactor recycling, full conversion of 20 mM (*R/S*)-1-PEA (**1**) was achieved. The conditions were applied to 10 mM racemic amine mixtures (**2** through **5**) and pure (*S*)-amine was obtained in all reactions (Table 4.6, Figure 4.7). Additional GC chromatograms and peak areas for both enantiomers are located Appendix E (Figure E.1 to Figure E.5).

Table 4.6 Enantioselectivity of oxidative deamination reaction of racemic amine mixtures

	Enantioselectivity (%)
1-PEA (1)	99.20
1-(2-napthyl)ethylamine (2)	99.32
2-aminohexane (3)	99.59
1,3-DMBA (4)	99.09
3,3-DMBA (5)	99.70

All enantioselectivity was determined by GC, except 1-(2-napthyl)ethylamine which was determined by HPLC.

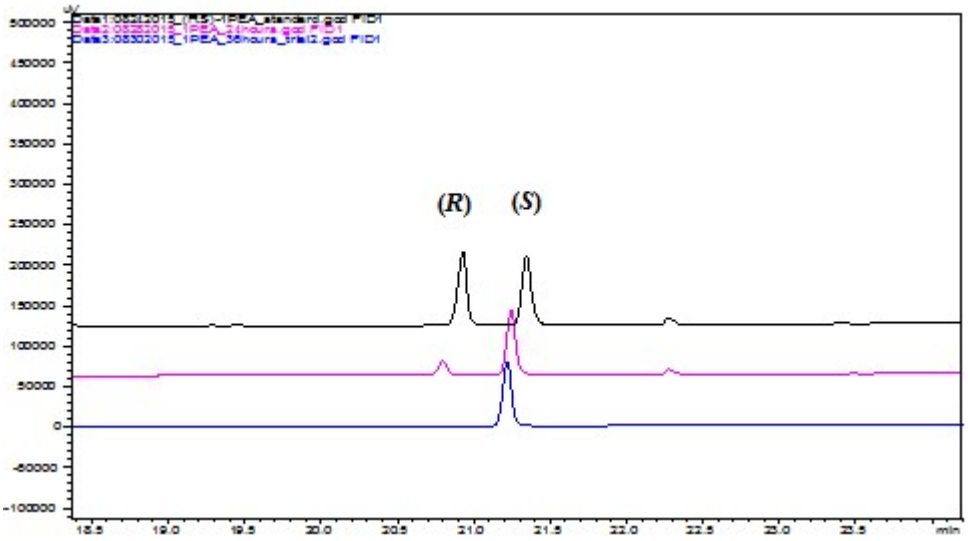

Figure 4.7 GC chromatogram of oxidative deamination of racemic mixture (*R/S*)- 1-phenylethylamine (1-PEA) to leave pure (*S*)-1-PEA. Standard of (*R/S*)-1-PEA (black), reaction sample (pink/blue).

4.4 Conclusion

Amine dehydrogenases (AmDHs) exhibit high enantioselectivity towards the (*R*)-amine and can be utilized to deracemize a racemic mixture in order to obtain enantiomerically pure (*S*)-amine (>99% *e.e.*). Protein engineering to improve oxidative deamination activity of all AmDHs and the thermostability of the NADH oxidase was achieved. Optimization of oxidative deamination reaction conditions was investigated and full conversion of (*R*)-amine was achieved. In summary, kinetic resolution of racemic amine mixtures was achieved for 1-phenylethylamine, 1-(2-napthyl)ethylamine, 2-aminohexane,

1,3-dimethylbutylamine and 3,3-dimethyl-2-butylamine to achieve their respective (*S*)-amines. Future work will look into optimizing the cofactor recycling system and application towards additional pharmaceutically relevant substrates.

CHAPTER 5

APPLICATION OF AQUEOUS TWO PHASE EXTRACTION SYSTEM FOR EFFICIENT PURIFICATION OF DEHYDROGENASES

5.1 Introduction & Motivation

The recently developed amine dehydrogenases (AmDHs) produce enantiomerically pure amines used as pharmaceutical precursors and intermediates. Their potential as a biocatalytic green alternative for production toward chiral amines has led to the development of a scalable, efficient purification strategy for these enzymes. The current purification procedure requires affinity chromatography, specifically involving purification through His-tagged proteins (Figure 5.1) [114, 115]. This purification is expensive, requires multiple steps and is not cost-effective on a larger industrial scale (greater than one liter). This work seeks to develop an efficient, 'one-step' purification procedure of enzymes.

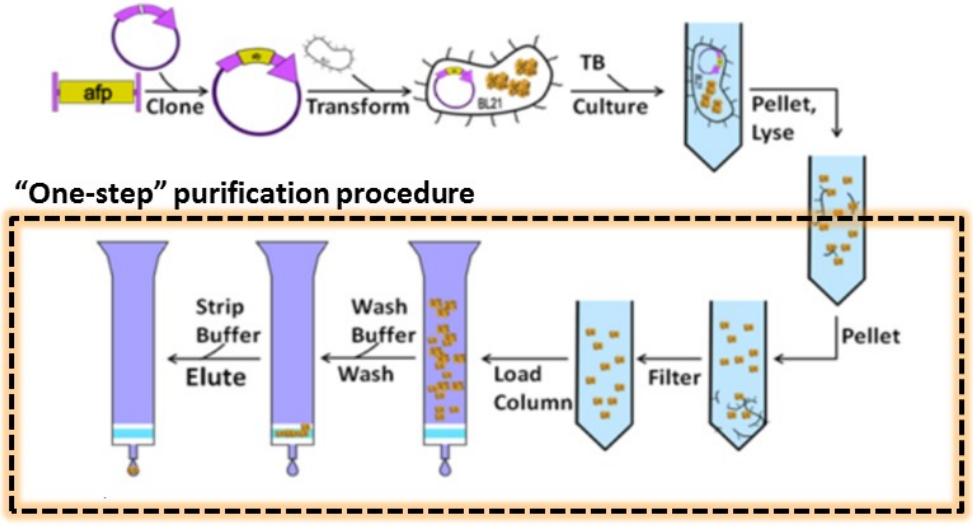

Figure 5.1 Current multi-step His-tag purification procedure [115]

This purification uses an aqueous two-phase extraction (ATPE) system with a polymer top phase and an aqueous salt buffer for the bottom phase. After homogenization of the bacterial cells, the cell lysate containing the desired protein was applied into the ATPE system. The ATPE system selectively partitions the desired enzyme (AmDH) into the top layer, while leaving the remaining cell debris and lysate to the bottom layer (Figure 5.2). The protein partitioning can be quickly determined by measuring the specific activity of the top and bottom layers. This ATPE is an economic, scalable and environmentally friendly alternative to traditional affinity protein purification. The polymer and salt components are cheap and non-toxic and no centrifugation or expensive Ni-NTA resin is required.

Notable recent separations with aqueous two-phase systems include amino acids [116], DNA [117], virus-like particles [118] and enzymes [119, 120]. Both phenylalanine dehydrogenase [121] and formate dehydrogenase [47, 122, 123] have been successfully purified with ATPE systems. This current thesis work involves 1) purification of F-AmDH through the ATPE system, 2) scaling-up the purification and 3) further application to various dehydrogenases, including amine dehydrogenase enzymes and the cofactor regeneration enzymes. In addition, phase diagrams are established with ammonium citrate as the salt in the ATPE system.

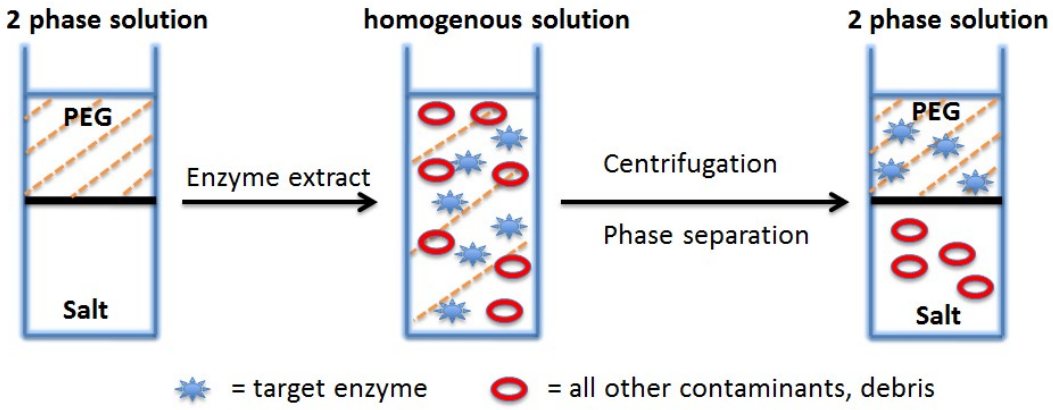

Figure 5.2 Aqueous two-phase extraction procedure

5.2 Materials & Methods

5.2.1 Chemicals

Substrates were obtained from suppliers and used without further purification. PEG 1000 was obtained from Spectrum Chemical (New Brunswick, NJ). PEG 1500 was obtained from Acros Organic (NJ, USA). PEG 4000, PEG 6000 and ammonium citrate tribasic were obtained from Alfa Aesar (War Hill, MA). PEG 8000 was obtained from GBiosciences (St. Louis, MO). Citric acid was obtained from Fisher Scientific (Fairlawn, NJ). Ammonium hydroxide was obtained from Ricca Chemical Company (Arlington, TX). Ammonium phosphate was obtained from Sigma Aldrich (St. Louis, MO) and ammonium bicarbonate was obtained from BDH Chemicals (West Chester, PA).

5.2.2 Protein expression

AmDH were expressed using the same procedure described in Section 2.2.2.

5.2.3 Enzyme activity assay

All UV-VIS analysis was performed as described in Section 2.2.3.

5.2.4 Preparation of cell debris and lysate

The cell debris is created by the resuspension of cell pellets in 50 mM NaH_2PO_4 buffer containing 20 mM imidazole and 300 mM NaCl at pH 8.0. The mixture is sonicated at 14 W for 1 minute ten times. To create the cell lysate, the sonicated cells were centrifuged at 10,000 rpm for 30 minutes.

5.2.5 Aqueous two-phase extraction procedure

To create a small-scale ATPE system, the salt ammonium citrate is first added into the system. Next, potassium phosphate buffer pH 8.0 or Tris-Cl buffer pH 10.4 is added and the system is adjusted to the desired pH with ammonium hydroxide. Next, the polymer polyethylene glycol (PEG) is added and the mixture is vortexed to form a homogenous solution. All components are added based on the desired weight percent and the entire system was a total weight of 10 grams. The cell lysate is then added 20% (w/w) and the ATPE system is mixed for an hour to again form a homogenous solution. The system is then centrifuged for 30 minutes at 4000 rpm at room temperature to form two distinct layers. For a large-scale ATPE system, citric acid is added and ammonium hydroxide is added to obtain the desired pH. The same procedure is followed with the desired volume and weight percent of each component and the cell lysate is added last at 20% (w/w).

The top and bottom layers are measured for catalytic activity UV-VIS spectrophotometry to quickly determine the partitioning of the enzyme. The protein concentration was determined by Bradford assay [75]. The enzymatic units in the top and bottom layers were calculated and compared to the total enzymatic units put into the system to determine the partitioning of the enzyme and if there was any loss of enzymatic

activity during the purification process (check of the mass balances). In addition, the top and bottom phases are run on a SDS-PAGE gel to observe the enzyme's purity. The salt is removed from the sample solution through trichloroacetic acid (TCA) precipitation of the protein. One volume of 100% (w/v) TCA solution is added to four volumes of protein sample. The protein is precipitated from the mixture by centrifugation and then washed five times with acetone.

5.2.6 Determination of phase diagrams

To determine the binodal curve, stock solution of both the polymer and salt solution are prepared. The stock solutions are added drop-wise at known weights until the first sign of turbidity is observed, the cloud point. The solution is vortexed for one minute and then centrifuged for five minutes to form two distinct layers. Next, the diluent water is added to get below the cloud point to obtain a clear mixture and the procedure is repeated again. The amount of each component in the system to form one or two layers is recorded [124, 125].

To define the tie-lines of a phase diagram, the composition of polymer and salt in the top and bottom phases must be determined. The top and bottom phases were diluted 1:10 with water and then measured by a conductivity meter (Corning Conductivity Meter 441) to determine the salt composition. The polymer concentration was determined by a refractometer (G.N. Wood, Newton, PA). The top and bottom phases were diluted 1:10 with water. Both the sample and the standard (consisting of the known amount of salt in each phase previously determined by the conductivity meter) were measured. Samples were measured in triplicates and with light at four different wavelengths

(green/blue/red/orange). The standard curve for amount of PEG 6000 in presence of 3.42% ammonium citrate is shown in Figure 5.3. The y-axis represents the difference in the light source reading between the sample and solvent. The composition of the polymer can also be determined by lyophilizing the top and bottom phases and obtaining the dry weight of polymer and salt. The previously determined salt composition was subtracted from the total dry weight of the phase to determine the polymer composition [124, 125].

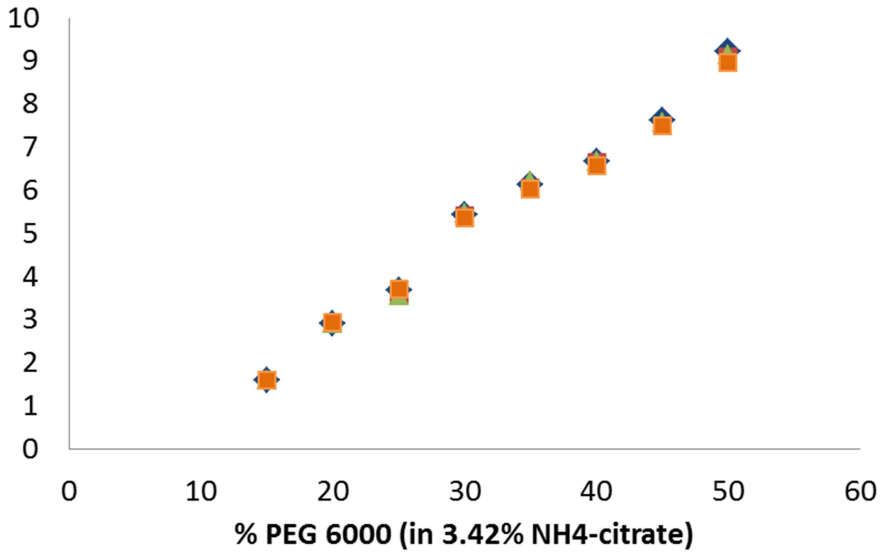

Figure 5.3 Standard curve of the amount of PEG 6000 in 3.42% of ammonium citrate

5.3 Results & Discussion

5.3.1 Screening of various conditions for the F-AmDH

Various conditions were tested to achieve optimal separation of the phenylalanine amine dehydrogenase (F-AmDH) in an aqueous two-phase extraction (ATPE) system. Previous work showed purification of *B. sphaericus* phenylalanine dehydrogenase with 9% (w/w) PEG 6000 and 16% (w/w) $(NH_4)_2SO_4$ at pH 8.0 [121]. Various salts were considered (Table 5.1) and ammonium citrate was chosen as the best salt for the system. Ammonium

citrate is not expensive and non-toxic, which leads to easy disposal. Ammonium citrate has not been utilized in ATPE systems thus far, so its development in this work will be completely novel. Various amounts of ammonium citrate are added into the system (14 to 16%) and optimal separation was achieved with 16% ammonium citrate (Table 5.2). All this work was performed with 9% (w/w) PEG 6000 at pH 8.0. The top and bottom layers for purification of F-AmDH in ATPE are shown in Figure 5.4.

Table 5.1 Ratio of catalytic activity of top and bottom layers for F-AmDH with various salts (PEG 6000, pH 8.0)

	Ratio
$(NH_4)_3PO_4$ (phosphate)	8.98
$(NH_4)HCO_3$ (bicarbonate)	Did not separate
$NH_4C_6H_{17}N_3O_7$ (citrate)	10.06

Table 5.2 Ratio of catalytic activity of top and bottom layers for F-AmDH at various concentrations of ammonium citrate (PEG 6000, pH 8.0)

Ammonium citrate	**Top Layer (U/mg)**	**Bottom Layer (U/mg)**	**Ratio**
14%	6.12	1.43	4.29
14.5%	6.39	1.04	6.17
15%	6.09	0.48	12.59
16%	6.46	0.053	123

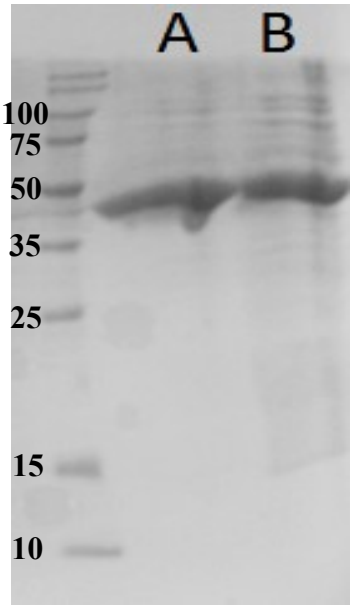

Figure 5.4 SDS purification of F-AmDH through ATPE, (A) top layer 1:10, (B) bottom layer

5.3.2 Scale-up of F-AmDH ATPE purification

The ATPE purification of F-AmDH was scaled up ten times (total weight 100 grams) using the optimal conditions described in the previous section. No centrifugation was performed because centrifugation is not feasible on a larger industrial scale. The system was allowed to settle in the 4°C fridge over a course of 3 days (Figure 5.5A through Figure 5.5C). Optimal separation was achieved after two days with a ratio of 7.68 of top to bottom layer catalytic activity.

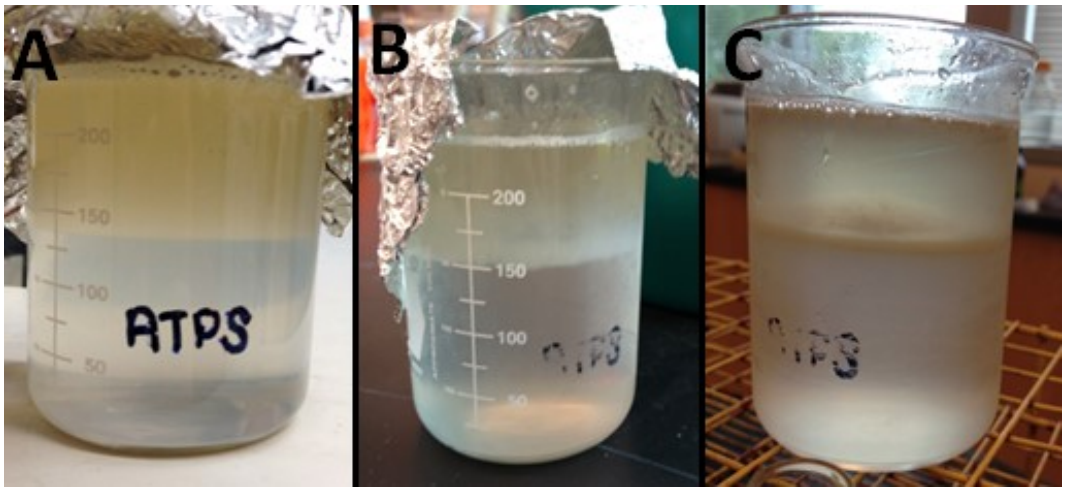

Figure 5.5 Larger-scale purification of F-AmDH through ATPE after (A) 30 minutes, (B) one day, (C) two days

5.3.3 Application to various dehydrogenases

The same conditions for the F-AmDH ATPE purification were applied to various dehydrogenases. There was no success in selectively partitioning the enzyme into the top layer with other dehydrogenases following the same conditions (Table 5.3). In addition, there was limited success with varying the molecular weight of the polymer. The ratios of the catalytic activity of the top to bottom layers are shown in Table 5.3. Values greater than unity represent more of the desired enzyme into the top layer (highlighted in green), while values less than unity represent more into the bottom layer (highlighted in red). Only F-AmDH and L-AmDH achieved sufficient protein purification into the top layer by varying the molecular weight.

Table 5.3 ATPE purification of various dehydrogenases

	PEG 400	PEG 1000	PEG 1500	PEG 4000	PEG 6000	PEG 8000
F-AmDH		89.34	38.98	47.45	123	6.2
cFL1-AmDH	0.44	0.081	0.115	0.275	0.067	
L-AmDH		16.19	19.34	1.6	0.17	
Formate DH	0.935	0.07	0.155	0.0205	0.085	
Glucose DH		0.63	0.0004	0.0044	0.031	0.0086

Partition coefficient= $[\text{target protein}]_{top}/[\text{target protein}]_{bot}$

The impact of pH was investigated in the ATPE purification of cFL1-AmDH. As shown in Table 5.4, as the pH is increased, more of the cFL1-AmDH moved into the top layer. It is hypothesized that the pH of the ATPE can play a role in the folding of the protein (depending on its isoelectric point and the charge/pKa of its amino acids responsible for the protein structure). In addition, cFL1-AmDH has a high temperature optimum (>60°C) so the cell debris is incubated at 45°C for 30 minutes. Many of the other unwanted proteins in the solution begin to denature and become insoluble, allow for easier and cleaner protein separation and purification. The protein purification of cFL1-AmDH is shown on a SDS-PAGE gel (Figure 5.6).

Table 5.4 Impact of pH on the purification of cFL1-AmDH (PEG 1500, cell lysate is treated to incubation at 45°C)

pH	Top Layer (U/mg)	Bottom Layer (U/mg)	Ratio
8.0	0.49	0.18	2.75
9.0	0.65	0.13	5
9.5	0.54	0.035	15.42

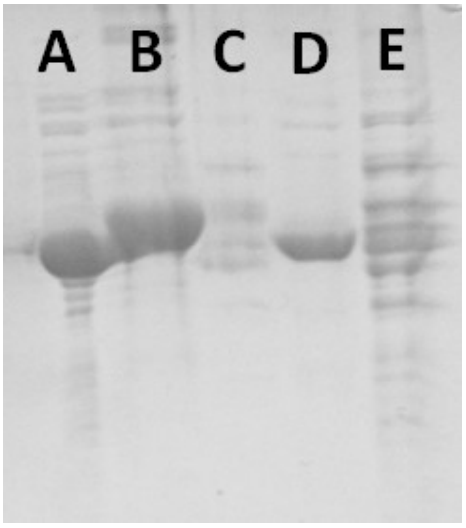

Figure 5.6 SDS purification of cFL1-AmDH through ATPE, (A) cell lysate incubated at 45°C, (B) PEG 1000 top layer, (C) PEG 1000 bottom layer, (D) PEG 1500 top layer, (E) PEG 1500 bottom layer

Raising the pH for the ATPE systems also improved the protein partitioning of the cofactor regeneration enzymes formate and glucose dehydrogenase. However, the ATPE purification was still not acceptable as a protein purification method. Previous studies have shown the addition of salts, such as NaCl, can strongly affect the ATPE. The effect can be attributed to hydrophobic interactions [126, 127]. The addition of NaCl helped to improve the partitioning of the cofactor regeneration enzymes and achieve protein purification similar to His-tagged purification. The addition of NaCl did not help the partitioning of any of the AmDHs. The optimized conditions for each enzyme are listed in Table 5.5. Activity yield describes how much protein activity units are present in the system, top or bottom layer (ideally should be 100%). Purification yield indicates how clean the desired protein is in the top layer (activity of ATPE purified protein compared to activity of His-tagged purified protein). Further work includes scaling-up the ATPE, back extraction out of the polymer layer and ammonium sulfate precipitation of the protein solution [data not shown, work performed by Dr. Bettina Bommarius].

Table 5.5 Optimal ATPE purification conditions

	Best ATPS condition	**Activity Yield**	**Purification Yield**
F-AmDH:	PEG 6000 pH 8.0	85.7%	99.4%
L-AmDH:	PEG 1500 pH 8.0	94.1%	100.1%
cFL1-AmDH:	PEG 4000 pH 9.5	90.28%	89.23%
Formate DH:	PEG 1500 pH 10.0, 10% NaCl	89.8%	89.2%
Glucose DH:	PEG 1000 pH 10.0, 10% NaCl	98.83%	91.38%

5.3.4 Phase diagrams: Determination of binodal curve

A binodal curve was established to determine the region of component concentrations that will form two phases in the ATPE system. All components above the curve will form

two immiscible aqueous phases; all components below the curve will only form one phase. Previously established phase diagrams are listed in Table 5.6. No phase diagrams have been determined using ammonium citrate as the salt. As can be seen from Figure 5.7, different binodal curves are observed depending on the polymer used in the ATPE system. The larger the molecular weight of the polymer, the less amount of polymer and salt must be added into the system to form two layers.

Table 5.6 Phase diagrams previously established in literature

PEG	Salt	Ref
2000, 4000, 6000, 8000	Potassium phosphate, sodium citrate	[127]
1500, 8000	Potassium citrate/formate, sodium citrate/formate	[128]
1000, 2000, 3400	Potassium phosphate, ammonium sulfate, K_2CO_3, Li_2SO_4, $MnSO_4$, NaOH, $ZnSO_4$	[129]
1000, 3350, 8000	Potassium phosphate, ammonium sulfate, sodium carbonate/sulfate, magnesium sulfate	[130]
600, 1000,1450, 3350, 8000	Sodium citrate	[131]
2000	Sodium citrate	[132]
6000	Potassium citrate	[133]

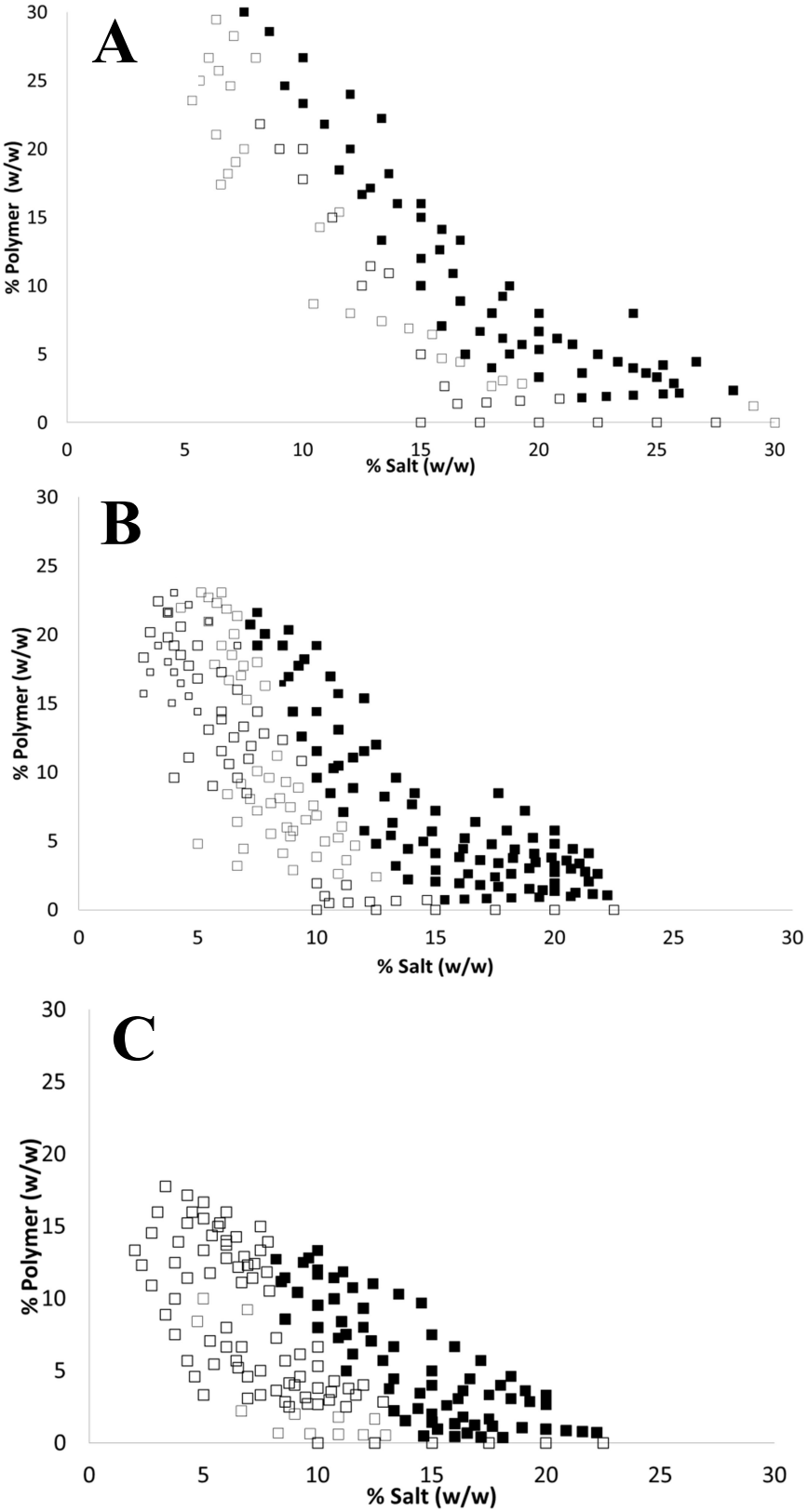

Figure 5.7 Binodal curve diagrams for PEG 1500 (A), PEG 6000 (B) and PEG 8000 (C) with ammonium citrate as the salt (at pH 8.0)

5.3.5 Phase diagrams: Determination of tie-lines

After the determination of the binodal curve, all systems that form two immiscible aqueous phases will lie on a tie-line. All systems along a tie-line will have the same final concentration of polymer and salt components in both the top and bottom phases, respectively, but different total compositions and phase ratios [124, 125, 134]. The tie-line length (TLL) is described by Equation 5.1 and the slope of the tie-line (STL) is described by Equation 5.2. ΔX is the difference in the salt composition between the top and bottom phases, ΔY is the difference in the polymer composition between the top and bottom phases. All components on a tie-lie will have the same TLL and STL.

$$TLL = (\Delta X^2 + \Delta Y^2)^{1/2} \qquad \text{[Equation 5.1]}$$

$$STL = \left({}^{\Delta Y}/_{\Delta X}\right) \qquad \text{[Equation 5.2]}$$

The phase diagram consisting of PEG 6000 at pH 8.0 with its respective tie-lines are shown in Figure 5.8. The salt concentration was determined by a conductivity meter and the polymer concentration was determined by a refractometer. The slopes of the tie-lines are not truly parallel and future work will look at improving the mass balances (approximately 10% off). Tie-lines are useful in determining the optimal conditions to achieve protein separation by knowing the polymer and salt composition of the top and bottom phases. In addition, phase diagrams will likely change when the cell lysate is added to the ATPE system [135].

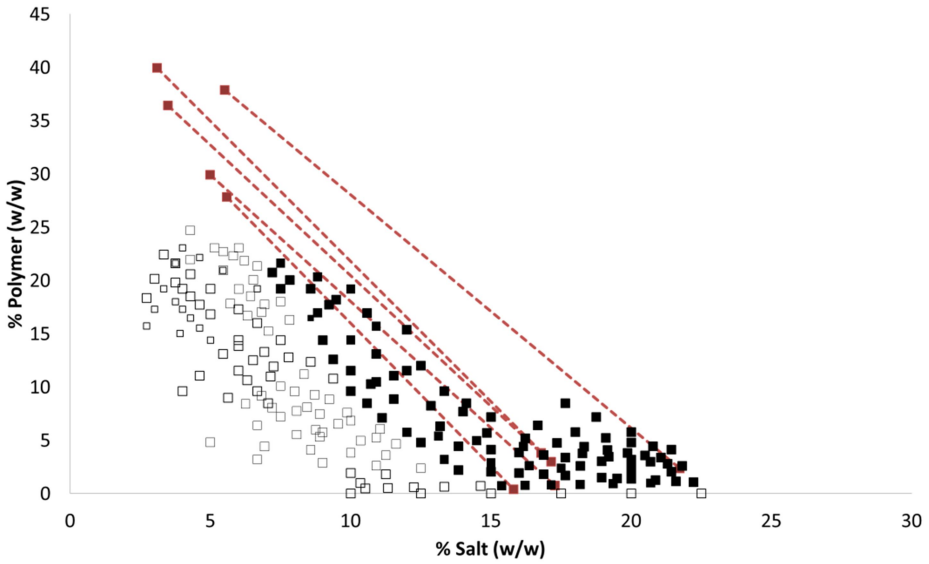

Figure 5.8 Tie-lie diagrams for PEG 6000 with ammonium citrate as the salt (at pH 8.0)

5.4 Conclusion

An efficient aqueous two-phase extraction (ATPE) system has been developed for the F-AmDH and applied to other dehydrogenases, including the amine dehydrogenase family. Successful small-scale purification of dehydrogenases was achieved and further work includes large-scale purification and back extraction out of the top polymer phase [work performed by Dr. Bettina Bommarius]. Initial phase diagrams have been created for our purification system. This purification procedure offers an efficient and environmentally friendly alternative to standard affinity protein purification.

CHAPTER 6

RECOMMENDATIONS AND CONCLUSIONS

6.1 Recommendations

6.1.1 Create variants to lower K_M value of ammonia of the amine dehydrogenases

The affinity towards ammonia for the amine dehydrogenases is still twenty times lower than for the amino acid dehydrogenases. Further work should focus on improving the K_M value toward the ammonia substrate. The work described in Section 3.3.7 in Chapter 3 suggests that cysteine or histidine may be the residue responsible for the binding of ammonia substrate. First, the same pH studies involving k_{cat} and K_M value towards ammonia should be repeated with the F-AmDH (as shown in Figure 3.16) in deuterated ammonia and fit to a double ionization model. If a cysteine residue is truly responsible for the binding of ammonia, pKa1 will shift 0.2 pH units. Cysteines located within the binding pocket of the F-AmDH include C52, C78, C141, C252 and C354. These cysteines should be mutated to alanine to determine if they are critical for catalysis and substrate binding. After determining which residue is important, surrounding residues should be mutated to maintain the correct protonation state within the active site (it is desired to deprotonate the cysteine residue). There is no histidine within the binding pocket of the F-AmDH. In addition, the residues R53, T123 and D131, should be closely investigated because previous mutations caused a dramatic decrease in the binding of ammonia and increase in the K_M value (Appendix B, Figure 6.1).

In addition, further work should look at different substrates with more electron withdrawing groups. Different substituents on the phenyl ring (Hammett correlation,

Figure C.2) did not have an impact on the binding of the ammonia substrate but did have an impact on catalytic activity [data discussed in Section 3.3.4]. Substituents on the methyl group should now be investigated because the difference between the substrates of the amino acid dehydrogenase and an amine dehydrogenase is the carboxyl attached instead of the methyl group. 2-chloro acetophenone and 2,2,2-trifluoro acetophenone both contain a substituent on the methyl group but the amine dehydrogenase showed no activity toward either substrate.

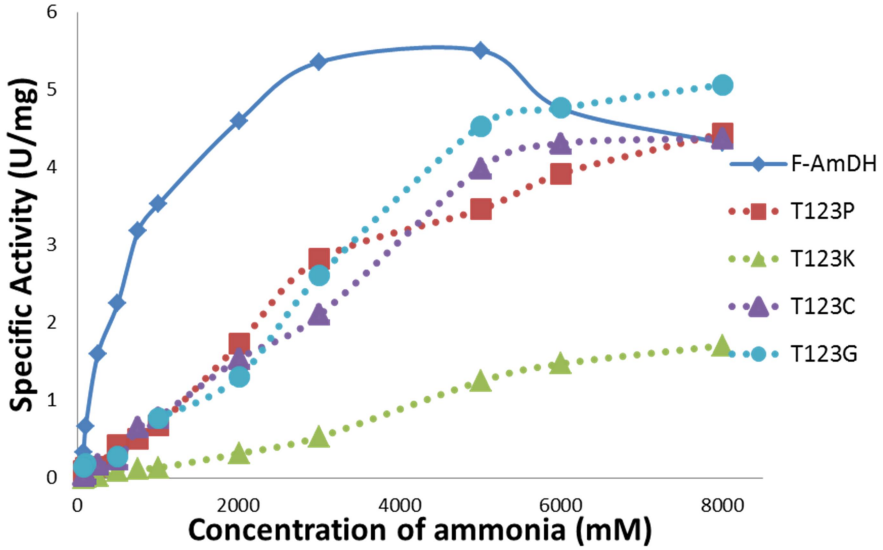

Figure 6.1 Impact of T123 mutations on the binding of ammonia

6.1.2 Expand the amine dehydrogenase family (V-AmDH and F-AmDH)

During the evolutionary route of creating AmDHs, the K77S and N275L mutations (PheDH nomenclature) were identified as essential to produce chiral amines. It is further suspected that these mutations are broadly applicable across the Glu-Leu-Phe-Val dehydrogenase sub-family. *Streptomyces cinnamonensis* valine dehydrogenase was chosen as the scaffold because it has previously been expressed in the pET-28a/ BL21

system [136, 137]. Previous work (performed by M.J. Abrahamson) codon optimized the gene because of the high GC content (around 71% GC-pairs). Characterization of the codon optimized valine dehydrogenase (ValDH) led to poor expression and only 9 to 16 U/mg of catalytic activity towards L-valine.

With the addition of mutations K76S and N272L, valine amine dehydrogenase (V-AmDH) was created exhibiting conversion of 2-methyl-3-butanone to (*R*)-1,2-dimethylpropyl amine (Figure 6.2). Conversion was observed *via* HPLC analysis, mass spectrometry and NMR [data not shown]. It exhibits a K_M value of around 20 mM for 2-methyl-3-butanone and 13 μM for NADH. The substrate profile for the V-AmDH is listed in Table 6.1. V-AmDH unexpectedly has activity toward *p*FPA but not for MIBK. Further work should focus on improving the catalytic activity, substrate range and protein expression of the V-AmDH. Switching to another valine dehydrogenase gene may be necessary to improve the protein expression; possible genes could include *Streptomyces aureofaciens* [138] and *Streptomyces albus* [139].

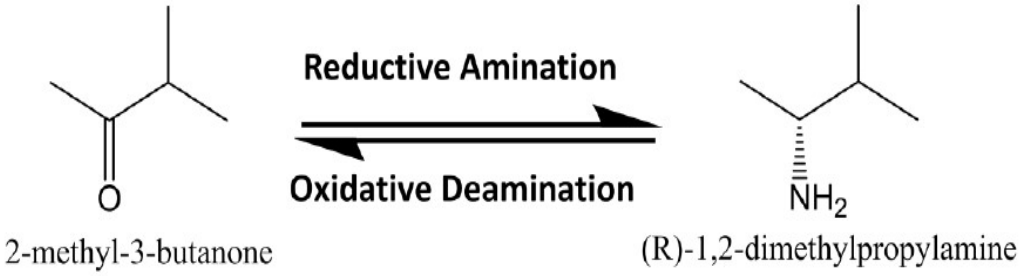

Figure 6.2 Valine AmDH reaction scheme

Table 6.1 Valine AmDH substrate profile

	Val-AmDH activity (U/mg)
Methyl isobutyl ketone (MIBK):	0.06
Para-fluoro phenyl acetone (*p*FPA):	0.44
Acetophenone:	0.04
3-methyl-2-butanone:	0.55
Pinacolone:	0.039

The *Rhodococcus sp.* phenylalanine DH could not be successfully mutated to create F-AmDH because adding mutations within the active site caused the protein to express in the insoluble fraction [data not shown]. However, Ye et al. were able to develop the *Rhodococcus sp.* F-AmDH [35]. It is critical that we develop our own *Rhodococcus sp.* F-AmDH because 1) the *Rhodococcus sp.* PheDH has been extensively studied- both the crystal structure and mechanism have been published [92, 93] and 2) the K_M value of ammonia was not reported for the *Rhodococcus sp.* F-AmDH. It is worth developing another F-AmDH to investigate any differences in the substrate profile and binding of ammonia. Future work should first look into improving the low expression of the wild-type *Rhodococcus sp.* phenylalanine dehydrogenase.

6.1.3 Improvement of kinetic resolution reaction conditions

The kinetic resolution reaction described in Chapter 4 exhibited poor reaction conditions- a significant amount of enzyme and cofactor NAD^+ had to be added to the reaction. When working with stoichiometric amounts of NAD^+, the reaction would drastically slow down around 80 to 90% conversion, giving less than 95% *e.e.* To convert 5 mM of (*R*)-amine, 5 to 10 equivalents of NAD^+ had to be added to drive the reaction to completion

and achieve greater than 99% *e.e.* (procedure described in Section 4.2.6). Further work should investigate and seek to improve the reaction conditions.

First, the conditions of the kinetic resolution reaction should be changed to allow for more oxygen transfer for the *Lactobacillus plantarum* NADH oxidase. The reaction vessel should change from a 1.7 mL Eppendorf tube to a 4 mL glass tube. A stir bar should be implemented to facilitate oxygen transfer in the beginning. Furthermore, a different NADH oxidase should also be investigated because it is suspected there is inefficient cofactor recycling in the reaction, causing a large amount of NAD^+ to be added into the reaction to achieve full conversion. *Lactobacillus plantarum* NADH oxidase currently exhibits high instability and begins to deactivate after 2 hours at room temperature [previously determined by Dr. Jonathan T. Park]. Without any NADH oxidase present, 78.17% conversion can already be achieved by just constantly adding NAD^+ into the system. Another NADH oxidase from *Lactobacillus sanfrancensis* should be expressed and purified to determine if it can be a more effective cofactor regeneration enzyme for kinetic resolution reactions. Temperature stability and activity studies should be performed.

The incorporation of a biphasic organic solvent system should be investigated. Different organic solvents include heptane, MTBE, toluene and chloroform and the reaction conditions described in Chapter 2 should be utilized. The product can be constantly removed by partitioning into the organic solvent from the aqueous medium [140]. The substrate can also be constantly added throughout the reaction to avoid any substrate inhibition.

6.1.4 Switch the enantioselectivity of the amine dehydrogenases

Asymmetric synthesis offers an advantage over kinetic resolution (as described in Chapter 4) in the production of pure enantiomers because of its 100% theoretical yield compared to 50% for kinetic resolution [141, 142]. However, the "mirror-image" enzyme most often is not available and thus only one but not both enantiomers are accessible through asymmetric synthesis. To develop a broad spectrum of possible API candidates for testing of drug efficacy, both enantiomers of the product amine are desired. To change the selectivity of the enzyme, residues located in the active site close to the residues participating in the chemical conversion of the substrate should be investigated. Studies of naturally occurring enantiocomplementary enzymes show that even though the pair catalyzes the same reaction, they can have different overall protein structures along with different functional groups located in the active site [142]. Inversion of enantioselectivity has been achieved by changing the location of key catalytic residues in a reaction mechanism. Successful inversion was accomplished in arylmalonate decarboxylase by exchanging the proton-donating cysteine to the opposite side of the active site [143-145]. Substitutions with larger residues into the active site cause steric effects that can affect the binding of the substrate and lead to a switch of enantioselectivity [146].

A high-throughput library was created with the attempt to switch the enantioselectivity of the AmDH from (*R*) to (*S*)-selectivity. The libraries were screened with *Bacillus badius* PheDH genes containing two different mutations located in the active site. The previous mutations introduced on the *B. badius* PheDH changed the substrate selectivity (K77 and N275), while these two new mutations are introduced with hopes to change the enantioselectivity (M74 and V308). Preservation of *(S)*-selectivity of

the PheDH will lead to formation of phenylpyruvate from (*S*)-phenylalanine. Wild-type activity toward phenylalanine was chosen as an assay for determining if inversion of enantioselectivity had been achieved because it is easier to screen in the deamination direction using an amine with already the desired enantioselectivity as the substrate. The substrate for F-AmDH, 1-(4-fluorophenyl)-propyl-2-amine, is only available as a racemate and is expensive. Successful variants will oxidize *(R)*-phenylalanine to phenylpyruvate. If these enantioselectivity mutations are successful, the addition of the previous mutations (K77S and N275L) can change substrate specificity toward *p*FPA.

Restricted libraries on both residues were performed synergistically as M74VWS and V308DDS on the wild-type PheDH. 1152 colonies were expressed at 25 and 30°C and screened for activity towards (*R*)-phenylalanine. The wild-type PheDH has an activity of 0.14 U/mg towards (*R*)-phenylalanine so this must be taken into account when screening for hits. 20 clones showing the highest activities were expressed and purified but there was no improved activity toward (*R*)-phenylalanine compared to the wild-type phenylalanine dehydrogenase. Further work should look at further mutations within the active site. Mutations to the M74 residue have resulted in inactive protein because it is probably essential for catalysis so another residue should be investigated instead. The same high throughput screening method involving (*R*) and (*S*) phenylalanine should be incorporated.

6.1.5 Investigate and expand the substrate profile of the amine dehydrogenases

As shown in Table 4.3 in Chapter 4, L-AmDH unexpectedly shows activity toward (*R*)-1-phenylethylamine (1-PEA) but little activity toward the ketone acetophenone (0.97 U/mg for deamination compared to 0.059 U/mg for amination, respectively). The same phenomenon was observed with the substrate (*R*)-3,3-DMBA and pinacolone with the L-AmDH (1.43 U/mg for deamination compared to 0.054 U/mg for amination, respectively). There should be further investigation to determine why the L-AmDH displays drastic activity differences between reductive amination and oxidative deamination. Further mutations and their impact on the substrate profile on the L-AmDH are listed in Table 6.2. Neither the F-AmDH nor the cFL1-AmDH displays this unique substrate profile.

Table 6.2 Mutations and substrate profile of the L-AmDH

	K67S/ N260L	**K67S/ N261L**	**K67M/ N260V**	**K67M/ N261L**	**K67M/ N260V/ N261L**	**K67M/ N260V/ N261V**
MIBK	0.91	0	0.77	0.046	0.092	0.48
1,3-DMBA	0.33	0.035	1.08	0.041	0.26	0.59
Acetophenone	0.049	0	0.4	0	0.052	0.24
PEA	0.7	0.017	0.93	0.06	0.2	0.79

There are many pharmaceutically relevant substrates that were not substrates of the amine dehydrogenases, such as 5-diethylamine-2-pentanone, 2-acetylpyridine, mexiletine and 1-(1-napthyl)ethylamine. Desired substrates should be modeled in AutoDock Vina® to determine the optimal binding conformation and what residues interact with the substrate. Rational design and directed evolution can be implemented to expand the current substrate profile of the amine dehydrogenases. The Y76 mutations opened up space in the binding pocket and improved catalytic activity of the F-AmDH towards *p*FPA up to 16

U/mg. Further work should test bulkier substrates with the Y76A variant and perform additional mutations within the active site (Figure 6.3).

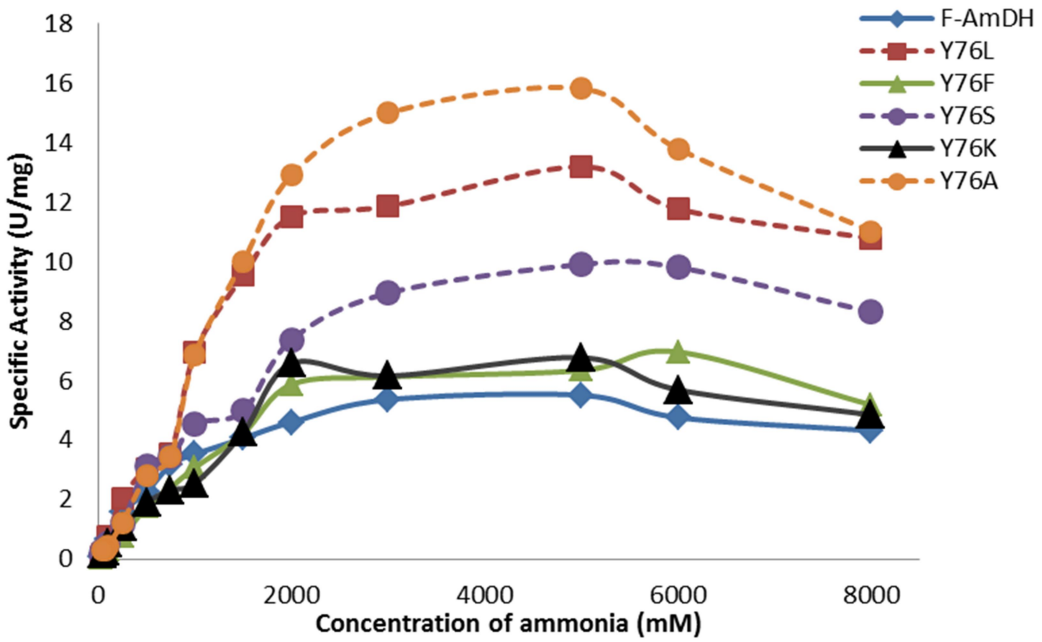

Figure 6.3 Impact of Y76 mutations on the catalytic activity of F-AmDH

6.1.6 Develop model to predict aqueous two-phase extraction system

So far, the aqueous two-phase extraction (ATPE) systems have only been applied to amine dehydrogenases and the cofactor regeneration enzymes, glucose and formate dehydrogenases. The main disadvantage of the ATPE is in the inability to predict partitioning behavior and testing numerous conditions can be tedious and time-consuming. Future work should focus on the purification of other enzymes beyond dehydrogenases and to develop a model to predict the partitioning behavior in an ATPE system.

First, the phase ratios at various polymer and salt concentrations (including NaCl) in an ATPE system should be thoroughly recorded and analyzed. The volume of each

phase is influenced by the amount of salt in the system (Figure 6.4) and molecular weight of the polymer (Figure 6.5) and can have an important impact on how the protein partitions between the two layers. The addition of NaCl affects the phase ratio as well as the formation of two immiscible aqueous layers (Figure 6.5). The pH did not have an impact on the phase ratios.

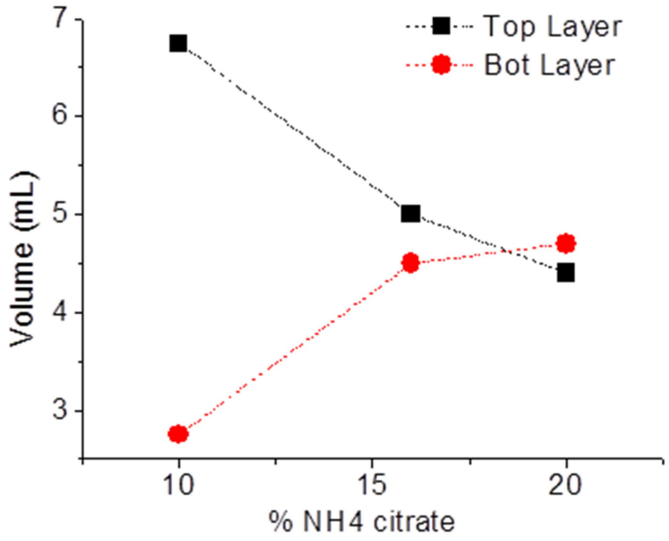

Figure 6.4 Impact of % (w/w) ammonium citrate on the volume ratio (PEG 1500, pH 5.5)

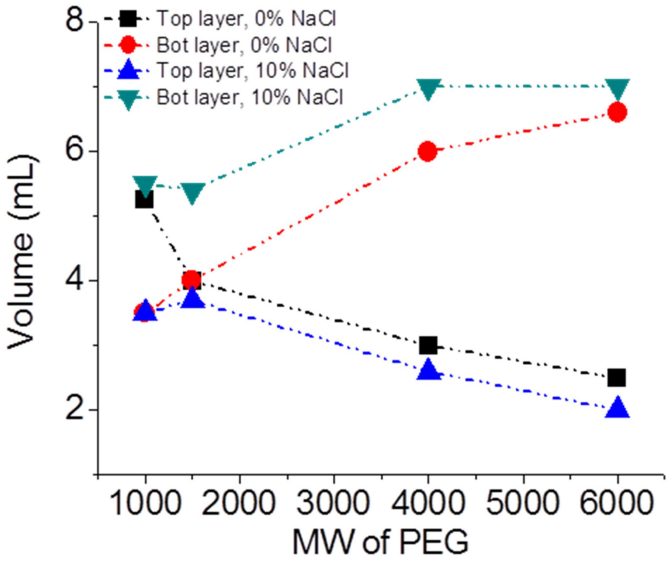

Figure 6.5 Impact of MW of PEG and addition of NaCl on the volume ratio (16 % (w/w) of ammonium citrate in the system, pH 8.0)

A model to predict which conditions are optimal for separation of each enzyme should take into account the molecular weight and amount of PEG, pH and type and amount of salt. If the molecular weight of the polymer is lower, the interfacial tension is decreased between the two phases [147]. In addition, the concentration of PEG impacts the hydrophobic interactions between the enzyme and polymer [148]. pH can impact the ATPE system through electrostatic interactions, depending on the isoelectric point and charge of the protein [149]. Lastly, the salts in the system affect the hydrophobicity and the 'salting-out' effect, which forces enzymes to move out of salt-rich phase to a PEG-rich phase [150]. Some potentially important characteristic of the dehydrogenases from Chapter 5 that can be used to build a universal model and procedure for ATPE systems are listed in Table 6.3.

Table 6.3 Characteristics of the dehydrogenases used in ATPE system

	# of aas	Molecular weight	Isoelectric point	Hydrophobicity index	Net Charge at pH 7.0
L-AmDH	367	40.46	5.56	-0.29	-8.5
cFL1-AmDH	376	41.04	5.75	-0.23	-8.5
F-AmDH	380	41.35	4.94	-0.2	-14.7
GluDH	330	34.76	4.8	0.01	-8.9
FDH	364	40.37	6.26	-0.28	-5.9

6.2 Conclusions

This work describes the development of the amine dehydrogenase for the enzymatic production of chiral amines. The substrate profile of the AmDHs was expanded to previously unattainable hydrophobic substrates with the incorporation of a biphasic organic solvent system. The initial study on the mechanism and binding of the ammonia substrate was extensively investigated on the novel AmDH through protein and reaction

engineering. Successful kinetic resolution reactions allowed for us to obtain the enantiomerically pure (*S*)-enantiomer (>99% *e.e.*). Lastly, the development of an aqueous two-phase extraction system was established and applied to dehydrogenases. The established purification protocol was very comparable to protein purification through affinity chromatography. Throughout the thesis work, various substrates were tested and protein engineering was performed with hopes to improve the specificity, activity and stability.

Future work should focus on preparing the amine dehydrogenase for industrial applications. The binding towards the ammonia substrate has to improve in order for the enzyme to be economically comparable to transaminases. Catalytically important amino acids within the active site of the AmDH should be investigated and mutated to maintain the correct protonation state. Any substrate or product inhibition should be studied so reactions of the AmDH can be continuously run at the optimal conditions. The substrate profile of the AmDH should constantly be expanded to cover more pharmaceutically relevant substrates and (*S*)-amines. Lastly, the aqueous two-phase extraction system should be applied to various enzymes, such as the alcohol dehydrogenases. A model should be developed to predict the protein partitioning in ATPE systems to avoid testing a large amount of conditions.

Appendix A

CHROMATOGRAMS FOR DEVELOPMENT OF BIPHASIC SYSTEM (CHAPTER 2)

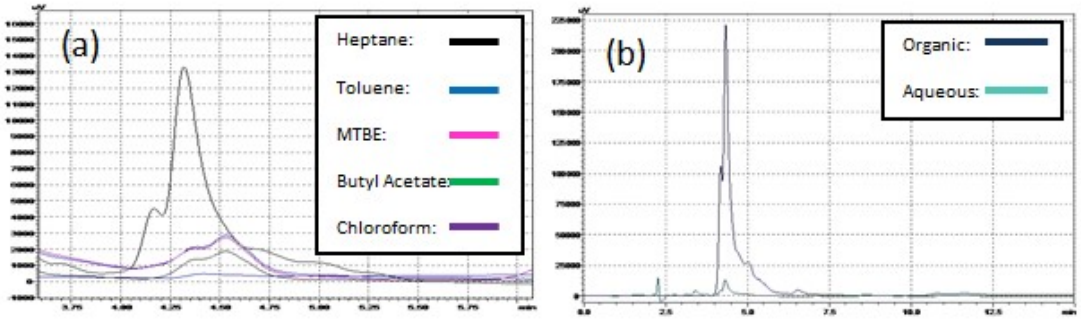

Figure A.1 Investigation of partition coefficient of *p*FPA: aqueous layers partitioning with various organic solvents (a), partition comparison between heptane and aqueous layer (b).

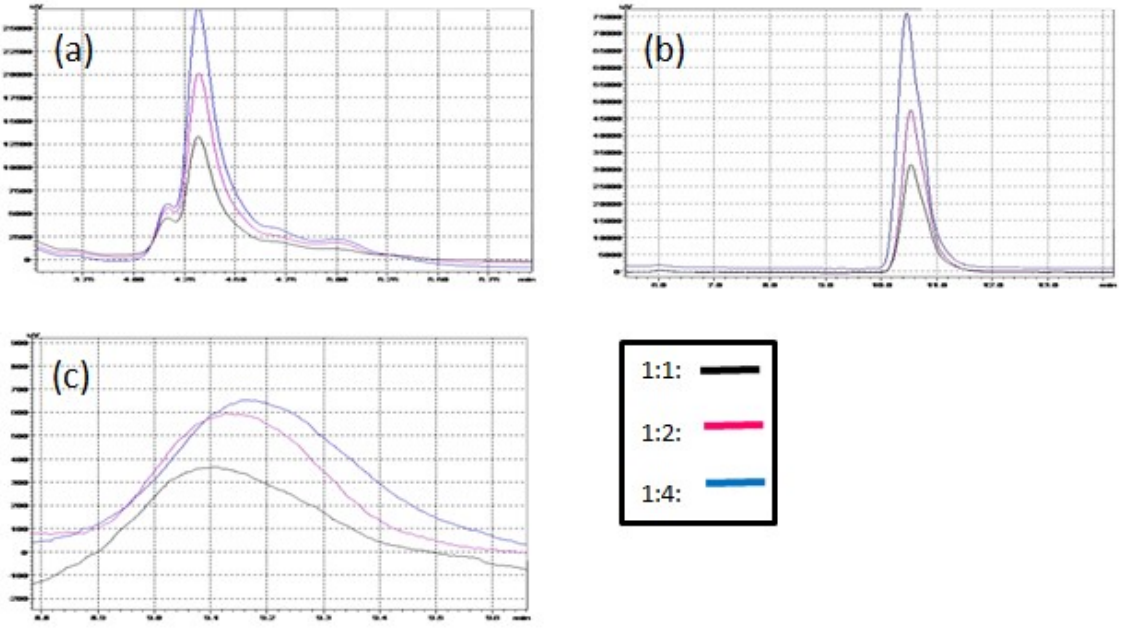

Figure A.2 The effect of the phase ratio on the partitioning of hydrophobic substrates in the aqueous layer: *p*FPA (a), acetophenone (b), 3-methyl-1-phenyl-2-butanone (c).Very little 1-adamantyl methyl ketone is present in the aqueous phase so no respective chromatogram is shown.

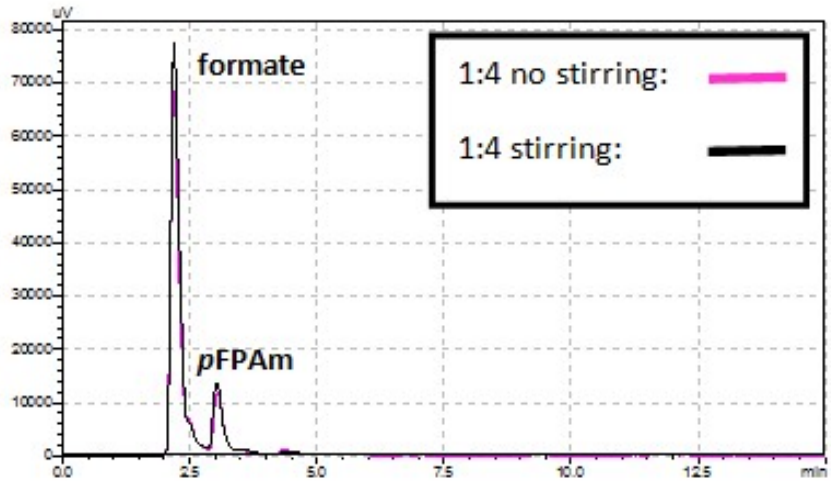

Figure A.3 Effect of stirring in the biphasic conversion of *p*FPA in the aqueous layer

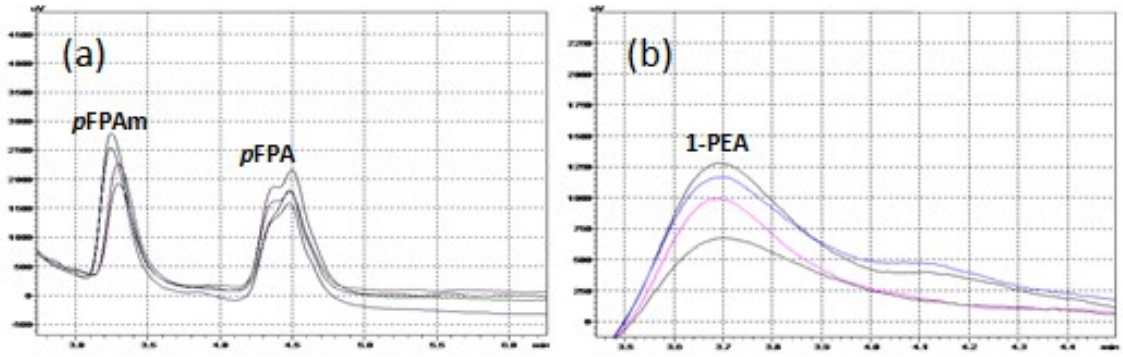

Figure A.4 Initial monophasic conversion of *p*FPA (a) and acetophenone (b).

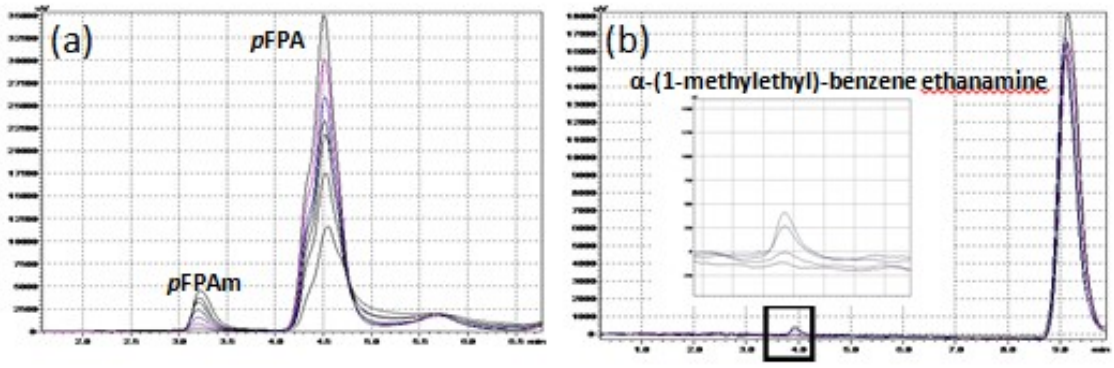

Figure A.5 Initial biphasic conversion of *p*FPA (a) and 3-methyl-1-phenyl-2-butanone (b) in heptane.

Appendix B

PHENYLALANINE AMINE DEHYDROGENASE (F-AMDH) VARIANTS (CHAPTER 3)

Table B.1 F-AmDH variants (base case= K77S/N275L) and their respective activity and K_M-NH_4. All activity was measured in 5 M $NH_4OH/CHOO^-$ buffer at 25°C.

Variant	Specific Activity	K_M-NH_4
R53D	None	N/A
R69D	No change	No change
K192D	No change	No change
A236D	No change	No change
G200H/L202H	No change	No change
R286D	1.5X less	No change
L49S	7X less	No change
L49A	3.5X less	No change
V143F	None	N/A
V143S	1.5X less	No change
Y76L	2X more	No change
Y76F	No change	No change
Y76K	No change	No change
Y76S	1.5X more	No change
Y76A	2.5X more	No change
D124K	None	N/A
D124H	None	N/A
D124A	None	N/A
T123P	No change	Worse (>1.5 M)
T123C	No change	Worse (>1.5 M)
T123G	No change	Worse (>1.5 M)
T123N	No change	Worse (>1.5 M)
T123K	4X less	Worse (>1.5 M)
N275K	4X less	Worse (>1.5 M)
K77K	50X less	No change
N276L	2.5X less	No change
N276Q	1.5X less	No change
N276H	No change	No change
K89S	No change	No change
K89S/Y76A	No change	Worse (>1.5 M)
K89S (w/o K77S)	100X less	N/A
K89S (w/o N275L)	100X less	N/A

Table B.1 (continued)

K89S (w/o K77S/N275L)	None	N/A
G50K	None	N/A
G122K	None	N/A
D82E	No change	No change
D82K	4X less	No change
D131E	No change	Worse (>1.5 M)
D131K	1.5X less	Worse (>1.5 M)
S155G	5X less	Worse (>1.5 M)
S155A	2X less	No change
S155K	None	N/A
T123K/D131K	6X less	Worse (>1.5 M)
D124K/D131K	None	N/A
K89M	10X less	No change
K89M/D124E	None	N/A
G51K	None	N/A
R53K	No change	Worse (>1.5 M)
D88K	None	N/A
N276K	2X less	Worse (>1.5 M)
Y298A	2X more	No change

Appendix C

AFFINITY TOWARDS AMMONIA AT VARIOUS BUFFER CONDITIONS (CHAPTER 3)

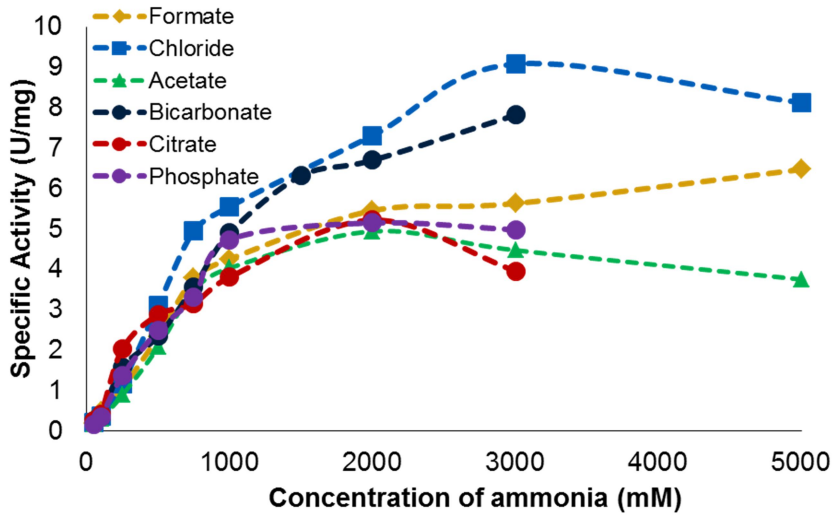

Figure C.1 Affinity towards ammonia with different ammonia buffers with F-AmDH. Activity measured at 25°C.

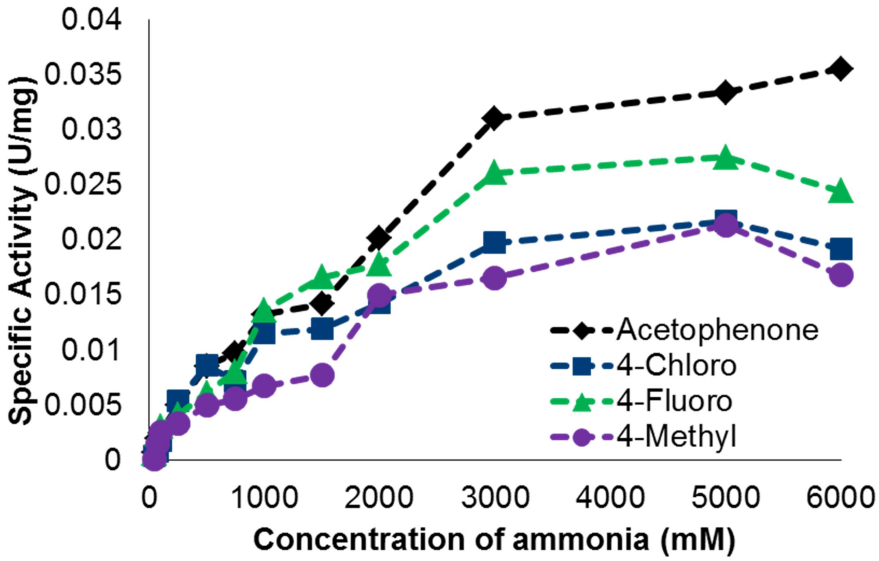

Figure C.2 Affinity towards ammonia with different substituents on the phenyl ring with cFL1-AmDH. Activity measured at 25°C.

Table C.1 Affinity towards *p*FPA at different pHs

5 M $NH_4/CHOO^-$ buffer	Specific Activity (U/mg)	K_M-*p*FPA (mM)
pH 11.5	1.65	2.87
pH 11.0	4.08	2.09
pH 10.0	5.34	3.03
pH 9.6	6.47	4.61
pH 9.0	5.39	2.19
pH 8.0	2.74	1.99
pH 7.0	1.21	1.3
pH 6.0	0.49	1.03

Table C.2 Affinity towards NADH at different pHs

5 M $NH_4/CHOO^-$ buffer	Specific Activity (U/mg)	K_M-NADH (mM)
pH 11.5	1.59	0.039
pH 11.0	2.23	0.035
pH 10.0	5.84	0.035
pH 9.6	6.47	0.04
pH 9.0	4.98	0.033
pH 8.0	2.69	0.051
pH 7.0	1.13	0.033
pH 6.0	0.84	0.057

Table C.3 Affinity towards ammonia at different pHs

5 M $NH_4/CHOO^-$ buffer	Specific Activity (U/mg)	K_M-*p*FPA (mM)
pH 11.5	1.09	675
pH 11.0	3.5	796
pH 10.0	5.68	698
pH 9.6	6.47	637
pH 9.0	5.33	799
pH 8.0	2.65	779
pH 7.0	1.31	1372
pH 6.0	0.23	1251

Appendix D

OPTIMIZED REACTION CONDITIONS FOR OXIDATIVE DEAMINATION (CHAPTER 4)

Table D.1 Activity of L-AmDH and NADH oxidase in various reaction buffers

Reaction buffer	pH	L-AmDH (U/mg)	NADH oxidase (U/mg)
1 M NH_4CHOO^-/OH	9.6	0.66	2.81
1 M NH_4CHOO^-/OH	8.0	0.15	51.93
0.1 M TEA	7.5	0.93	152.8
0.1 M glycine	8.0	1.09	93.02
0.1 M glycine	7.5	0.98	98.45
0.05 M Tris	8.0	1.32	80.38

Table D.2 Investigation of various reaction temperatures

(R/S)-1-PEA (mM)	NAD^+ (mM)	Temperature (°C)	Ratio of Units (L-AmDH to Nox)	Time (hours)	Conversion (%)
30	10	25	3 to 1	24	64.01
30	10	35	3 to 1	24	75.42
30	10	45	3 to 1	24	67.77

Table D.3 Investigation of various enzyme ratios of L-AmDH to NoxV

(R/S)-1-PEA (mM)	NAD^+ (mM)	Temperature (°C)	Ratio of Units (L-AmDH to Nox)	Time (hours)	Conversion (%)
30	10	25	1 to 1	24	38.71
30	10	25	2 to 1	24	47.19
30	10	25	3 to 1	24	64.01
30	10	25	4 to 1	24	66.66
30	10	25	5 to 1	24	71.14
30	10	25	6 to 1	24	78.69
30	10	25	7 to 1	24	67.32
30	10	25	8 to 1	24	62.33

Table D.4 Investigation of various initial concentrations of NAD^+

(R/S)-1-PEA (mM)	NAD^+ (mM)	Temperature (°C)	Ratio of Units (L-AmDH to Nox)	Time (hours)	Conversion (%)
30	22.5	25	3 to 1	24	66.35
30	10	25	3 to 1	24	66.12
30	5	25	3 to 1	24	35.29
30	2.5	25	3 to 1	24	20.37

Appendix E

CHROMATOGRAMS TO OBTAIN ENANTIOMERICALLY PURE (S)-AMINES (CHAPTER 4)

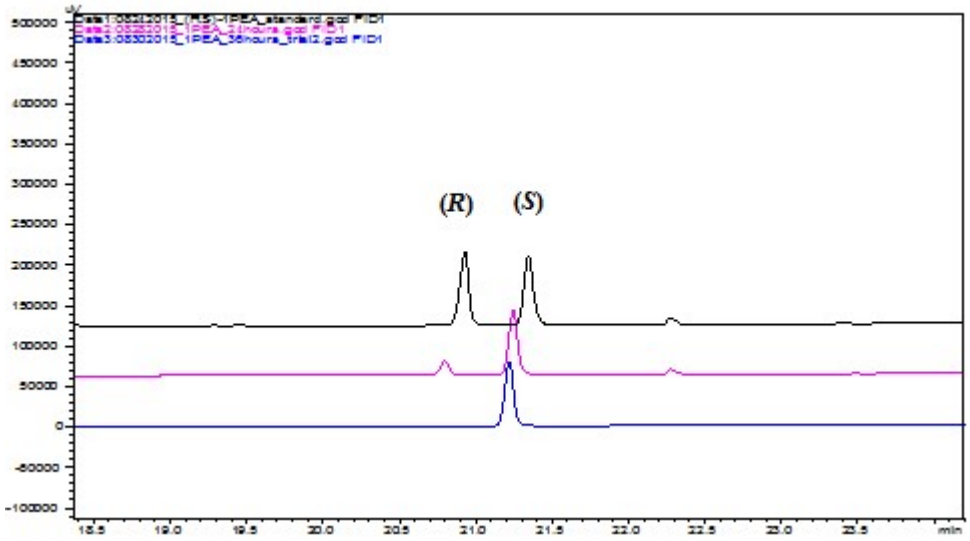

Figure E.1 GC chromatogram of oxidative deamination of racemic mixture (*R/S*)- 1-phenylethylamine (1-PEA) to leave pure (*S*)-1-PEA. Standard of (*R/S*)-1-PEA (black), reaction sample (pink/blue)

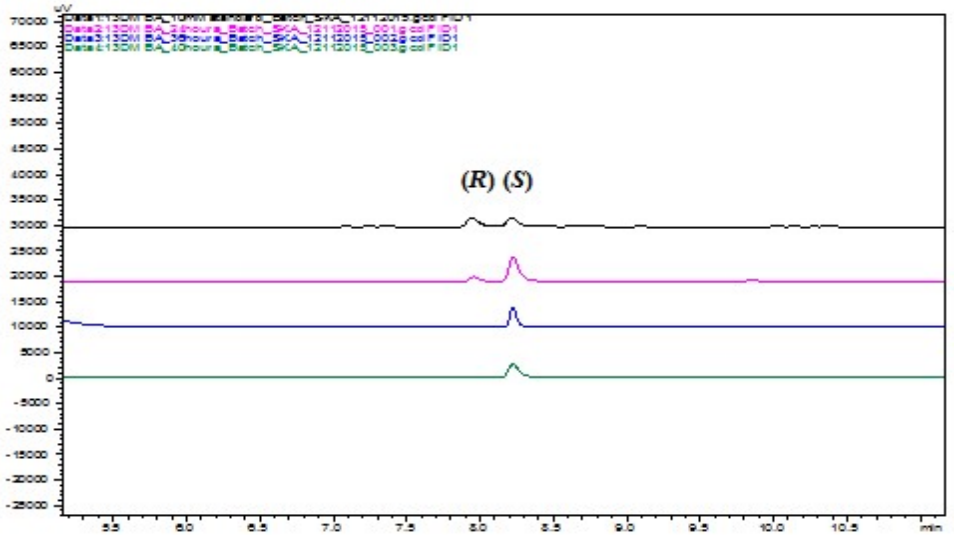

Figure E.2 GC chromatogram of oxidative deamination of racemic mixture (*R/S*)-1,3-dimethylbutylamine (DMBA) to leave pure (*S*)-1,3-DMBA. Standard of (*R/S*)-1,3-DMBA (black), reaction sample (pink/blue/green).

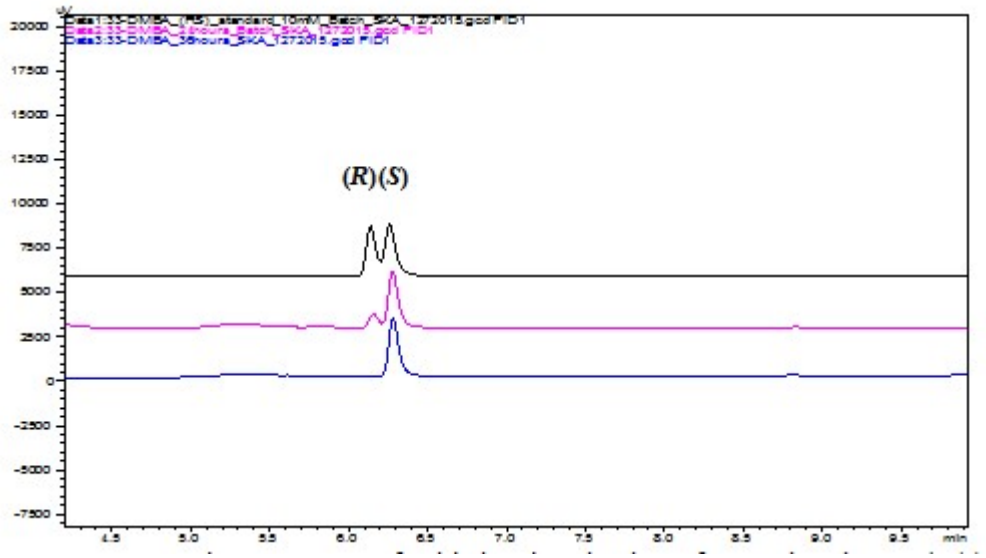

Figure E.3 GC chromatogram of oxidative deamination of racemic mixture (*R/S*)-3,3-dimethyl-2-butyl amine to leave pure (*S*)-3,3-DMBA. Standard of (*R/S*)-3,3-DMBA (black), reaction sample (pink/blue).

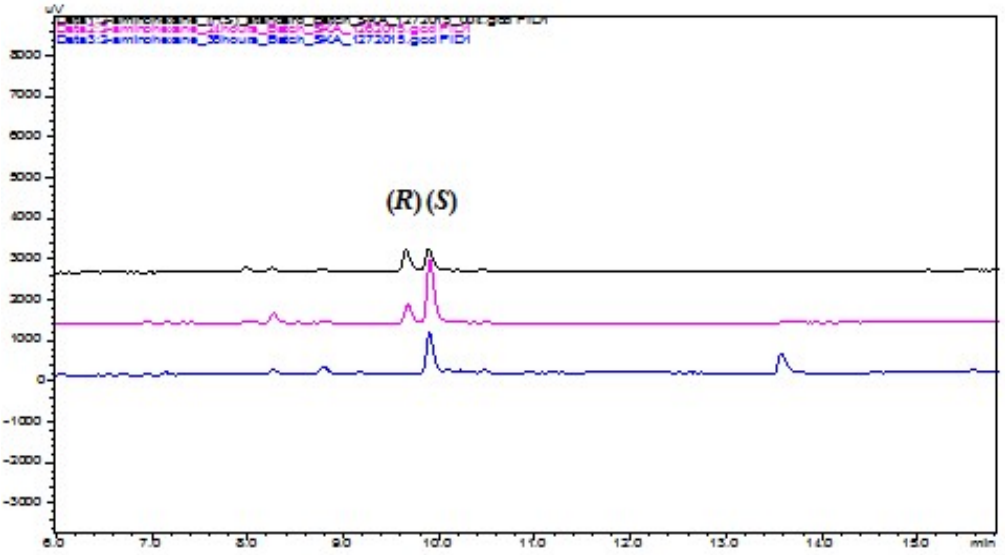

Figure E.4 GC chromatogram of oxidative deamination of racemic mixture (*R/S*)-2-aminohexane to leave pure (*S*)-2-aminohexane. Standard of (*R/S*)-2-aminohexane (black), reaction sample (pink/blue).

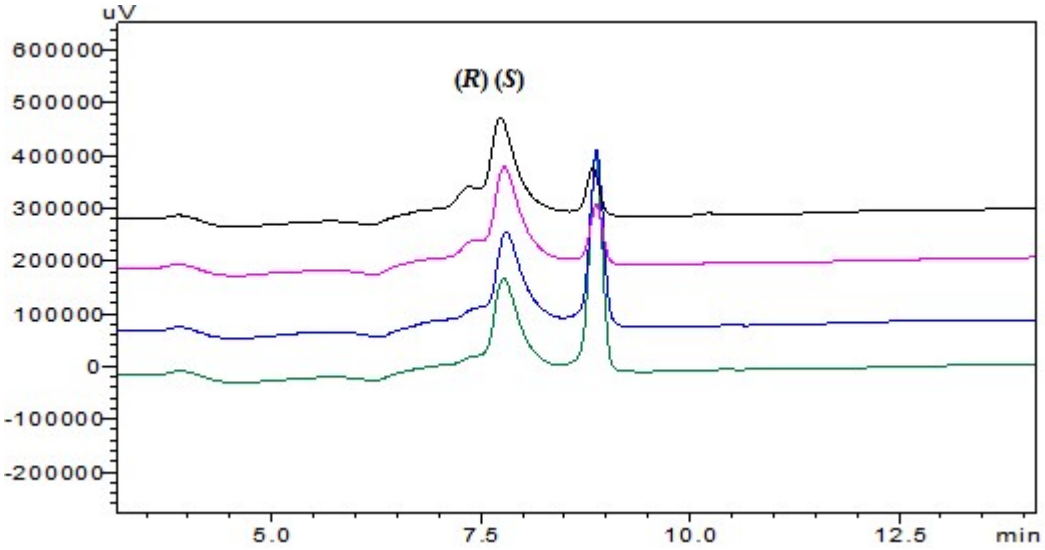

Figure E.5 HPLC chromatogram of oxidative deamination of 10 mM racemic mixture (*R/S*)-1-(2-napthyl)ethylamine to leave pure (*S*)-1-(2-napthyl)ethylamine. Time points: 12 hours (black), 24 hours (pink), 36 hours (blue) and 48 hours (green). Reaction samples are diluted with isopropanal before injection.

REFERENCES

1. Wolfenden, R. and M.J. Snider, *The depth of chemical time and the power of enzymes as catalysts.* Accounts of Chemical Research, 2001. **34**(12): p. 938-945.

2. Bommarius, A.S.R.-B., B.R., *Biocatalysis*. 2004: Wiley-Blackwell. 634.

3. de Carvalho, C.C.C.R., *Enzymatic and whole cell catalysis: Finding new strategies for old processes.* Biotechnology Advances, 2011. **29**(1): p. 75-83.

4. Chotani, G., et al., *The commercial production of chemicals using pathway engineering.* Biochimica Et Biophysica Acta-Protein Structure and Molecular Enzymology, 2000. **1543**(2): p. 434-455.

5. Pollard, D.J. and J.M. Woodley, *Biocatalysis for pharmaceutical intermediates: the future is now.* Trends in Biotechnology, 2007. **25**(2): p. 66-73.

6. Thayer, A.M., *Centering on chirality.* Chemical & Engineering News, 2007. **85**(32): p. 11-19.

7. Fazlena, H., A.H. Kamaruddin, and M.M.D. Zulkali, *Dynamic kinetic resolution: alternative approach in optimizing S-ibuprofen production.* Bioprocess and Biosystems Engineering, 2006. **28**(4): p. 227-233.

8. Carey, J.S., et al., *Analysis of the reactions used for the preparation of drug candidate molecules.* Organic & Biomolecular Chemistry, 2006. **4**(12): p. 2337-2347.

9. Mack, D.J., et al. *Top 200 Brand Name Drugs by US Retail Sales in 2010*. 2010; Available from: http://cbc.arizona.edu/njardarson/group/top-pharmaceuticals-poster.

10. Hansen, K.B., et al., *Highly Efficient Asymmetric Synthesis of Sitagliptin.* Journal of the American Chemical Society, 2009. **131**(25): p. 8798-8804.

11. Kadyrov, R. and T.H. Riermeier, *Highly enantioselective hydrogen-transfer reductive amination: Catalytic asymmetric synthesis of primary amines.* Angewandte Chemie-International Edition, 2003. **42**(44): p. 5472-5474.

12. Gomez, S., J.A. Peters, and T. Maschmeyer, *The reductive amination of aldehydes and ketones and the hydrogenation of nitriles: Mechanistic aspects and selectivity control.* Advanced Synthesis & Catalysis, 2002. **344**(10): p. 1037-1057.

13. Nugent, T.C., *Chiral Amine Synthesis: Methods, Developments and Applications*. 2010: John Wiley & Sons.

14. Constable, D.J.C., et al., *Key green chemistry research areas - a perspective from pharmaceutical manufacturers.* Green Chemistry, 2007. **9**(5): p. 411-420.

15. Koszelewski, D., et al., *omega-Transaminases for the synthesis of non-racemic alpha-chiral primary amines.* Trends in Biotechnology, 2010. **28**(6): p. 324-332.

16. Mathew, S. and H. Yun, *omega-Transaminases for the Production of Optically Pure Amines and Unnatural Amino Acids.* Acs Catalysis, 2012. **2**(6): p. 993-1001.

17. Tufvesson, P., et al., *Process Considerations for the Asymmetric Synthesis of Chiral Amines Using Transaminases.* Biotechnology and Bioengineering, 2011. **108**(7): p. 1479-1493.

18. Hohn, M. and U.T. Bornscheuer, *Biocatalytic Routes to Optically Active Amines.* Chemcatchem, 2009. **1**(1): p. 42-51.

19. Park, E.S., M. Kim, and J.S. Shin, *Molecular determinants for substrate selectivity of omega-transaminases.* Applied Microbiology and Biotechnology, 2012. **93**(6): p. 2425-2435.

20. Steffen-Munsberg, F., et al., *Revealing the Structural Basis of Promiscuous Amine Transaminase Activity.* Chemcatchem, 2013. **5**(1): p. 154-157.

21. Pressnitz, D., et al., *Asymmetric Amination of Tetralone and Chromanone Derivatives Employing w-transaminase.* ACS Catal., 2013. **3**: p. 555-559.

22. Busto, E., et al., *Cutting Short the Asymmetric Synthesis of the Ramotroban Precursor by Employing w-transaminases.* Advanced Synthesis & Catalysis, 2014.

23. Koszelewski, D., et al., *Deracemization of Mexiletine Biocatalyzed by omega-Transaminases.* Organic Letters, 2009. **11**(21): p. 4810-4812.

24. Simon, R.C., et al., *Enzymatic asymmetric synthesis of the silodosin amine intermediate.* Tetrahedron-Asymmetry, 2014. **25**(3): p. 284-288.

25. Mutti, F.G., et al., *Stereoselectivity of Four (R)-Selective Transaminases for the Asymmetric Amination of Ketones.* Advanced Synthesis & Catalysis, 2011. **353**(17): p. 3227-3233.

26. Schatzle, S., et al., *Enzymatic Asymmetric Synthesis of Enantiomerically Pure Aliphatic, Aromatic and Arylaliphatic Amines with (R)-Selective Amine Transaminases.* Advanced Synthesis & Catalysis, 2011. **353**(13): p. 2439-2445.

27. Deepankumar, K., et al., *Enhancing Thermostability and Organic Solvent Tolerance of w-Transaminase through Global Incorporation of Fluorotyrosine.* Advanced Synthesis & Catalysis, 2014. **356**(5): p. 993-998.

28. Green, A.P., N.J. Turner, and E. O'Reilly, *Chiral Amine Synthesis Using omega-Transaminases: An Amine Donor that Displaces Equilibria and Enables High-Throughput Screening.* Angewandte Chemie-International Edition, 2014. **53**(40): p. 10714-10717.

29. Willies, S.C., et al., *A stereospecific solid-phase screening assay for colonies expressing both (R)- and (S)-selective omega-aminotransferases.* Philosophical Transactions of the Royal Society a-Mathematical Physical and Engineering Sciences, 2016. **374**(2061).

30. Savile, C.K., et al., *Biocatalytic Asymmetric Synthesis of Chiral Amines from Ketones Applied to Sitagliptin Manufacture.* Science, 2010. **329**(5989): p. 305-309.

31. Bommarius, A.S. and S.K. Au, *Chapter 2.4.1. Amino Acid and Amine Dehydrogenases*. Science of Synthesis Reference Library: Biocatalysis in Organic Synthesis (Vol. 2). 2015.

32. Abrahamson, M.J., et al., *Development of an Amine Dehydrogenase for Synthesis of Chiral Amines.* Angewandte Chemie-International Edition, 2012. **51**(16): p. 3969-3972.

33. Abrahamson, M.J., J.W. Wong, and A.S. Bommarius, *The Evolution of an Amine Dehydrogenase Biocatalyst for the Asymmetric Production of Chiral Amines.* Advanced Synthesis & Catalysis, 2013. **355**(9): p. 1780-1786.

34. Bommarius, B.R., M. Schurmann, and A.S. Bommarius, *A novel chimeric amine dehydrogenase shows altered substrate specificity compared to its parent enzymes.* Chemical Communications, 2014. **50**(95): p. 14953-14955.

35. Ye, L.J., et al., *Engineering of Amine Dehydrogenase for Asymmetric Reductive Amination of Ketone by Evolving Rhodococcus Phenylalanine Dehydrogenase.* Acs Catalysis, 2015. **5**(2): p. 1119-1122.

36. Abu, R. and J.M. Woodley, *Application of Enzyme Coupling Reactions to Shift Thermodynamically Limited Biocatalytic Reactions.* Chemcatchem, 2015. **7**(19): p. 3094-3105.

37. Schrittwieser, J.H., et al., *Recent biocatalytic oxidation-reduction cascades.* Current Opinion in Chemical Biology, 2011. **15**(2): p. 249-256.

38. Mutti, F.G., et al., *Conversion of alcohols to enantiopure amines through dual-enzyme hydrogen-borrowing cascades.* Science, 2015. **349**(6255): p. 1525-1529.

39. Wang, J.R., M.T., *Chiral Cascades.* Nature Chemistry, 2015. **7**.

40. Chen, F.F.L., Y.Y.; Zhen, G.W.; Xu, J.H, *Asymmetric amination of secondary alcohols by using a redox-neutral two-enzyme cascade.* ChemCatChem, 2015. **7**(28): p. 3838-3841.

41. Paul, C.E., I.W.C.E. Arends, and F. Hollmann, *Is Simpler Better? Synthetic Nicotinamide Cofactor Analogues for Redox Chemistry.* Acs Catalysis, 2014. **4**(3): p. 788-797.

42. Bommarius, B., et al., *Data-driven de novo protein design*, in *Zing Biocatalysis*2012, December Xcaret, Mexico.

43. Vazquez-Figueroa, E., J. Chaparro-Riggers, and A.S. Bommarius, *Development of a thermostable glucose dehydrogenase by a structure-guided consensus concept.* Chembiochem, 2007. **8**(18): p. 2295-2301.

44. Labrou, N.E., D.J. Rigden, and Y.D. Clonis, *Characterization of the NAD(+) binding site of Candida boidinii formate dehydrogenase by affinity labelling and site-directed mutagenesis.* European Journal of Biochemistry, 2000. **267**(22): p. 6657-6664.

45. Schirwitz, K., A. Schmidt, and V.S. Lamzin, *High-resolution structures of formate dehydrogenase from Candida boidinii.* Protein Science, 2007. **16**(6): p. 1146-1156.

46. Slusarczyk, H., et al., *Stabilization of NAD-dependent formate dehydrogenase from Candida boidinii by site-directed mutagenesis of cysteine residues.* European Journal of Biochemistry, 2000. **267**(5): p. 1280-1289.

47. Ansorge-Schumacher, M.B., et al., *Directed evolution of formate dehydrogenase from Candida boidinii for improved stability during entrapment in polyacrylamide.* Febs Journal, 2006. **273**(17): p. 3938-3945.

48. Zhang, Y.W., et al., *Cloning and characterization of a thermostable H2O-forming NADH oxidase from Lactobacillus rhamnosus.* Enzyme and Microbial Technology, 2012. **50**(4-5): p. 255-262.

49. Park, J.T., et al., *NAD(P)H oxidase V from Lactobacillus plantarum (NoxV) displays enhanced operational stability even in absence of reducing agents.* Journal of Molecular Catalysis B-Enzymatic, 2011. **71**(3-4): p. 159-165.

50. Riebel, B.R., et al., *Cofactor regeneration of both NAD(+) from NADH and NADP(+) from NADPH : NADH oxidase from Lactobacillus sanfranciscensis.* Advanced Synthesis & Catalysis, 2003. **345**(6-7): p. 707-712.

51. Lountos, G.T., et al., *The crystal structure of NAD(P)H oxidase from Lactobacillus sanfranciscensis: Insights into the conversion of O-2 into two water molecules by the flavoenzyme.* Biochemistry, 2006. **45**(32): p. 9648-9659.

52. Geueke, B., B. Riebel, and W. Hummel, *NADH oxidase from Lactobacillus brevis: a new catalyst for the regeneration of NAD.* Enzyme and Microbial Technology, 2003. **32**(2): p. 205-211.

53. Hummel, W. and B. Riebel, *Isolation and biochemical characterization of a new NADH oxidase from Lactobacillus brevis.* Biotechnology Letters, 2003. **25**(1): p. 51-54.

54. Kuzu, M., et al., *Crystallization and preliminary crystallographic analysis of a flavoprotein NADH oxidase from Lactobacillus brevis.* Acta Crystallographica Section F-Structural Biology and Crystallization Communications, 2005. **61**: p. 528-530.

55. Gao, H., et al., *Role of surface residue 184 in the catalytic activity of NADH oxidase from Streptococcus pyogenes.* Applied Microbiology and Biotechnology, 2014. **98**(16): p. 7081-7088.

56. Bommarius, A.S., J.K. Blum, and M.J. Abrahamson, *Status of protein engineering for biocatalysts: how to design an industrially useful biocatalyst.* Current Opinion in Chemical Biology, 2011. **15**(2): p. 194-200.

57. Bloom, J.D. and F.H. Arnold, *In the light of directed evolution: Pathways of adaptive protein evolution.* Proceedings of the National Academy of Sciences of the United States of America, 2009. **106**: p. 9995-10000.

58. Peisajovich, S.G. and D.S. Tawfik, *Protein engineers turned evolutionists.* Nature Methods, 2007. **4**(12): p. 991-994.

59. Klibanov, A.M., *Improving enzymes by using them in organic solvents.* Nature, 2001. **409**(6817): p. 241-246.

60. Zaks, A. and A.M. Klibanov, *Enzyme-Catalyzed Processes in Organic-Solvents.* Proceedings of the National Academy of Sciences of the United States of America, 1985. **82**(10): p. 3192-3196.

61. Mutti, F.G. and W. Kroutil, *Asymmetric Bio-amination of Ketones in Organic Solvents.* Advanced Synthesis & Catalysis, 2012. **354**(18): p. 3409-3413.

62. Truppo, M.D., H. Strotman, and G. Hughes, *Development of an Immobilized Transaminase Capable of Operating in Organic Solvent.* Chemcatchem, 2012. **4**(8): p. 1071-1074.

63. Klibanov, A.M., *Asymmetric enzymatic oxidoreductions in organic solvents.* Current Opinion in Biotechnology, 2003. **14**(4): p. 427-431.

64. Cainelli, G., et al., *Engineered phenylalanine dehydrogenase in organic solvents: homogeneous and biphasic enzymatic reactions.* Organic & Biomolecular Chemistry, 2005. **3**(24): p. 4316-4320.

65. De Temino, D.M., W. Hartmeier, and M.B. Ansorge-Schumacher, *Entrapment of the alcohol dehydrogenase from Lactobacillus kefir in polyvinyl alcohol for the synthesis of chiral hydrophobic alcohols in organic solvents.* Enzyme and Microbial Technology, 2005. **36**(1): p. 3-9.

66. Stepankova, V., et al., *Strategies for Stabilization of Enzymes in Organic Solvents.* ACS Catal., 2013. **3**: p. 2823-2836.

67. Luetz, S., L. Giver, and J. Lalonde, *Engineered Enzymes for Chemical Production.* Biotechnol Bioeng, 2008. **101**(4): p. 647-653.

68. Gorman, L.A.S. and J.S. Dordick, *Organic-Solvents Strip Water Off Enzymes.* Biotechnol Bioeng, 1992. **39**(4): p. 392-397.

69. Groger, H., et al., *Preparative asymmetric reduction of ketones in a biphasic medium with an (S)-alcohol dehydrogenase under in situ-cofactor-recycling with a formate dehydrogenase.* Tetrahedron, 2004. **60**(3): p. 633-640.

70. Groger, H., et al., *Practical asymmetric enzymatic reduction through discovery of a dehydrogenase-compatible biphasic reaction media.* Org Lett, 2003. **5**(2): p. 173-176.

71. Mohamadi, H.S., E. Omidinia, and R. Dinarvand, *Evaluation of recombinant phenylalanine dehydrogenase behavior in aqueous two-phase partitioning.* Process Biochemistry, 2007. **42**(9): p. 1296-1301.

72. Chen, S.H. and P.C. Engel, *An engineered mutant, L307V of phenylalanine dehydrogenase from Bacillus sphaericus: high activity and stability in organic-aqueous solvent mixtures and utility for synthesis of non-natural L-amino acids.* Enzyme and Microbial Technology, 2007. **40**(5): p. 1407-1411.

73. Kim, D., et al., *(2R)-4-Oxo-4-[3-(trifluoromethyl)-5,6-dihydro[1,2,4]triazolo[4,3-alpha]pyrazin-7(8H)-yl]-1-(2,4,5-trifluorophenyl)butan-2-amine: A potent, orally active dipeptidyl peptidase IV inhibitor for the treatment of type 2 diabetes.* J Med Chem, 2005. **48**(1): p. 141-151.

74. Augeri, D.J., et al., *Discovery and preclinical profile of saxagliptin (BMS-477118): A highly potent, long-acting, orally active dipeptidyl peptidase IV inhibitor for the treatment of type 2 diabetes.* J Med Chem, 2005. **48**(15): p. 5025-5037.

75. Bradford, M.M., *Rapid and Sensitive Method for Quantitation of Microgram Quantities of Protein Utilizing Principle of Protein-Dye Binding.* Analytical Biochemistry, 1976. **72**(1-2): p. 248-254.

76. Zhao, L.M., L.Y. Zhu, and H.K. Lee, *Analysis of aromatic amines in water samples by liquid-liquid-liquid microextraction with hollow fibers and high-*

performance liquid chromatography. Journal of Chromatography A, 2002. **963**(1-2): p. 239-248.

77. Stepankova, V., J. Damborsky, and R. Chaloupkova, *Organic co-solvents affect activity, stability and enantioselectivity of haloalkane dehalogenases.* Biotechnol J, 2013. **8**(6): p. 719-729.

78. Dordick, J.S., *Enzymatic Catalysis in Monophasic Organic-Solvents.* Enzyme and Microbial Technology, 1989. **11**(4): p. 194-211.

79. *ACS GCI pharmaceutical roundtable solvent selection guide*, 2011, American Chemical society, GCI, Pharmaceutical Roundtable: www.acs.org.gcipharmaroundtable.

80. Villela, M., et al., *Is log P a convenient criterion to guide the choice of solvents for biphasic enzymatic reactions?* Angewandte Chemie-International Edition, 2003. **42**(26): p. 2993-2996.

81. (ACD/Labs), A.C.D., 1994-2013.

82. Carrea, G., *Biocatalysis in Water-Organic Solvent 2-Phase Systems.* Trends Biotechnol, 1984. **2**(4): p. 102-106.

83. Klibanov, A.M., et al., *A new approach to preparative enzymatic synthesis (Reprinted from Biotechnology and Bioengineering, vol 19, pg 1351-1361, 1977).* Biotechnol Bioeng, 2000. **67**(6): p. 737-747.

84. Laane, C., et al., *Rules for Optimization of Biocatalysis in Organic-Solvents.* Biotechnol Bioeng, 1987. **30**(1): p. 81-87.

85. Faber, K., *Biotransformations in organic chemistry*. 2011, New York: Springer.

86. Baldascini, H., et al., *Effect of mass transfer limitations on the enzymatic kinetic resolution of epoxides in a two-liquid-phase system.* Biotechnol Bioeng, 2001. **73**(1): p. 44-54.

87. Willeman, W.F., et al., *Development of (R)-4-hydroxymandelonitrile synthesis in an aqueous-organic biphasic stirred tank batch reactor.* Biotechnol Bioeng, 2002. **79**(2): p. 154-164.

88. Ducret, A., M. Trani, and R. Lortie, *Lipase-catalyzed enantioselective esterification of ibuprofen in organic solvents under controlled water activity.* Enzyme and Microbial Technology, 1998. **22**(4): p. 212-216.

89. Ghanem, A. and H.Y. Aboul-Enein, *Lipase-mediated chiral resolution of racemates in organic solvents.* Tetrahedron-Asymmetry, 2004. **15**(21): p. 3331-3351.

90. Ho, S.N., et al., *Site-Directed Mutagenesis by Overlap Extension Using the Polymerase Chain-Reaction.* Gene, 1989. **77**(1): p. 51-59.

91. Higuchi, R., B. Krummel, and R.K. Saiki, *A general method of in vitro preparation and specific mutagenesis of DNA fragments: study of protein and DNA interactions.* Nucleic Acids Res, 1988. **16**(15): p. 7351-67.

92. Brunhuber, N.M.W., et al., *Rhodococcus L-phenylalanine dehydrogenase: Kinetics, mechanism, and structural basis for catalytic specifity.* Biochemistry, 2000. **39**(31): p. 9174-9187.

93. Vanhooke, J.L., et al., *Phenylalanine dehydrogenase from Rhodococcus sp. M4: High-resolution X-ray analyses of inhibitory ternary complexes reveal key features in the oxidative deamination mechanism.* Biochemistry, 1999. **38**(8): p. 2326-2339.

94. Brunhuber, N.M.W. and J.S. Blanchard, *The Biochemistry and Enzymology of Amino-Acid Dehydrogenases.* Critical Reviews in Biochemistry and Molecular Biology, 1994. **29**(6): p. 415-467.

95. Steffen-Munsberg, F., et al., *Bacillus anthracis w-amino acid: pyruvate transaminase employs a different mechanism for dual substrate recognition than other amine transaminases.* Appl Microbil Biotechnol, 2016.

96. Asano, Y., et al., *Phenylalanine Dehydrogenase of Bacillus-Badius - Purification, Characterization and Gene Cloning.* European Journal of Biochemistry, 1987. **168**(1): p. 153-159.

97. Viola, R.E. and W.W. Cleland, *Initial Velocity Analysis for Terreactant Mechanisms.* Methods in Enzymology, 1982. **87**: p. 353-366.

98. Rife, J.E. and W.W. Cleland, *Kinetic Mechanism of Glutamate-Dehydrogenase.* Biochemistry, 1980. **19**(11): p. 2321-2328.

99. Rife, J.E. and W.W. Cleland, *Determination of the Chemical Mechanism of Glutamate-Dehydrogenase from Ph Studies.* Biochemistry, 1980. **19**(11): p. 2328-2333.

100. Plowman, K.M. and W.W. Cleland, *Purification and Kinetic Studies of Citrate Cleavage Enzyme.* Journal of Biological Chemistry, 1967. **242**(18): p. 4239-&.

101. Robbins, J.M. and H.R. Ellis, *Identification of Critical Steps Governing the Two-Component Alkanesulfonate Monooxygenase Catalytic Mechanism.* Biochemistry, 2012. **51**(32): p. 6378-6387.

102. Shin, J.S. and B.G. Kim, *Kinetic resolution of alpha-methylbenzylamine with omega-transaminase screened from soil microorganisms: Application of a*

biphasic system to overcame product inhibition. Biotechnology and Bioengineering, 1997. **55**(2): p. 348-358.

103. Alexeeva, M., et al., *Deracemization of alpha-methylbenzylamine using an enzyme obtained by in vitro evolution.* Angewandte Chemie-International Edition, 2002. **41**(17): p. 3177-+.

104. Bea, H.S., et al., *Kinetic Resolution of alpha-methylbenzylamine by Recombinant Pichia pastoris Expressing omega-transaminase.* Biotechnology and Bioprocess Engineering, 2010. **15**(3): p. 429-434.

105. Shin;, G., S. Mathew;, and H. Yun;, *Kinetic resolution of amines by (R)-selective omega-transaminse from Mycobacterium vanbaalenii.* Journal of Industrial and Engineering Chemistry, 2014.

106. Truppo, M.D., N.J. Turner, and J.D. Rozzell, *Efficient kinetic resolution of racemic amines using a transaminase in combination with an amino acid oxidase.* Chemical Communications, 2009(16): p. 2127-2129.

107. Ghislieri, D., et al., *Monoamine Oxidase (MAO-N) Catalyzed Deracemization of Tetrahydro-beta-carbolines: Substrate Dependent Switch in Enantioselectivity.* Acs Catalysis, 2013. **3**(12): p. 2869-2872.

108. Yasukawa;, K., S. Nakano;, and Y. Asano, *Tailoring D-Amino Acid Oxidase from the Pig Kidney to R-Stereoselective Amine Oxidase and its Use in the Deracemization of alpha-Methylbenzylamine.* Angewandte Chemie-International Edition, 2014. **53**: p. 4428-4431.

109. Schrittwieser;, J.H., et al., *Deracemisation of Benzylisoquinoline Alkaloids Employing Monoamine Oxidase Variants.*

110. O'Reilly, E., C. Iglesias, and N.J. Turner, *Monoamine Oxidase- w- Transaminase Cascade for the Deracemisation and Dealkylation of Amines.* Chemcatchem, 2014. **6**(4): p. 992-995.

111. Au, S.K., B.R. Bommarius, and A.S. Bommarius, *Biphasic Reaction System Allows for Conversion of Hydrophobic Substrates by Amine Dehydrogenases.* Acs Catalysis, 2014. **4**(11): p. 4021-4026.

112. Sokalingam, S., et al., *A Study on the Effect of Surface Lysine to Arginine Mutagenesis on Protein Stability and Structure Using Green Fluorescent Protein.* Plos One, 2012. **7**(7).

113. Iqbal, J., M. Zaidi, and A.E. Schneider, *Cinacalcet hydrochloride - Amgen.* Idrugs, 2003. **6**(6): p. 587-592.

114. Graslund, S., et al., *Protein production and purification.* Nature Methods, 2008. **5**(2): p. 135-146.

115. *BioRad Micro Column Protein Prep Protocol*. 2009 [cited 2016 February 26]; Available from: http://2009.igem.org/Team:Washington/Notebook/IMAC_protocol.

116. van Berlo, M., et al., *Partitioning behavior of amino acids in aqueous two-phase systems with recyclable volatile salts.* Journal of Chromatography B, 2000. **743**(1-2): p. 317-325.

117. Johansson, H.O., et al., *Plasmid DNA partitioning and separation using poly(ethylene glycol)/poly(acrylate)/salt aqueous two-phase systems.* Journal of Chromatography A, 2012. **1233**: p. 30-35.

118. Vijayaragavan, K.S., et al., *Separation of porcine parvovirus from bovine serum albumin using PEG-salt aqueous two-phase system.* Journal of Chromatography B-Analytical Technologies in the Biomedical and Life Sciences, 2014. **967**: p. 118-126.

119. Asenjo, J.A. and B.A. Andrews, *Aqueous two-phase systems for protein separation: A perspective.* Journal of Chromatography A, 2011. **1218**(49): p. 8826-8835.

120. Raja, S., et al., *Aqueous Two Phase Systems for the Recovery of Biomolecules- A Review.* Science and Technology, 2011. **1**(1): p. 7-16.

121. Shahbaz Mohammadi, H., E. Omidinia, and H. Taherkhani, *Rapid one-step separation and purification of recombinant phenylalanine dehydrogenase in aqueous two-phase systems.* Iran Biomed J, 2008. **12**(2): p. 115-22.

122. Carter, J.L.L., et al., *Directed Evolution of a Formate Dehydrogenase for Increased Tolerance to Ionic Liquids Reveals a New Site for Increasing the Stability.* Chembiochem, 2014. **15**(18): p. 2710-2718.

123. Schutte, H., et al., *Purification and Properties of Formaldehyde Dehydrogenase and Formate Dehydrogenase from Candida-Boidinii.* European Journal of Biochemistry, 1976. **62**(1): p. 151-160.

124. Hatti-Kaul, R., *Aqueous Two-Phases Systems: Methods and Protocols*. Vol. 11. 2000.

125. Albertsson, P.A. and F. Tjerneld, *Phase-Diagrams.* Aqueous Two-Phase Systems, 1994. **228**: p. 3-13.

126. Ferreira, L.A. and J.A. Teixeira, *Salt Effect on the Aqueous Two-Phase System PEG 8000-Sodium Sulfate.* Journal of Chemical and Engineering Data, 2011. **56**(1): p. 133-137.

127. Glyk, A., T. Scheper, and S. Beutel, *Influence of Different Phase-Forming Parameters on the Phase Diagram of Several PEG-Salt Aqueous Two-Phase Systems.* Journal of Chemical and Engineering Data, 2014. **59**(3): p. 850-859.

128. Silverio, S.C., et al., *Effect of Aqueous Two-Phase System Constituents in Different Poly(ethylene glycol)-Salt Phase Diagrams.* Journal of Chemical and Engineering Data, 2012. **57**(4): p. 1203-1208.

129. Huddleston, J.G., H.D. Willauer, and R.D. Rogers, *Phase diagram data for several PEG plus salt aqueous biphasic systems at 25 degrees C.* Journal of Chemical and Engineering Data, 2003. **48**(5): p. 1230-1236.

130. Snyder, S.M., K.D. Cole, and D.C. Szlag, *Phase Compositions, Viscosities, and Densities for Aqueous 2-Phase Systems Composed of Polyethylene-Glycol and Various Salts at 25-Degrees-C.* Journal of Chemical and Engineering Data, 1992. **37**(2): p. 268-274.

131. Tubio, G., et al., *Liquid-liquid equilibria of aqueous two-phase systems containing poly (ethylene glycols) of different molecular weight and sodium citrate.* Journal of Chemical and Engineering Data, 2006. **51**(1): p. 209-212.

132. Murugesan, T. and M. Perumalsamy, *Liquid-liquid equilibria of poly(ethylene glycol) 2000+sodium citrate plus water at (25, 30, 35, 40, and 45) degrees C.* Journal of Chemical and Engineering Data, 2005. **50**(4): p. 1392-1395.

133. Zafarani-Moattar, M.T. and A.A. Hamidi, *Liquid-liquid equilibria of aqueous two-phase poly(ethylene glycol)-potassium citrate system.* Journal of Chemical and Engineering Data, 2003. **48**(2): p. 262-265.

134. Zaslavsky, B.Y., *Use of the aqueous two-phase partition technique for characterization and quality control of recombinant proteins.* Aqueous Biphasic Separations, 1995: p. 177-183.

135. Kohler, K., L. Vonbonsdorfflindeberg, and S.O. Enfors, *Influence of Disrupted Biomass on the Partitioning of Beta-Galactosidase Fused Protein-A.* Enzyme and Microbial Technology, 1989. **11**(11): p. 730-735.

136. Leiser, A., A. Birch, and J.A. Robinson, *Cloning, sequencing, overexpression in Escherichia coli, and inactivation of the valine dehydrogenase gene in the polyether antibiotic producer Streptomyces cinnamonensis.* Gene, 1996. **177**(1-2): p. 217-222.

137. Priestley, N.D. and J.A. Robinson, *Purification and Catalytic Properties of L-Valine Dehydrogenase from Streptomyces-Cinnamonensis.* Biochemical Journal, 1989. **261**(3): p. 853-861.

138. Vancurova, I., et al., *Isolation and Characterization of Valine Dehydrogenase from Streptomyces-Aureofaciens.* Journal of Bacteriology, 1988. **170**(11): p. 5192-5196.

139. Hyun, C.G., S.S. Kim, and J.W. Suh, *Identification of essential amino acid residues in valine dehydrogenase from Streptomyces albus.* Journal of Microbiology, 2006. **44**(1): p. 50-53.

140. Galaction, A.I., et al., *Improvement of enzymatic conversion of methylbenzylamine by direct extraction of acetophenone.* Separation Science and Technology, 2016.

141. D. Miguel, T.T., K.J. Woyechowsky, D. Hilvert, *Minimalist Active-site Redesign: Teaching Old Enzymes New Tricks.* Angewante Chemie Int. Ed., 2007. **46**: p. 3213-3236.

142. P.F. Mugford, U.G.W., Y. Jiang, K. Faber, R.J. Kazlauskas, *Enantiocomplementary enzymes: Classification, molecular basis for their enantiopreference, and prospects for mirror-image biotransformations.* Angewante Chemie Int. Ed., 2008. **47**: p. 8782-8793.

143. Yoichiro Ijima, K.M., Yosuke Terao, Nobuhide Doi, Hiroshi Yanagawa and Hiromichi Ohta, *Inversion of enantioselectivity of asymmetric biocatalytic decarboxylation by site-directed mutagenesis based on the reaction mechanism.* Chem. Commun., 2005: p. 877-879.

144. Yosuke Terao, Y.I., Kenji Miyamoto, Hiromichi Ohta, *Inversion of enantioselectivity of arylmalonate decarboxylase via site-directed mutation based on the proposed reaction mechanism.* Journal of Molecular Catalysis B: Enzymatic, 2007. **45**: p. 15-20.

145. Nakasako, R.O.a.M., *Structural Basis for Inverting the Enantioselectivity of Arylmalonate Decarboxylase Revealed by the Structural Analysis of the Gly74Cys/Cys188Ser Mutant in the Liganded Form.* Biochemistry, 2010. **49**: p. 1963-1969.

146. Sebastian Bartsch, R.K., and Uwe T. Bornscheuer, *Complete Inversion of Enantioselectivity towards Acetylated Tertiary Alcohols by a Double Mutant of a Bacillus Subtilis Esterase.* Angewante Chemie Int. Ed., 2008. **47**: p. 1508-1511.

147. Johansson, G., et al., *Affinity Partitioning of Bio-Polymers and Membranes in Ficoll Dextran Aqueous 2-Phase Systems.* Journal of Chromatography, 1985. **331**(1): p. 11-21.

148. Gonzaleztello, P., F. Camacho, and G. Blazquez, *Density and Viscosity of Concentrated Aqueous-Solutions of Polyethylene-Glycol.* Journal of Chemical and Engineering Data, 1994. **39**(3): p. 611-614.

149. Asenjo, J.A., et al., *Model for Predicting the Partition Behavior of Proteins in Aqueous 2-Phase Systems.* Journal of Chromatography A, 1994. **668**(1): p. 47-54.

150. Zhi, W.B., et al., *Partial purification of alpha-amylase from culture supernatant of Bacillus subtilis in aqueous two-phase systems.* Bioprocess and Biosystems Engineering, 2004. **27**(1): p. 3-7.

VITA

SAMANTHA KALING AU

Samantha was born in Edison, New Jersey on Christmas day to David and Michelle Au. She graduated from North Gwinnett High School (Suwanee, GA) in 2007. She graduated *cum laude* from the University of Kentucky in 2011where she majored in chemical engineering and played varsity soccer. She then pursued a doctoral degree at Georgia Institute of Technology within the school of Chemical & Biomolecular Engineering.